For Reference

NOT TO BE TAKEN FROM THIS ROOM

For Reference

NOT TO BE TAKEN FROM THIS ROOM

Ex LIBRIS
UNIVERSITATIS
ALBERTAENSIS

University of Alberta
Printing Department

THE UNIVERSITY OF ALBERTA

HYDROCARBON VAPOR-LIQUID EQUILIBRIA IN THE PRESENCE OF HYDROGEN SULPHIDE AND CARBON DIOXIDE

BY

AVINASH C. SAXENA

A DISSERTATION

SUBMITTED TO THE FACULTY OF GRADUATE STUDIES

IN PARTIAL FULFILMENT OF THE REQUIREMENTS

FOR THE DEGREE OF DOCTOR OF PHILOSOPHY

IN CHEMICAL ENGINEERING

DEPARTMENT OF CHEMICAL AND PETROLEUM ENGINEERING

EDMONTON, ALBERTA

OCTOBER, 1966

UNIVERSITY OF ALBERTA

FACULTY OF GRADUATE STUDIES

The undersigned certify that they have read, and recommend to the Faculty of Graduate Studies for acceptance, a thesis entitled "Hydrocarbon Vapor-Liquid Equilibria in the Presence of Hydrogen Sulphide and Carbon Dioxide" submitted by A.C. Saxena, M.Sc., B. Chem. Eng., in partial fulfilment of the requirements for the degree of Doctor of Philosophy.

ABSTRACT

An extensive review of the literature pertaining to the prediction and correlation of vapor-liquid equilibria has been made. This has revealed that most of the techniques which have been developed in the past are limited in application to simple systems at low pressures, without non-condensible components. The Chao-Seader correlation, the Wilson equation and the concept of convergence pressure appeared to be less restrictive, in this respect. The usefulness of these methods in correlating hydrocarbon-non-hydrocarbon vapor-liquid equilibria has been assessed.

Experimental vapor-liquid equilibrium data were obtained in the methane-hydrogen sulphide-n-butane system and the methane-carbon dioxide-n-butane system. The investigations were conducted at temperatures of -20°, 40°, and 100°F and at pressures, 400, 800, and 1200 psia at each temperature. A windowed cell of variable volume using mercury as confining fluid, was employed for this purpose. Equilibrium between phases was readily attained by means of a new technique based on spraying the liquid phase into the vapor phase.

The experimental results have indicated that hydrogen sulphide and carbon dioxide significantly influence the K-values of hydrocarbon components. The Chao-Seader correlation could not predict quantitatively the data of the systems of this investigation. Deviations in K-values in excess of 40%

were obtained at concentrations of the non-hydrocarbon component exceeding 30% in the liquid phase. The Wilson model, on the other hand, failed to correlate even the binary data in the presence of non-condensible components.

The excess free energy, enthalpy, and entropy functions for many binary systems containing non-condensible components were calculated. These values were compared with the values taken from the literature for simpler systems, having components which are all condensible. The equality in the order of magnitude of the ΔH^E and the $T\Delta S^E$ terms make the assumption of a regular or athermal solution inadequate in correlating liquid-solution behavior of hypothetical liquids. No satisfactory method to predict the behavior of non-condensible components has been developed to date. Before any attempt in this direction can be fruitful, a knowledge of partial molal liquid volumes of non-condensible components as a function of pressure, temperature, and properties of the solvent is essential. These must be known to account for the effect of pressure on activity coefficients. Their knowledge will also provide a better understanding of the behavior of a non-condensible component and enable use of physically-real standard states for these components. The calculation of excess functions has further indicated that a comprehensive theory of solutions must take into account both the non-ideal enthalpy and the non-ideal entropy of mixing.

ACKNOWLEDGEMENTS

The author is deeply indebted to Dr. D.B. Robinson, the principal thesis advisor, and to Dr. F.D. Otto and Professor P.M. Dranchuk,the other members of the supervisory committee, for their guidance and encouragement throughout this investigation.

For financial support of the project, the author is grateful to the National Research Council of Canada and the Texas Gulf Sulphur Company.

TABLE OF CONTENTS

	Page
LIST OF FIGURES	iii
LIST OF TABLES	vi
I. INTRODUCTION	1
II. THEORY	4
A. The Criterion of Equilibrium	4
B. Ideal Equilibrium Ratios	4
C. Ideal Solutions	6
D. Excess Free Energy and Activity Coefficients	10
E. Regular Solutions	16
F. Athermal Solutions	19
G. Determination of Activity Coefficients	21
H. Reference States	23
I. The Relative Volatility	25
J. Generalized Fugacity Charts	27
K. Direct Expressions Relating the Composition of Two Phases	28
L. The Convergence Pressure	29
M. Other Solution Theories	30
N. Applicability of Correlations to Hydrocarbon-non-Hydrocarbon Systems	31
III. LITERATURE REVIEW	33
A. Survey of Previous Experimental Work	33
IV. EXPERIMENTAL STUDIES	36
A. Experimental Apparatus	36
B. Preparation of Mixtures	42
C. Experimental Procedures	42
D. Analysis	43
E. Materials	45

V. RESULTS AND DISCUSSION 46

A. Experimental Apparatus 46

B. Experimental Results 46

a) Binary Systems 46

b) Ternary Systems 47

1) The Methane-Hydrogen Sulphide-n-Butane System 47

2) The Methane-Carbon Dioxide-n-Butane System 56

C. Comparison of Experimental Results 70

a) Comparison with the NGPSA Engineering Data Book 70

b) Comparison with the Chao-Seader Correlation 76

c) Comparison with the Wilson Equation 86

D. Excess Functions in Hydrocarbon Systems 91

VI. CONCLUSIONS 99

NOMENCLATURE 103

BIBLIOGRAPHY 106

APPENDIX A - TABULATIONS 114

APPENDIX B - SUMMARY OF EQUATIONS USED IN THE CHAO-SEADER CORRELATION 137

APPENDIX C - SAMPLE CALCULATION OF EXCESS FUNCTIONS 140

APPENDIX D - CALIBRATIONS 146

LIST OF FIGURES

Figure No.	Title	Page
1	Assembly View of Equilibrium Cell	37
2	Schematic Layout of Experimental Equipment	38
3	Sectional View of Internal Valve Used in Establishing Equilibrium	40
4	Vapor-Liquid Equilibrium Data at 400 psia and 100°F for the Methane-Hydrogen Sulphide-n-Butane System	48
5	Vapor-Liquid Equilibrium Data at 800 psia and 100°F for the Methane-Hydrogen Sulphide-n-Butane System	49
6	Vapor-Liquid Equilibrium Data at 1200 psia and 100°F for the Methane-Hydrogen Sulphide-n-Butane System	50
7	Vapor-Liquid Equilibrium Data at 400 psia and 40°F for the Methane-Hydrogen Sulphide-n-Butane System	51
8	Vapor-Liquid Equilibrium Data at 800 psia and 40°F for the Methane-Hydrogen Sulphide-n-Butane System	52
9	Vapor-Liquid Equilibrium Data at 1200 psia and 40°F for the Methane-Hydrogen Sulphide-n-Butane System	53
10	Vapor-Liquid Equilibrium Data at 400 psia and -20°F for the Methane-Hydrogen Sulphide-n-Butane System	54
11	Vapor-Liquid Equilibrium Data at 800 psia and -20°F for the Methane-Hydrogen Sulphide-n-Butane System	55
12	Vapor-Liquid Equilibrium Data at 1200 psia and -20°F for the Methane-Hydrogen Sulphide-n-Butane System	57

13	Influence of Hydrogen Sulphide Concentration on K-factors in the Methane-Hydrogen Sulphide-n-Butane System	58
14	Vapor-Liquid Equilibrium Data at 400 psia and 100°F for the Methane-Carbon Dioxide-n-Butane System	59
15	Vapor-Liquid Equilibrium Data at 800 psia and 100°F for the Methane-Carbon Dioxide-n-Butane System	60
16	Vapor-Liquid Equilibrium Data at 1200 psia and 100°F for the Methane-Carbon Dioxide-n-Butane System	61
17	Vapor-Liquid Equilibrium Data at 400 psia and 40°F for the Methane-Carbon Dioxide-n-Butane System	62
18	Vapor-Liquid Equilibrium Data at 800 psia and 40°F for the Methane-Carbon Dioxide-n-Butane System	63
19	Vapor-Liquid Equilibrium Data at 1200 psia and 40°F for the Methane-Carbon Dioxide-n-Butane System	64
20	Vapor-Liquid Equilibrium Data at 400 psia and -20°F for the Methane-Carbon Dioxide-n-Butane System	66
21	Vapor-Liquid Equilibrium Data at 800 psia and -20°F for the Methane-Carbon Dioxide-n-Butane System	67
22	Vapor-Liquid Equilibrium Data at 1200 psia and -20°F for the Methane-Carbon Dioxide-n-Butane System	68
23	Influence of Carbon Dioxide Concentration on K-factors in the Methane-Carbon Dioxide-n-Butane System at 40°F	69
24	Comparison of Experimental and Predicted K-factors for Methane, Hydrogen Sulphide, and n-Butane at 40°F	71

LIST OF TABLES

Table No.	Title	Page No.
1	Experimental Data in the CH_4-H_2S-nC_4H_{10} System	115
2	Smoothed Data in the CH_4-H_2S-nC_4H_{10} System	118
3	Experimental Data in the CH_4-CO_2-nC_4H_{10} System	121
4	Smoothed Data in the CH_4-CO_2-nC_4H_{10} System	123
5	Comparisons with the Chao-Seader Correlation	126
6	Wilson Constants and Binary Interaction Energies in the Methane-Hydrogen Sulphide System	132
7	Calculated Values of Excess Functions	133
8	Values of Excess Function Taken from the Literature	134
9	Comparison with the NGPSA Engineering Data Book	136

I. INTRODUCTION

Design of contacting equipment like distillation columns and absorbers requires a knowledge of the composition and amounts of coexisting phases under heterogeneous equilibrium. In order to facilitate vapor-liquid equilibrium calculations, Souders, Selheimer, and Brown[111] developed the concept of 'equilibrium constants' which have been found to be a suitable measure of the vaporization characteristics of petroleum mixtures[50]. They arbitrarily defined the equilibrium constant, K, as the ratio of the mole fraction of a component in the vapor phase, y, to the mole fraction of the same component in the liquid phase, x, at a defined temperature and pressure of equilibrium. Equilibrium constants are functions of temperature, pressure, and composition of the system. The term 'constant' is thus misleading. Muskat[70] has proposed the term 'equilibrium ratio', often written as K-ratio or K-value.

The K-ratios for components of a mixture can be determined experimentally by finding the composition of the vapor and liquid in equilibrium at the desired conditions of pressure and temperature. Experimental measurements are expensive and time consuming and, for this reason, many attempts have been made to predict and correlate K-values using theoretical, semi-empirical and empirical methods. These methods, discussed in a later section, have been found to be useful only for

specific systems and for conditions of pressure and temperature at which they were derived. All attempts to devise a general correlation for vapor-liquid equilibria have been unsuccessful for lack of reliable experimental data as well as for lack of a comprehensive theory.

Petroleum reservoirs frequently contain large amounts of non-hydrocarbon components such as hydrogen sulphide and carbon dioxide. Due to their widely different molecular structure, these components are known to form highly non-ideal solutions with hydrocarbons. Vapor-liquid equilibrium data on a large number of hydrocarbon binaries containing these non-hydrocarbon components are available in the literature but data on ternary and multi-component systems of these components are scant. Experimental data on only a very few systems containing hydrogen sulphide are reported, possibly due to the extremely toxic properties of this substance. The experimental data are normally limited to room temperature and above. In the recent years, there has been a trend towards increased use of low temperatures in the petrochemical and natural gas industries. This has necessitated experimental information on hydrocarbon systems at temperatures much lower than the ambient.

In view of the above considerations, the objectives of this investigation may be stated as follows:

1. To extend the range of K-data available on systems con-

taining non-hydrocarbons like hydrogen sulphide and carbon dioxide.

2. To compare the influence of hydrogen sulphide and carbon dioxide on the K-values of hydrocarbons.
3. To review the prediction and correlation methods for vapor-liquid equilibria which have been proposed in the literature and to assess their applicability to hydrocarbon-non-hydrocarbon systems of this investigation.

II. THEORY

A. The Criterion of Equilibrium

Equilibrium in a closed system implies a situation in which there are no spontaneous or unaided changes. All spontaneous changes are accompanied by a decrease in the free energy of the system, therefore, expressed mathematically, the criterion of equilibrium at constant temperature and pressure is[34]

$$dF = 0 \qquad (1)$$

where, F is the free energy of the system.

Vapor-liquid equilibrium conditions can be assumed to exist in natural gas-condensate wells and many contacting equipments such as distillation columns. Expressions which relate vaporization equilibrium ratio K to system variables, pressure, temperature, and composition are, therefore, very useful. Many methods have been proposed in the literature for the correlation of equilibrium ratios. A review of the usefulness of these techniques and their limitations will be presented here.

B. Ideal Equilibrium Ratios

By definition, at equilibrium,

$$K_i = \frac{y_i}{x_i} \qquad (2)$$

If the molecules of the components of a solution are so similar in nature that the forces between unlike molecules are the same as those between like molecules and if the components mix without the complicating effects of molecular association or chemical combination, the solution would obey Raoult's law[88]:

$$p_i = x_i \cdot p_i^v \qquad (3)$$

where, p_i is the partial pressure of the i^{th} component of the solution and p_i^v, the vapor pressure of the i^{th} component in its pure state at the temperature of equilibrium.

Dalton's law[15] states that the total pressure of a gas is equal to the sum of the partial pressures of the components present, thus:

$$p_i = y_i \cdot P \qquad (4)$$

where, P is the total pressure of the system.

Equations (3) and (4) may be combined to give,

$$K_i = \frac{y_i}{x_i} = \frac{p_i^v}{P} \qquad (5)$$

This equation suggests a useful method of representing the equilibrium ratios graphically. Taking the logarithm of both sides one obtains,

$$\log K_i = \log p_i^v - \log P \qquad (6)$$

A log-log plot of K_i versus P will, therefore, yield a straight line of slope -1, passing through $K_i = 1$ where $P = p_i^v$ at the

temperature of the system.

Raoult's and Dalton's laws are not exact even in relatively simple mixtures of paraffin hydrocarbons. K-values predicted by this method are restricted to low pressures and some considerable distance from the critical pressure. n-Pentane and heavier n-paraffin hydrocarbons conform to these ideal laws over certain ranges of pressure and temperature, but the presence of components such as nitrogen, water, hydrogen, carbon dioxide, hydrogen sulphide, and olefins frequently causes significant departures from these laws.

C. Ideal Solutions

G.N. Lewis[61] proposed the use of fugacity in place of pressure whenever the fluids behave non-ideally. A closer approximation to actual K-values is obtained if partial pressure and pressure are replaced by fugacities in making equilibrium calculations. An ideal solution is defined as one in which the fugacity of each component is proportional to its mole fraction. Equilibrium ratios defined in terms of fugacity are sometimes called 'ideal solution equilibrium ratios'.

Fugacity, at constant temperature T, is defined as:

$$dF = RT\ d\ \ln f = v\ dp \qquad (7)$$

where, f is the fugacity; v, the molal volume of the component; and p, the system pressure. The Dalton's and Raoult's law type

equations now become:

$$\bar{f}_i^{\,v} = y_i f_i^{\,v} \tag{8}$$

$$\bar{f}_i^{\,l} = x_i f_i^{\,l} \tag{9}$$

where, the bar denotes the fugacity of a component in the mixture and v and l stand for vapor and liquid respectively.

The criterion of vapor-liquid equilibrium, making use of Equation (7), can be written as

$$\bar{f}_i^{\,v} = \bar{f}_i^{\,l} \tag{10}$$

giving

$$K_{ideal} = \frac{y_i}{x_i} = \frac{f_i^{\,l}}{f_i^{\,v}} \tag{11}$$

K_{ideal} is a function of pressure and temperature only and is independent of composition. The ideal solution is a limiting case which real solutions can approach, more or less closely, depending on system conditions.

For a quantitative thermodynamic treatment of real solutions it is customary to compare their behavior with the behavior of an ideal solution. In this regard, the introduction of special thermodynamic functions such as the activity, the activity coefficient, and the excess properties enables comparison to the made, quite simply, between the properties of a given solution and those of an ideal solution.

The activity is defined as the ratio of the fugacity of a component in the given state to the fugacity of this component at the same temperature, in some arbitrarily chosen standard state:

$$\bar{a}_i = \frac{f_i}{f_i^o} \tag{12}$$

where, $\bar{a}_i$ denotes the activity of the i^{th} component and f_i^o, the fugacity in the standard state, at the same temperature. For solutions of non-electrolytes, it is customary to choose as the standard state that of the pure component under its vapor pressure at the temperature of the system. Thus, the activity of a pure substance at its vapor pressure is always equal to unity:

$$(\bar{a}_i)_{x_i=1} = \frac{f_i^o}{f_i^o} = 1 \tag{13}$$

It follows from the definition that for an ideal solution the activity of a component is equal to its mole fraction.

The activity coefficient γ_i is defined as the ratio of the activity to the mole fraction of the i^{th} component:

$$\gamma_i = \frac{\bar{a}_i}{x_i} \tag{14}$$

For an ideal solution, the activity coefficient is always equal to unity. All deviations from ideal behavior are lumped into one factor, the activity coefficient and, in the characteriza-

tion of real solutions of non-electrolytes, attention is directed to predicting the dependence of the activity coefficient on temperature, pressure and especially composition. Thermodynamic relations of an ideal solution are valid even for real solutions provided the mole fraction x_i is replaced by the activity $\bar{a}_i$ or the product $\gamma_i x_i$. The activity and activity coefficient are functions of pressure, temperature and composition of the system. The influence of pressure on the activity coefficient is expressed by the following equation[38].

$$\left(\frac{\partial \ln \gamma_i}{\partial P}\right)_{T,x} = \left(\frac{\partial \ln \bar{a}_i}{\partial P}\right)_{T,x} = \frac{1}{RT}\left(\bar{V}_i - V_i^{o}\right) \qquad (15)$$

where, $\bar{V}_i$ is the partial molar volume of the i^{th} component and V_i^{o}, the molar volume of the pure i^{th} component at a given pressure and temperature.

The following equation [38] expresses the dependence of activity and activity coefficient on temperature:

$$\left(\frac{\partial \ln \gamma_i}{\partial T}\right)_{P,x} = \left(\frac{\partial \ln \bar{a}_i}{\partial T}\right)_{P,x} = -\frac{\bar{H}_i - H_i^{o}}{RT^2} \qquad (16)$$

where, the difference $(\bar{H}_i - H_i^{o})$ is the partial molar heat of mixing of the i^{th} component.

The well-known Gibbs-Duhem equation expresses the effect of composition at constant pressure and temperature, on the activity and activity coefficient[87]:

$$\sum_{i=1}^{N} x_i \frac{\partial \ln \bar{a}_i}{\partial x_j} = \sum_{i=1}^{N} x_i \frac{\partial \ln \gamma_i}{\partial x_j} = 0 \qquad (17)$$

where, N is the number of components and the subscripts i and j denote the i^{th} and the j^{th} component respectively. Integrated forms of the Gibbs-Duhem equation have been used to develop various expressions relating the activity coefficient to composition. Some of these equations are discussed in a later section.

D. Excess Free Energy and the Activity Coefficients

Scatchard[104] introduced the very useful concept of the excess free energy of a solution, ΔF^E, to express the non-idealities of a liquid mixture. The effects of differences in intermolecular forces, polarity, chemical structure, and molecular size, causing non-ideal solution behavior are included in the excess free energy. It has been found to be very useful and convenient to express the excess free energy as a function of liquid composition. The excess free energy of a solution is defined by the expression:

$$\Delta F^E = \Delta F_{mix} - \Delta F_{mix}^{ideal} \qquad (18)$$

where, ΔF_{mix} is the molar free energy of mixing of a real solution, and ΔF_{mix}^{ideal}, the molar free energy of mixing of the same solution if it were ideal. The activity coefficient γ_i for any

component i can be found by the exact relation[86]:

$$RT \ln \gamma_i = \left[\frac{\partial (n_T \Delta F^E)}{\partial n_i} \right]_{T,P,\text{all } n_k (k \neq 1)} \tag{19}$$

where, n_T is the total number of moles in the liquid solution and n_i, the number of moles of the i^{th} component.

Wohl[125] statistically developed a general expression for the dependence of ΔF^E on composition.

$$\frac{\Delta F^E}{RT(\sum_i q_i x_i)} = \sum_{i,j} Z_i Z_j a_{ij} + \sum_{i,j,k} Z_i Z_j Z_k a_{ijk} + \sum_{i,j,k,l} Z_i Z_j Z_k Z_l a_{ijkl} + \ldots \tag{20}$$

where, ΔF^E is the molal excess free energy; x_i, q_i and Z_i, respectively, the mole fraction, effective molal volume, and effective volume fraction of the i^{th} component; the empirical constants, a_{ij}, a_{ijk}, a_{ijkl}, ... measure the interaction in various groups of molecules, ij, ijk, ijkl, ... The effective volume fraction of any component i is defined by the relation

$$Z_i = \frac{q_i x_i}{\sum_j q_j x_j} \tag{21}$$

The first term on the right hand side of Equation (20) represents the contribution due to all possible binary interactions of unlike components and is designated as a two-

suffix term. The term $\sum_{ijk} Z_i Z_j Z_k a_{ijk}$ accounts for the interaction of unlike components in groups of three. A combination of the first and second terms represents a three-suffix equation. The remaining terms have a similar interpretation. The number of terms to be used is dictated by the complexity of the solution and the precision of the experimental data.

According to Equation (20), a third order Wohl expression for a binary system may be written as,

$$\frac{\Delta F^E}{RT(q_1 x_1 + q_2 x_2)} = 2Z_1 Z_2 a_{12} + 3Z_1{}^2 Z_2 a_{112} + 3Z_1 Z_2{}^2 a_{122} \quad (22)$$

or, since $Z_1 + Z_2 = 1.0$,

$$\frac{\Delta F^E}{RT} = (x_1 + \frac{q_2}{q_1} x_2) Z_1 Z_2 \left[Z_1 q_1 (2a_{12} + 3a_{112}) + Z_2 q_1 (2a_{12} + 3a_{122}) \right] \quad (23)$$

Using Equation (19) and the substitutions,

$$\left.\begin{aligned} A &= q_1 (2a_{12} + 3a_{122}) \\ B &= q_2 (2a_{12} + 3a_{112}) \end{aligned}\right] \quad (24)$$

the following expressions for the activity coefficients are obtained:

$$\ln \gamma_1 = Z_2{}^2 \left[A + 2Z_1 (B \frac{q_1}{q_2} - A) \right] \quad (25)$$

$$\ln \gamma_2 = Z_1{}^2 \left[B + 2Z_2 (A \frac{q_2}{q_1} - B) \right] \quad (26)$$

The constants A, B, and q_1/q_2 must be determined experimentally. The introduction of certain simplifying assumptions reduces these equations to relations proposed in the literature by other authors. Thus, if the effective molar volumes q_1 and q_2 are replaced by the molar volumes of the pure components, the Scatchard and Hamer[107] equations are obtained:

$$\ln \gamma_1 = Z_2^2 \left[A + 2Z_1\left(B \frac{V_1}{V_2} - A\right)\right] \tag{27}$$

$$\ln \gamma_2 = Z_1^2 \left[B + 2Z_2\left(A \frac{V_2}{V_1} - B\right)\right] \tag{28}$$

If it is assumed that $q_2/q_1 = B/A$, Equations (25) and (26) become the van Laar[116,117] equations of third order:

$$\ln \gamma_1 = AZ_2^2 = \frac{A}{\left(1 + \frac{x_1}{x_2}\cdot\frac{A}{B}\right)^2} \tag{29}$$

$$\ln \gamma_2 = BZ_1^2 = \frac{A}{\left(1 + \frac{x_2}{x_1}\cdot\frac{B}{A}\right)^2} \tag{30}$$

On the assumption, $q_2/q_1 = 1$, Equation (25) and (26) take the form of Margules[68] equations of third order

$$\ln \gamma_1 = x_2^2 \left[A + 2x_1(B - A)\right]$$

$$= x_2^2 (2B - A) + 2x_2^3(A - B) \tag{31}$$

$$\ln \gamma_2 = x_1^2 \left[B + 2x_2(A - B)\right]$$

$$= x_1^2 (2A - B) + 2x_1^3(B - A) \tag{32}$$

If A = B, both Margules and van Laar equations further simplify to the common form:

$$\ln \gamma_1 = Ax_2^2 \qquad (33)$$

$$\ln \gamma_2 = Ax_1^2$$

The constants A and B in all these equations are terminal values, defined as:

$$A = \lim_{x_1 \to 0} \ln \gamma_1 \qquad (35)$$

$$B = \lim_{x_2 \to 0} \ln \gamma_2$$

The methods of determining these constants are outlined by Carlson and Colburn[9]. Wohl equations of higher orders can be derived similarly, but they involve a greater number of constants.

These equations are found to be useful in predicting vapor-liquid equilibria in many ternary non-ideal systems at subatmospheric pressures, containing components which are all condensible at the system temperature[1]. Two or three constants, depending on the suffix of the equation used, are calculated from the experimental data for each of the component binaries. Sometimes a ternary constant, if the non-idealities are large, is calculated from ternary experimental data. These constants are then used to correlate ternary

vapor-liquid equilibria. In the presence of non-condensible components, that is components having a critical temperature lower than the system temperature, extrapolation of the properties of these components into hypothetical regions is necessary. This introduces many uncertainties and, as a result, only qualitative prediction of vapor-liquid equilibria has been possible in the systems of non-condensible components.

Chueh, Muirbrook, and Prausnitz[11] have recently developed a modified van Laar model which does not assume q_1 and q_2 to be independent of composition. Instead, they assumed q_1/q_2 to be constant and equal to the ratio of critical volumes of components 1 and 2. The model can easily be extended to multicomponent systems and requires data only on component binaries to predict multicomponent phase equilibria. The authors have used this model to predict vapor-liquid equilibria in the carbon dioxide-nitrogen-oxygen system, but only qualitative agreement with experimental data was obtained.

Various authors[3,120,63,53,75,76] have developed expressions for activity coefficients in terms of composition with terms involving functions of temperature. These equations are basically derived from the van Laar equations and have been found to be useful with systems containing condensible components of markedly different boiling points.

E. Regular Solutions

The excess free energy consists of two parts, an excess enthalpy and an excess entropy term:

$$\Delta F^E = \Delta H^E - T\Delta S^E \qquad (36)$$

Hildebrand[40], in 1929, proposed the concept of a 'regular solution', defined as a solution involving no entropy change when a small amount of one of its components is transferred to it from an ideal solution of the same composition, the total volume remaining unchanged. Thus, for a regular solution:

$$\Delta F^E = \Delta H^E \qquad (37)$$

where, ΔH^E is the excess enthalpy of mixing. Hildebrand and Scott[42] have shown that the enthalpy of mixing can be expressed as a function of the cohesive energy densities of the components. Thus, for a binary solution

$$\Delta F^E = \Delta H^E = (x_1V_1 + x_2V_2)\left[\left(\frac{\Delta E_1^V}{V_1}\right)^{\frac{1}{2}} - \left(\frac{\Delta E_2^V}{V_2}\right)^{\frac{1}{2}}\right]^2 \phi_1\phi_2 \qquad (38)$$

where, V_1 and V_2 are the pure liquid volumes; ΔE_1^V and ΔE_2^V, the corresponding molar energies required to vaporize the liquid to infinite volume; and ϕ_1 and ϕ_2, the volume fractions for components 1 and 2 respectively. This equation is generally known as the Scatchard-Hildebrand[106] equation.

Defining the solubility parameter δ_i as the square

root of cohesive energy density,

$$\delta_i = \left(\frac{\Delta E_i^V}{V_i}\right)^{\frac{1}{2}} \tag{39}$$

and utilizing Equation (19), the following general equation is obtained. It expresses the activity coefficients in a multi-component regular liquid solution.

$$\ln \gamma_i = \frac{V_i}{RT} (\delta_i - \bar{\delta})^2 \tag{40}$$

The quantity $\bar{\delta}$ designates an average value of the solubility parameter for the solution:

$$\bar{\delta} = \frac{\sum_i x_i V_i \delta_i}{\sum_i x_i V_i} \tag{41}$$

According to Equation (40), two constants are required for each component - the solubility parameter δ_i and the molar liquid volume V_i. Regular solutions are endothermic, heat or enthalpy of mixing being always positive. The excess entropy of mixing is assumed negligible in comparison, i.e. $\Delta S^E \simeq 0$. The activity coefficients are all greater than unity, $\gamma_i > 1.0$.

Equation (40) reduces to the familiar van Laar Equations (27) and (28), if the constants A and B are defined as follows:

$$A = \frac{V_1}{RT} (\delta_1 - \delta_2)^2 \tag{42}$$

$$B = \frac{V_2}{RT} (\delta_2 - \delta_1)^2 \tag{43}$$

The concept of regular solutions has been used recently in correlating K-values. The necessary derivations are outlined below. Utilizing equation (10), K_i may be expressed as:

$$K_i = \frac{\dfrac{\bar{f}_i^{\,l}}{f_i^{\,l} x_i}}{\dfrac{\bar{f}_i^{\,v}}{P y_i}} \left(\frac{f^l}{P}\right)_i = \frac{\gamma_i^{\,l} \nu_i}{\phi_i'}$$

where

$\gamma_i^{\,l} = (\bar{f}/fx)_i^{\,l}$ = activity coefficient of component i in a liquid mixture

$\nu_i = (f/P)_i^{\,l}$ = fugacity coefficient of component i as a pure liquid

$\phi_i' = (\bar{f}/Py)_i^{\,v}$ = fugacity coefficient of component i in a vapor mixture

Chao and Seader[10] have used this expression for K_i to develop a general correlation of vapor-liquid equilibria in hydrocarbon mixtures. The quantity $\gamma_i^{\,l}$ is calculated from Hildebrand's Equation (40), with regular solutions assumed. The solubility parameters for various components are derived from a best fit of experimental vapor-liquid equilibrium data. The quantity ν_i is correlated utilizing a modified form of Pitzer's[14,82] principle of corresponding states. The Redlich Kwong[95] equation of state is employed to calculate the vapor phase fugacity coefficient ϕ_i. All necessary equations are given in Appendix B. Chao and Seader[10] have calculated

the solubility parameter, the acentric factor, and the constants required in the expansion of ν_i in terms of reduced properties, for various components, including paraffins, olefins, aromatics, and naphthenes.

F. Athermal Solutions

In the study of polymer solutions, Flory[26] and Huggins[47] independently developed the concept of 'athermal solutions' for which the heat of mixing is ideal, i.e. $\Delta H^E = 0$, and all non-idealities are due to the excess entropy of mixing, $\Delta S^E \neq 0$. The mole fraction in the expression for excess entropy of mixing in an ideal solution is replaced by volume fraction. The Flory-Huggins expression for athermal mixtures is,

$$\Delta F^E = -T\Delta S^E = RT \sum_i x_i(\ln \phi_i - \ln x_i) \qquad (45)$$

where, ϕ_i is the volume fraction of the i^{th} component:

$$\phi_i = \frac{x_i V_i}{\sum_i x_i V_i} \qquad (46)$$

For mixtures of components with equal molar liquid volumes, $\phi_i = x_i$, and the Flory-Huggins equation predicts ideal entropy of mixing, $\Delta S^E = 0$.

Recently, Wilson[122] has proposed a different expression for excess Gibb's free energy involving logarithmic functions of composition. To derive the Wilson equation[79],

consider a binary solution of components i and j. If attention is focussed on a central molecule of type i, the probability of finding amolecule of type j, compared to finding a molecule of type i, about this central molecule is defined by:

$$P(j/i) = \frac{x_j \exp - \frac{\lambda_{ij}}{RT}}{x_i \exp - \frac{\lambda_{ii}}{RT}} \tag{47}$$

where, λ_{ij} and λ_{ii} are proportional to the i-j and i-i interaction energies, $\lambda_{ij} = \lambda_{ji}$. Using the definition embodied in Equation (47), Wilson has empirically defined a local volume fraction, ξ_i, i.e.

$$\xi_i = \frac{x_i V_i \exp\left(-\frac{\lambda_{ii}}{RT}\right)}{x_i V_i \exp\left(-\frac{\lambda_{ii}}{RT}\right) + x_j V_j \exp\left(-\frac{\lambda_{ij}}{RT}\right)} \tag{48}$$

Defining,

$$\Lambda_{ij} = \frac{V_j}{V_i} \exp\left(\frac{\lambda_{ij} - \lambda_{ii}}{RT}\right) \tag{49}$$

and replacing ϕ_i by ξ_i in the Flory-Huggins expression, the following relation for excess free energy in a multicomponent solution is obtained:

$$\Delta F^E = -RT \sum_{i=1}^{N} x_i \ln\left(\sum_{j=1}^{N} x_j \Lambda_{ij}\right) \tag{50}$$

The expression for the activity coefficient for any component k is readily obtained by a partial differentiation of Equation (50) according to Equation (19).

$$\ln \gamma_k = -\ln \left(\sum_{j=1}^{N} x_j \Lambda_{kj} \right) + 1 - \sum_{i=1}^{N} \frac{x_i \Lambda_{ik}}{\sum_{j=1}^{N} x_j \Lambda_{ij}} \qquad (51)$$

To predict vapor-liquid equilibria, the Wilson equation requires data only on component binary systems. The Boltzmann factors, $\exp(-\lambda_{ij}/RT)$ provide a built-in temperature dependence, and for simple systems the quantities $(\lambda_{ij} - \lambda_{ii})$ and $(\lambda_{ij} - \lambda_{jj})$ may be considered independent of temperature over modest ranges of temperature, enabling extension of data from one temperature to other temperatures not too far removed. No simplifying assumptions about additivity of intermolecular forces are made and the equation can be used for systems which exhibit negative or positive deviations from Raoult's law. In its present form, the Wilson equation cannot account for a system of limited solubility and it is not possible to calculate Wilson parameters which reproduce maxima and minima in activity coefficients.

G. Determination of Activity Coefficients

Deal and coworkers[17,81,123] suggested that in any solvent environment the partial molal excess free energy of solution of a solute molecule can be taken as the sum of individual contributions from each of its structural groupings. These contributions depend, in some way, upon the number and kind of structural groupings which make up the environment.

No extension of a group approach to excess free energies or activity coefficients has, however, appeared recently. Predictions using this approach were not sufficiently precise and could only be used for a qualitative description of phase behavior.

Reference to the literature indicates that many attempts have been made to express the behavior of real solutions in terms of the known properties of the pure components. Ewell and coworkers[25] classified liquids into five groups, according to their ability to form hydrogen bonds. Their classification enables a qualitative estimation of the direction of deviation in real solutions from ideal behavior[27,91]. For solutions whose constituents neither associate nor form hydrogen bonds, Redlich, Kister and Turnquist[94] have presented relations for approximate calculation of constants for van Laar type equations. The method of Hala et al[37] may be used with polar components to calculate van Laar constants from the parachors of components and from known values of constants for standard binary systems. Erdös[24] calculated the van Laar constants from the parachors and heats of vaporization of pure components. The results of these approaches are fragmentary and can be used only for a semi-quantitative estimate of the behavior of real solutions.

A knowledge of total pressure over a binary solution as a function of the composition of liquid phase is sufficient

for a complete description of vapor-liquid equilibria. It is a very cumbersome task to obtain a vapor sample truly in equilibrium with the liquid phase, in particular with components of high relative volatility. Using the total pressure approach, however, activity coefficients can be calculated, with due allowance for the non-idealities of the vapor phase, without knowledge of the vapor composition. The results are comparable in accuracy with those obtained from the experimentally more difficult partial pressure measurements[105].

The method has been successfully employed for binary mixtures which do not deviate greatly from ideal behavior[60]. The calculations involved with the use of this method are tedious[69,93]. Barker[2] has developed a convenient method of least squares, requiring successive approximations for the calculation of activity coefficients. Small experimental errors, it should be remembered, may entail large errors in the resulting activity coefficients.

H. Reference States

There are two systems of reference states commonly employed in defining activity coefficients, one symmetrical and the other non-symmetrical[87]. Confining discussion to binary systems for the sake of simplicity, the symmetrical system can be defined as:

$$\begin{aligned} \gamma_1 &\longrightarrow 1 \quad \text{as} \quad x_1 \longrightarrow 1 \\ \gamma_2 &\longrightarrow 1 \quad \text{as} \quad x_2 \longrightarrow 1 \end{aligned} \tag{52}$$

This definition implies a reference state for both components; that of pure liquid under its vapor pressure at the temperature of the solution. The symmetrical reference system is found to be very convenient and the reference state has a definite physical meaning provided the temperature of the mixture is not beyond the critical temperature of any of the components. All the components of the system are treated in the same manner and the reference system is particularly valuable in the treatment of concentrated solutions.

The unsymmetrical convention employs an ideal dilute solution as the reference state, when the component may be assumed to obey Henry's law. This system can be expressed mathematically as:

$$\begin{aligned} \gamma_1^* &\longrightarrow 1 \quad \text{as} \quad x_2 \longrightarrow 0 \\ \gamma_2^* &\longrightarrow 1 \quad \text{as} \quad x_1 \longrightarrow 1 \end{aligned} \tag{53}$$

It can be seen that the activity coefficients defined in this manner are no longer symmetrical. The asterisks are used to indicate that an unsymmetrical reference system has been employed. Prigogine and Defay[87] have derived the necessary equations for change from one system to another.

The unsymmetrical reference system is useful in the presence of non-condensible components[85,77], because the reference fugacity is defined very unambiguously and it is not necessary to extrapolate the properties of pure liquid beyond its critical point. It should be noted, however, that

the reference state is not that of a pure component but depends also on the properties of the solvent. In order that this reference system may be employed it is necessary, therefore, to know the infinite dilution fugacity of the non-condensible component in the heavier constituents. Employing the Henry's constant as the reference fugacity for a non-condensible component does not completely solve the problem of its hypothetical existence. In order to account for the effect of pressure on activity coefficient, it is necessary to evaluate the integral $\left[\int_{P_{reference}}^{P_{system}} \frac{V_i}{RT}\, dP\right]$. The molar liquid volume V_i is a hypothetical liquid property, for a non-condensible component.

I. <u>The Relative Volatility</u>

In the case of non-ideal solutions whose vapor phase behaves ideally, the following assumptions can be made:

1) The relative volatility is independent of pressure.
2) Dependence of relative volatility on temperature is also small, certainly smaller than the dependence of activity coefficient.

The relative volatility is defined as:

$$\alpha_{ij} = \frac{\frac{y_i}{x_i}}{\frac{y_j}{x_j}} = \frac{K_i}{K_j} \qquad (54)$$

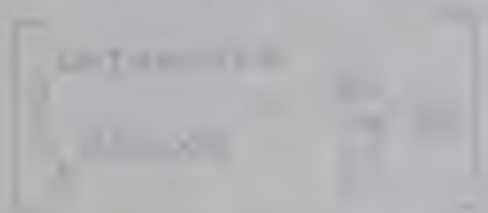

If the dependence of the relative volatility on the composition of the liquid is known, it is possible to calculate the composition of the equilibrium vapor according to the following equations:

$$y_i p = \gamma_i x_i p_i^v ; \qquad y_j p = \gamma_j x_j p_j^v \tag{55}$$

which on combination yield,

$$\alpha_{ij} = \frac{\gamma_i}{\gamma_j} \frac{p_i^v}{p_j^v} \tag{56}$$

This equation implies that to express dependence of relative volatility, it is necessary to know the dependence of the ratio of activity coefficients on state variables. Relations expressing the dependence of the relative volatility on composition can be derived from Equation (19).

$$\ln \gamma_k - \ln \gamma_1 = \ln \frac{\gamma_k}{\gamma_1} = \left(\frac{\partial}{\partial n_k} - \frac{\partial}{\partial n_1}\right)\left(n_T \frac{\Delta F^E}{RT}\right) \tag{57}$$

ΔF^E can be expressed by means of the Wohl expansion (20). This treatment leads to the well-known Margules-Wohl[126] and Redlich-Kister[92] equations. The Margules-Wohl equations are found to be useful for systems which depict extrema in activity coefficients, with respect to composition. The Redlich-Kister equations have been successfully employed for systems in which the effect of temperature on activity coefficients is negligible.

J. Generalized Fugacity Charts

Equations (8) and (9) can be combined as follows:

$$K_i = \frac{\bar{f}_i^{\,l}}{\bar{f}_i^{\,v}} \left(\frac{y_i}{x_i}\right) = \frac{\left(\frac{\bar{f}}{xf}\right)_i^{l}}{\left(\frac{\bar{f}}{yf}\right)_i^{v}} \left(\frac{f_i^{\,l}}{f_i^{\,v}}\right) = \frac{\gamma_i^{\,l}}{\gamma_i^{\,v}} K_{ideal} \qquad (58)$$

The fugacity and the activity coefficients in the above equations can be calculated from pressure-volume-temperature-composition data. Empirical treatment for both liquid and vapor phases is required in the presence of components in hypothetical states.

Many K-value charts, utilizing different rearrangements of the above equation, have been prepared. The most well-known and widely used of these are the Polyco or Kellogg PTC-K charts of Benedict et al[3], utilizing the Benedict-Webb-Rubin equation of state; the new Kellogg charts prepared by Edmister and Ruby[22]; the MIT K-charts[62]; the DePriester[18] K-value correlations; the Smith and Smith charts[110]; and the K-value charts presented recently by Edmister[21]. These charts have been found to be very useful for prediction of fugacity coefficients, activity coefficients, and K-values in hydrocarbon systems under conditions removed from the critical.

Many equations of state have been used for the calculation of fugacity and activity coefficients. In the treatment of mixtures various empirical mixing rules have been

employed. The most important equations of state are the equation proposed by Benedict, Webb, and Rubin[3]; the Redlich and Kwong[95] equations of state and the Black[5] equation of state. The Redlich-Kwong and the Black equations of state are widely employed at the present time to describe the behavior of vapors.

K. Direct Expressions Relating the Composition of Two Phases

In the preceding pages, relationships expressing the dependence of the activity coefficient on state variables, particularly liquid composition, were discussed. Various authors have recently proposed a series of empirical relations which are intended to express algebraically the mutual dependence of the equilibrium composition of the vapor and liquid phases, sometimes utilizing special functions like enrichment factor and equilibrium ratio. The greatest advantage of these equations is that they permit the use of simple algebraic procedures in vapor-liquid equilibrium calculations. All these equations have been found to be useful only for binary systems and are special cases of the following relation[38]

$$\alpha_{12} = \frac{1 + a_{11}x_1}{a_{20} + a_{21}x_2 + a_{22}x_2^2} \qquad (59)$$

where, all a's are empirical constants. The expression proposed by the following authors fall in this group: Clark[12]; Prahl[84]; Kretschmer and Wiebe[52]; Spinner, Lu, and Gray-

don[112]; Mayo and Lewis[67]; Wall[118]; Hirata[43,44]; Othmer and Gilmont[31,80]; Scheibel and Friedland[108]; Gilmont and coworkers[28,29,30]; and Edwards and coworkers[23].

These equations only relate equilibrium compositions in a system at a known pressure and temperature. Their usefulness lies in extension of experimental data in binary systems.

L. The Convergence Pressure

The observation that K-ratios, when plotted on log K vs log P coordinates, converge to unity for each temperature chosen,has led to the concept of convergence pressure[35]. Thus, the convergence pressure is defined as the pressure at which K's for all components appear to converge to unity at the system temperature. The K-values are continuous to K = 1 when the equilibrium temperature happens to be the critical temperature of the system. At temperatures other than the critical, the discontinuous curves on a log K vs. log P plot, when extended, converge to unity.

Gibb's phase rule states for two phase equilibria,

$$K = f'(P,T, \text{composition of } (N-2) \text{ components}) \quad (60)$$

If we express,

$$K = f''(P,P_{cv}) \quad (61)$$

then

$$P_{cv} = f'''(T, \text{composition of } (N-2) \text{ components}) \quad (62)$$

where P_{cv} is the convergence pressure of the system. For a binary system, the convergence pressure is the critical pressure of the mixture having a critical temperature equal to the system temperature. The application of convergence pressure to multicomponent systems requires treating the multicomponent mixture as a hypothetical binary to estimate K-values. Many methods have been presented to calculate the convergence pressure[35, 57, 59, 124] and charts are available[6,36,58,71,73] to obtain the equilibrium ratios when the convergence pressure is known.

For mixtures of paraffin hydrocarbons the concept of convergence pressure yields a satisfactory parameter to account for the influence of composition on K-values. The presence of non-hydrocarbons may, however, destroy the usefulness of convergence pressure type correlations.

M. Other Solution Theories

Many complex approaches to characterize the behavior of liquid mixtures have been reported in the literature. Most of these are useful only for mixtures of simple, non-polar components at very moderate pressures. Some of these methods are listed below.

1) Theory of conformal solutions - Longuet-Higgins[64].
2) Quasi-crystalline model for solutions - Sweeny and Rose[114].
3) Cluster theory of vapor-liquid equilibria - Lu, Li, and Ting[65].

4) Theory of cells - Priggogine[86].

5) Corresponding state theory - Scott[109]; Leland and co-workers[55,56]; Pitzer et al[14,82]; Lyderson, Greenkorn, and Hougen[66].

N. Applicability of Correlations to Hydrocarbon-Non-Hydrocarbon Systems

Most of the prediction and correlation methods which have been discussed in the previous sections are limited in application to specific systems and conditions. For example, some are useful for correlation of low pressure vapor-liquid equilibria while others are limited strictly to binary systems. The presence of non-condensible, polar, and components of widely different molecular structures impairs their usefulness. For paraffin-non-hydrocarbon systems these methods have been useful only for a qualitative prediction of vapor-liquid equilibria. Very little is known about the systems of hydrogen sulphide and carbon dioxide due to the lack of experimental data.

The concept of convergence pressure has been very useful in the correlation of K-values in hydrocarbon systems. The applicability of this approach to systems of hydrogen sulphide and carbon dioxide, however, has not been assessed conclusively.

The Chao-Seader correlation is attracting much

attention at the present time, perhaps due to its simplicity and adaptability to computer programming. Furthermore, this correlation requires data only on pure components to predict multicomponent vapor-liquid equilibria. The correlation is claimed to be very general in application and has been used with components of many different molecular types. Its applicability to systems of non-hydrocarbon components such as hydrogen sulphide and carbon dioxide has not been assessed quantitatively due to the lack of data.

The Wilson equation is probably the most recent technique for the correlation and prediction of vapor-liquid equilibrium data. It has been used with great success for many systems at low pressures[20]. It requires data only on the component binaries to predict ternary and multicomponent data. There is little information available in the literature on the applicability of the Wilson equation to high pressure systems containing non-condensible components.

This investigation provides vapor-liquid equilibrium data for the methane-hydrogen sulphide-n-butane and the methane-carbon dioxide-n-butane systems. Some of the assumptions and sources of error associated with the above methods have already been discussed, but nevertheless, an appraisal of their applicability to the systems of this investigation will be useful. A comparison of the experimental data with results predicted using the above methods is presented in a later section.

III. LITERATURE REVIEW

A. Survey of Previous Experimental Work

Experimental vapor-liquid equilibrium data have been reported on few systems containing hydrogen sulphide and/or carbon dioxide. Saxena[103] has compiled references on hydrogen sulphide and carbon dioxide systems for which phase behavior data are available.

Many hydrocarbon-non-hydrocarbon binaries and some complex natural gas systems containing non-hydrocarbons have been investigated but, surprisingly, very little information is available on ternary systems. Donnelly and Katz[19] investigated the methane-carbon dioxide binary in the temperature range, -100 to 29°F and for pressures up to 1150 psia. Kurata and coworkers[16] have investigated the solid-liquid-vapor phase behavior of this system. Poettmann and Katz[83] have reported vapor-liquid equilibria in carbon dioxide-n-butane system. Their data cover the whole two phase region for this binary at room temperature and above. Olds, Reamer, Sage, and Lacey[78] have reported volumetric behavior in the carbon dioxide-n-butane system in the temperature interval 100 to 280°F and for pressures up to 1200 psia.

The phase and volumetric behavior in the methane-hydrogen sulphide system was reported by Reamer, Sage, and Lacey[90]. They studied this system at temperatures between

40 and 340°F and at pressures up to 10,000 psia. Kohn and Kurata[51] reported some discrepancies in the data of Reamer, Sage, and Lacey and extended information on this system to temperatures as low as -300°F. Sandercock[102] studied the phase behavior in the hydrogen sulphide-n-butane system at 100°F and Hughes[48] has reported data on this system in the temperature range, 125 to 275°F and pressures up to 1780 psia.

The system methane-n-butane has been studied extensively by Sage and coworkers[89,100,101] and by other workers[74,96]. The combined data of these investigators embrace the range of temperatures from -4 to 460°F and pressures from 147 to 10,000 psia. The carbon dioxide-hydrogen sulphide binary has been investigated by Bierlein and Kay[4] and other workers[54,113,115]. These data cover the range of temperatures from -50 to 207°F for pressures up to 1250 psia. The methane-carbon dioxide-n-butane system was investigated by Wang and McKetta[119], between -140 and 100°F in the pressure range of 400 to 1700 psia.

During the course of the present work, some inconsistencies, which will be discussed later, were noticed in the results of Wang and McKetta, as a result it was decided to study vapor-liquid equilibria in this system at -20, 40, and 100°F and at pressures of 400, 800 and 1200 psia.

Robinson and coworkers[97,98] have reported phase equilibria in methane-carbon dioxide-hydrogen sulphide system

at temperatures of 40, 100 and 160°F and pressures between 400 and 1600 psia. Hensel and Massoth[39] investigated the same system at -29, 68 and -59.8°F at pressures of 300, 500 and 700 psia. Clark and Din[13] studied the system carbon dioxide-ethylene-ethane at low temperatures and sub-atmospheric pressures. Saxena[103] has investigated the vapor-liquid equilibria in a quaternary natural gas system. The system contained 68 mole percent hydrogen sulphide and 9.5 mole percent carbon dioxide. The experimental data were obtained at nine temperatures between 35° and 180°F and for pressures in the range 246 to 1945 psia.

IV. EXPERIMENTAL STUDIES

A. Experimental Apparatus

Sandercock[102] has presented a detailed description of the basic experimental apparatus used in this work. Hughes[49] and Saxena[103] reported some modifications in the cell assembly. It is basically, a windowed cell of variable volume. A sectional view of the cell assembly is presented in Figure (1), and Figure (2) shows the schematic arrangement of the cell and accessories. The main aspects of this apparatus are:

a) The cell is fabricated from 316 stainless steel and has a total volume of about 600 ml. It is designed to withstand pressures up to 8000 psia at a maximum temperature of 300°F. The freezing point of mercury, the confining fluid, determines the minimum operating temperature. Type 316 stainless steel was found to suitably resist attack by hydrogen sulphide. Teflon rings and gaskets were equally resistant but neoprene rings were observed to become hard and brittle after prolonged exposure to hydrogen sulphide.

b) A positive displacement pump connected to the bottom of the cell enables the volume of the sample in the cell to be increased or decreased as desired, by withdrawal or addition of mercury to the cell.

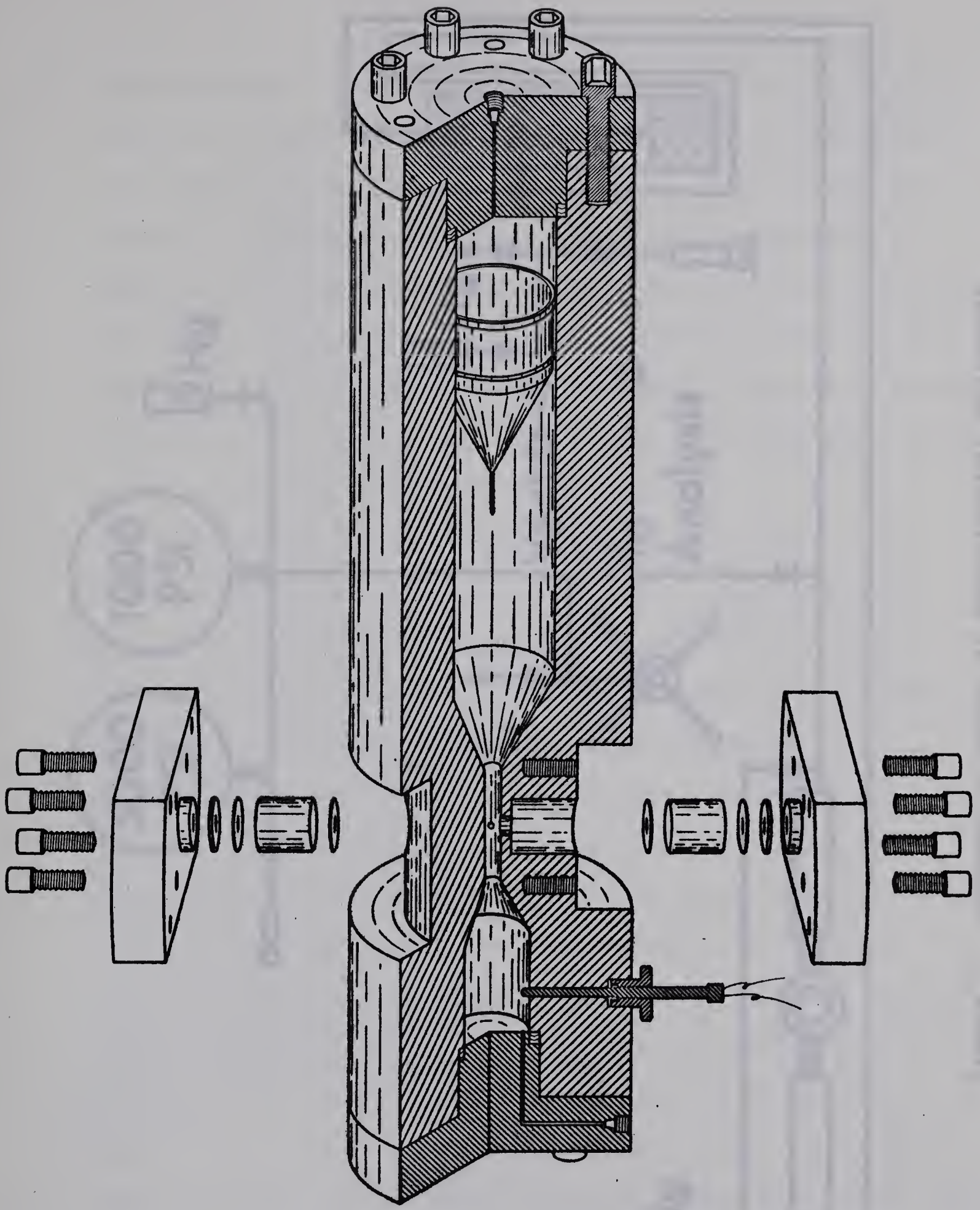

Fig. 1 Assembly View of Equilibrium Cell

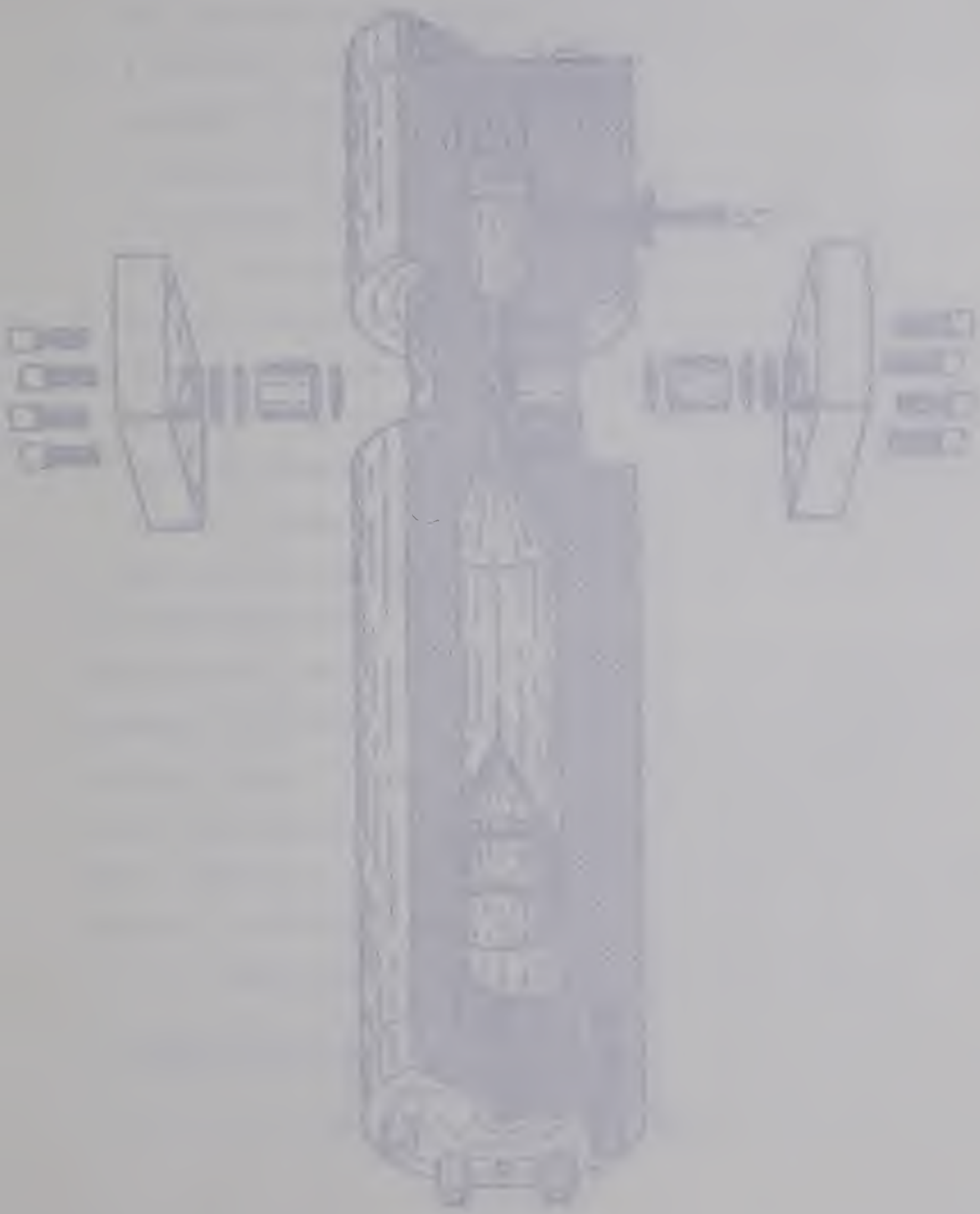

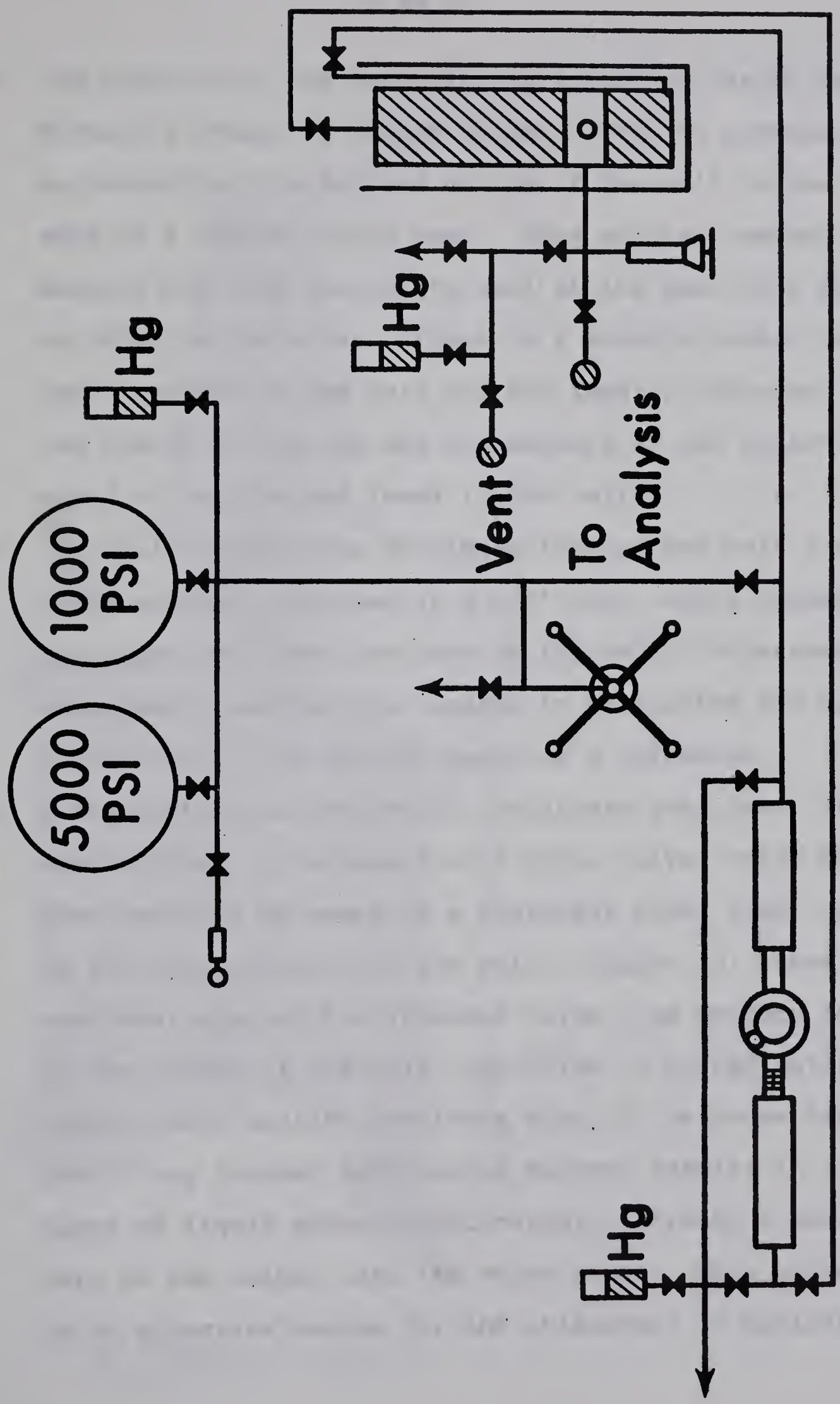

Figure 2 Schematic Layout of Experimental Equipment

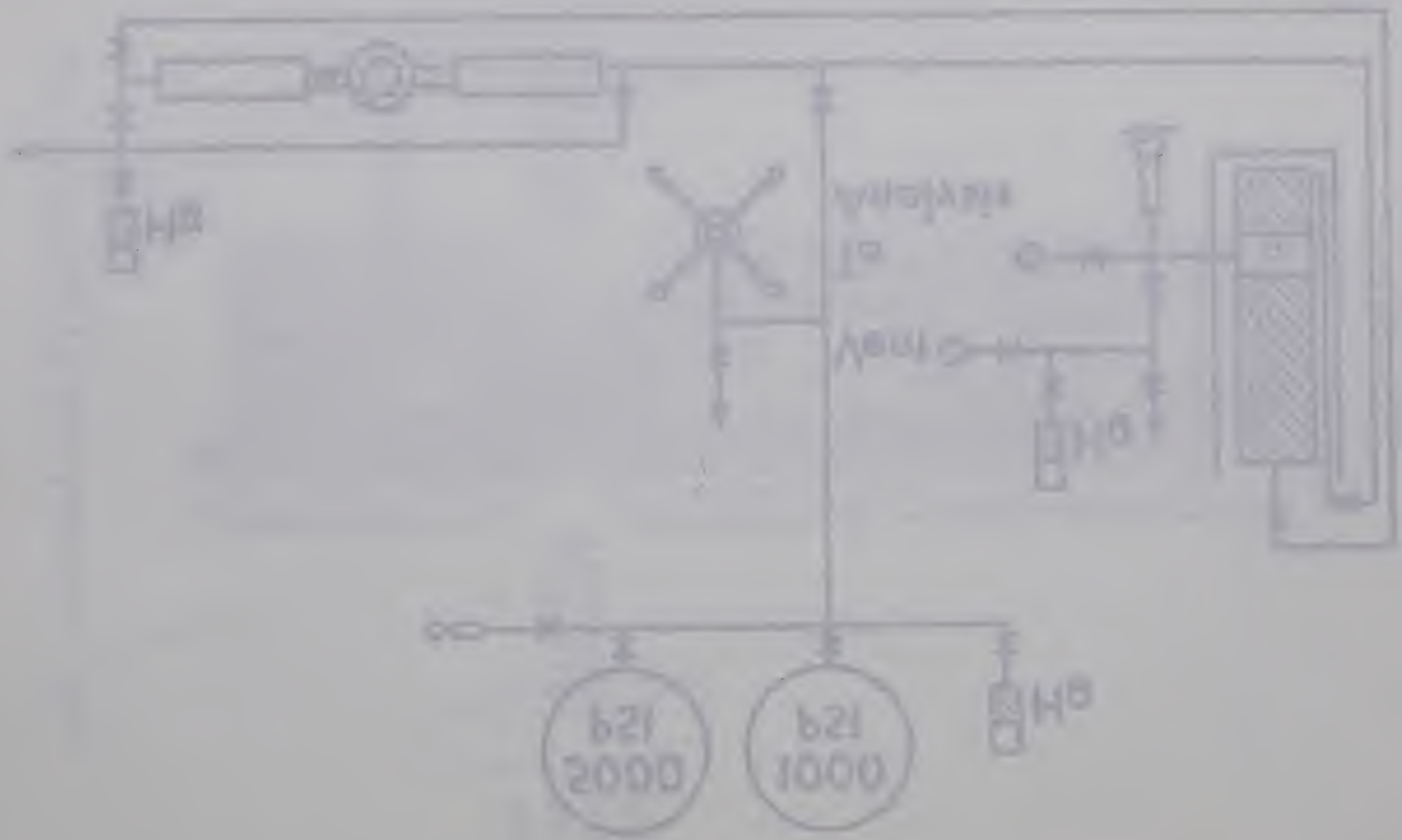
621
2000
621
1000

c) The position of the vapor-liquid interface can be changed without a change in sample volume. This is accomplished by connecting the top and bottom of the cell to the two ends of a double acting pump. This enables removal of mercury from one end of the cell at the same rate that it is added to the other. There is a movable piston in the upper section of the cell and the sample, contained between the piston at the top and the mercury at the bottom, can be moved to any desired level in the cell.

d) The cell contents can be viewed through two bull's eye glass windows, situated in a 3/8" port, which connects the upper and lower sections of the cell. A periscope arrangement enables the windows to be lighted and viewed at the top of the cell by means of a telescope.

e) A new system was devised to facilitate attainment of equilibrium. It consists of a nylon valve, which has been weighted by means of a stainless steel ring, placed in the lower section of the cell. Figure (3) shows a sectional view of the internal valve. As mercury is added to the bottom of the cell, the valve is lifted until it makes a seal against the lower edge of the connecting port. Any further addition of mercury results in a fine spray of liquid phase and/or mercury, through a small aperture in the valve, into the vapor phase. This proved to be an effective device for the attainment of equilibrium.

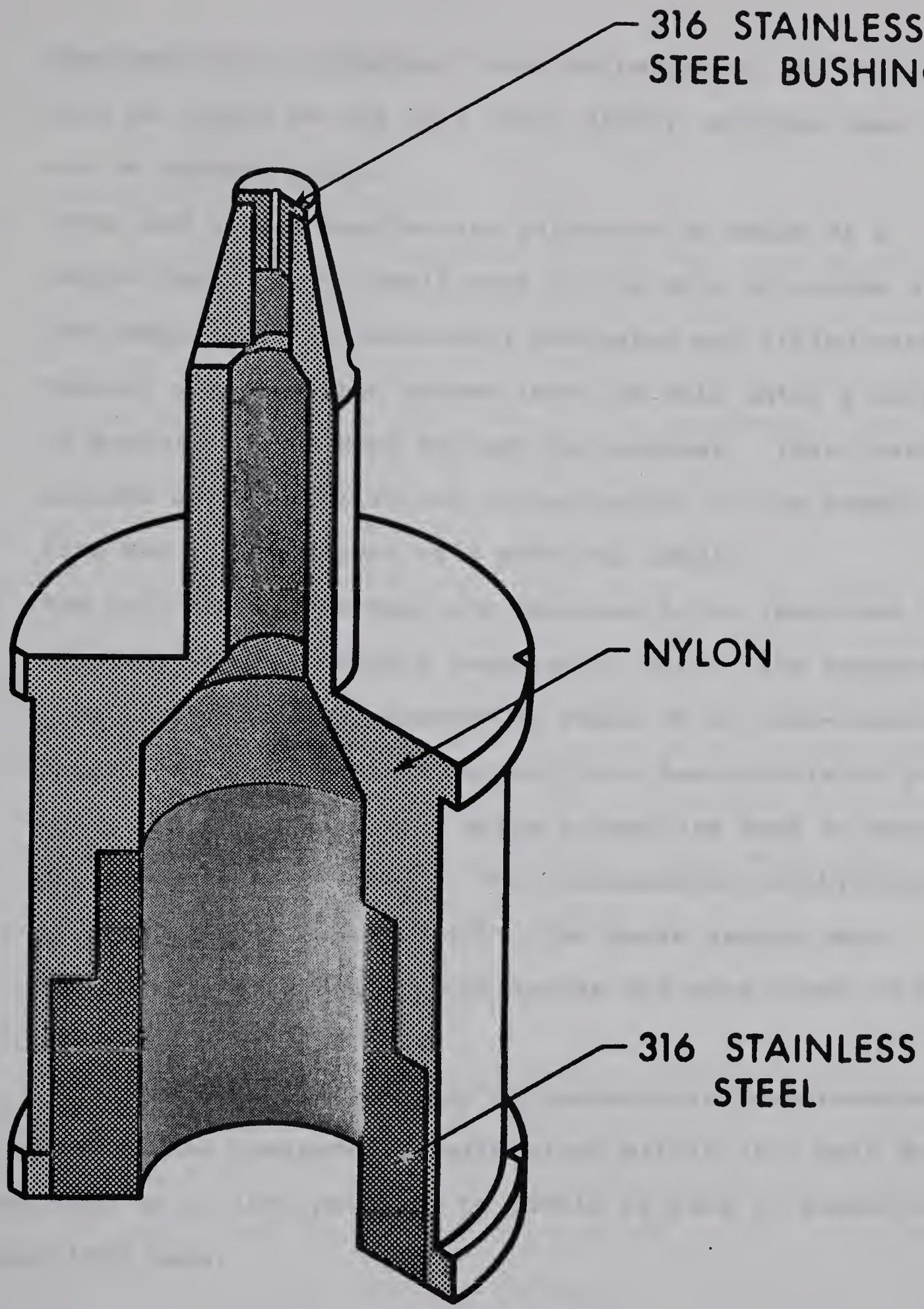

Figure 3 Sectional View of Internal Valve Used in Establishing Equilibrium

When mercury is withdrawn from the bottom of the cell, the film of liquid on the cell walls slowly trickles down and can be sprayed again.

f) Vapor and liquid samples are withdrawn by means of a sample pump, from a small port in the cell at window level. The sample pump is previously evacuated and filled with mercury which is then pushed into the cell until a drop of mercury can be seen through the windows. This insures against any possibility of contamination in the sample line due to the traces of a previous sample.

g) The cell and sample pump are immersed in an insulated ethylene glycol constant temperature bath. The temperature in the cell is measured by means of an iron-constantan thermocouple and a Leeds and Northrup semi-precision portable K-2 potentiometer. Heise gauges are used to measure the pressure in the cell. The thermocouple calibration is presented in Appendix (D). The Heise gauges were tested against a dead weight tester and were found to be accurate up to 3000 psia.

The expected accuracy of temperature measurements is $\pm 0.05^{\circ}F$; the pressure was maintained within ±0.5 psia for pressures up to 1000 psia and to within ±3 psia at pressure above 1000 psia.

B. Preparation of Mixtures

According to their vapor pressures,n-butane and the non-hydrocarbon component, in this order, were added to the cell in the desired proportions. Methane was then added. The pressure in the cell was regulated, by adding more methane or by actuating the positive displacement pump, to make sure two phases were present. The procedure was repeated starting with a different proportion of n-butane to non-hydrocarbon component. Sometimes, n-butane, contained as liquid at high pressure in a separate pump, was added directly to the existing mixture in the cell, in order to vary the overall composition. Hydrogen sulphide or carbon dioxide could be added to a cell mixture, only if the cell contents could be expanded to a pressure below the vapor pressure of hydrogen sulphide at room temperature. Venting a portion of the cell mixture was sometimes necessary to achieve this.

C. Experimental Procedures

Once two phases were present at the desired condition of pressure, temperature, and composition, all system variables were held constant and the liquid phase was sprayed into the vapor phase once every ten minutes, until any further spraying did not change the cell pressure. Equilibrium was then assumed to have been reached and the cell contents were allowed to stand for an hour for adequate separation of phases

before any sampling of phases was done. The temperature and pressure of equilibrium were simultaneously recorded.

D. Analysis

The phase desired to be sampled was brought in contact with the sample port, under visual observation. The desired amount of sample, about 0.5 ml for vapor and 0.1 ml for liquid, was then withdrawn from the cell. After the liquid phase had been withdrawn, the mercury level was raised to cover the sample port and about 0.5 ml of mercury was withdrawn to flush traces of liquid in the sample line. No mercury was withdrawn after vapor samples for fear of contamination with liquid. Mercury was added to the cell bottom during sampling to keep the cell pressure constant. After a sample had been withdrawn, including followup mercury for liquid samples, the cell was isolated from the sample pump. The sample was then vaporized in the sample pump and later in a glass gas-burette, to a few inches of mercury above atmospheric pressure, for analysis.

A Burrell K-2 gas chromatograph was used for analysis. A two-meter hairpin type glass column packed with 30% ansul ether on fire brick was used. Helium was the carrier gas and a thermal conductivity detector was employed. The chromatograph variables were maintained at the following values:

Column	:	20% ansul ether on firebrick
Column size	:	2 meters
Carrier gas	:	Helium at 78.5 ml/min.
Detector current	:	200 mA
Column temperature	:	100^{o}F
Sample size	:	1.85 ml

Separation of components in the column was excellent; and sharp, well-defined peaks were obtained for all components. A calibration based on peak heights was found to be satisfactory. Seven samplers of different sizes were used to obtain peak height vs. sample volume charts. These are presented in Appendix (D). Several mixtures of known composition containing components of both the ternary systems of this work were made in a gas-burette. Known volume of sample of these mixtures was analyzed on the chromatograph. Knowing peak heights for each component thus obtained, the composition of the mixtures was calculated using the calibration curves presented in Figure (34) and compared with the actual composition. The components in the methane-hydrogen sulphide-n-butane system showed very slight interaction. Figure (35) presents corrections required in the calculated value of composition for this system. Methane, carbon dioxide, and n-butane did not exhibit appreciable interaction and no correction in the calculated composition was necessary for this system. In both systems, after correction in the hydrogen sulphide system, the mole

fraction of every component could be determined to within 1% of its actual value.

E. Materials

Mercury was used as displacement fluid. Since the combination of mercury and hydrogen sulphide in the presence of even traces of moisture causes almost instantaneous blackening of mercury due to formation of mercuric sulphide, triple distilled mercury was used. The procedure employed for purification and distillation of mercury has been reported previously[102]. All gases were dried before introducing them into the cell.

Matheson of Canada supplied methane of purity between 99.3 and 99.65%, as indicated by a chromatographic analysis. The instrument grade n-butane and C.P. hydrogen sulphide, also supplied by Matheson of Canada, had a minimum purity of 99.5%. Carbon dioxide supplied by Canadian Liquid Air Company was specified to have a minimum purity of 99.95%.

V. RESULTS AND DISCUSSION

A. Experimental Apparatus

The internal valve, used to spray liquid phase and mercury into the vapor phase, was found to work very efficiently. Equilibrium conditions were readily attained, even when the amount of liquid present was small. In spite of being subjected to heavy duty for a period of more than a year, the nylon part still makes a good seal with the sharp edges of the channel and a very adequate spray is obtained.

The vertical sample pump which was incorporated approximately three years ago[103] is functioning well. High pressure samples of both phases of the required size can be obtained without any contamination.

B. Experimental Results

a) Binary Systems

Data on all component binaries were available in the literature. For further assurance, it was decided to obtain vapor-liquid equilibrium data on all binaries of interest as well. The agreement with all previous authors was excellent with the exception of methane-n-butane system, reported by Wang and McKetta[119], at -20° and 40°F for pressures of 400, 800 and 1200 psia.

According to the results of Wang and McKetta the binary system methane-carbon dioxide does not exist in two

phases at -20°F and 400 and 800 psia, and at 40°F at 800 and 1200 psia. The data of Donnelly and Katz[19] show, on the other hand, that this system does separate into equilibrium liquid and vapor phases at the above conditions of pressure and temperature. To resolve this disagreement, vapor-liquid equilibria in the methane-carbon dioxide system were studied at temperatures of -20°, 40°, and 100°F and at pressures, 400, 800, and 1200 psia. Excellent agreement with the results of Donnelly and Katz was obtained and it was concluded, therefore, that the data of Wang and McKetta are in error.

b) Ternary Systems

1) The Methane-Hydrogen Sulphide-n-Butane System

Raw and smoothed experimental data respectively are presented in Tables (1) and (2). Graphical interpolation was used to obtain the data of Table (2), which presents composition of equilibrium phases at equal increments of mole fraction of H_2S in the liquid phase.

Experimental vapor-liquid equilibrium data at constant pressure and temperature are plotted on conventional triangular diagrams, showing compositions,in mole fractions, of equilibrium vapor and liquid phases. Figure (4), (5) and (6) present data on this system at 100°F and at pressures of 400, 800, and 1200 psia respectively. Experimental data at 40°F and pressures of 400, 800, and 1200 psia respectively are presented in Figures (7), (8), and (9). Figures (10), (11),

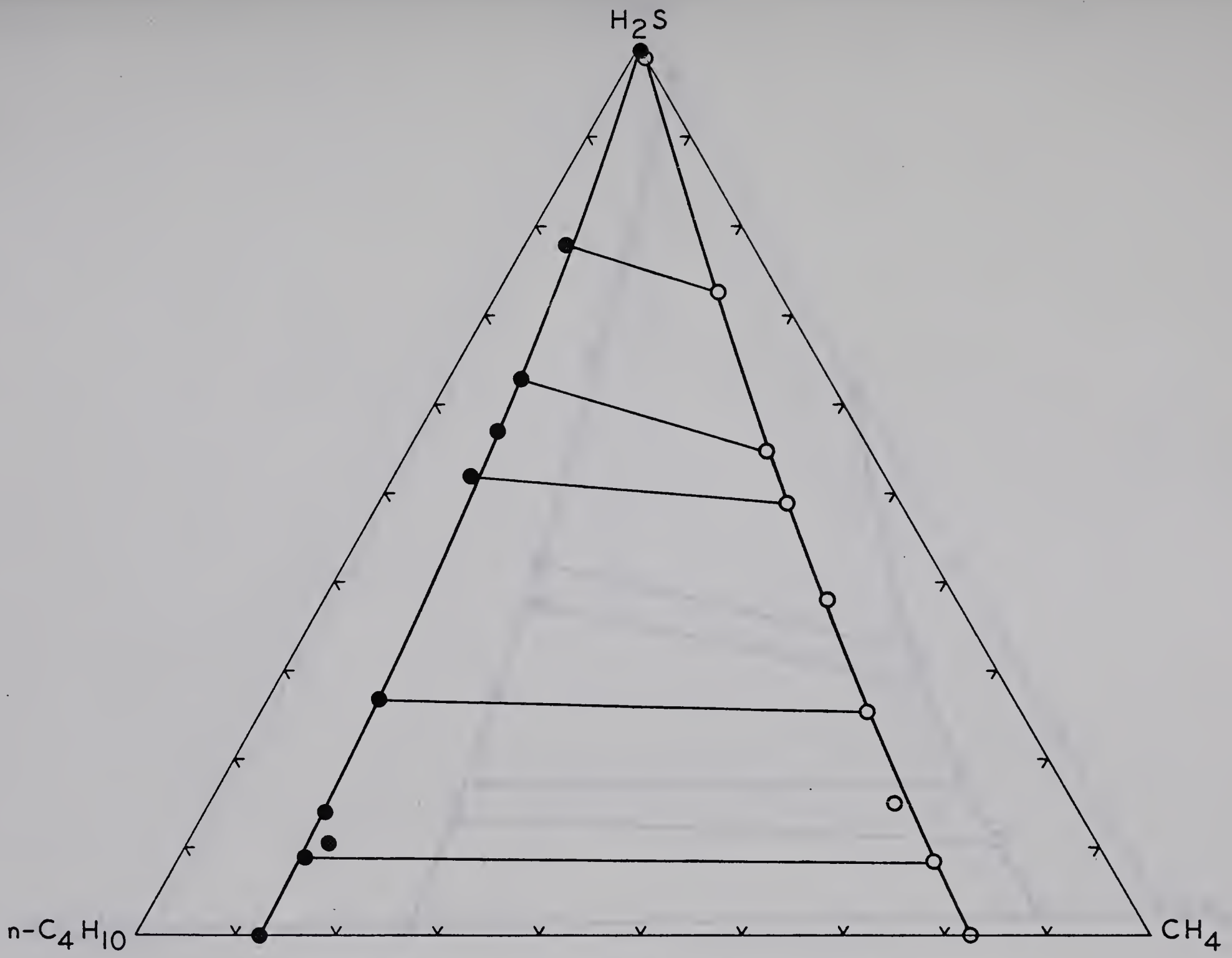

FIG. 4 Vapour-Liquid Equilibrium Data at 400 psia and 100°F for the Methane-Hydrogen Sulfide-n-Butane System

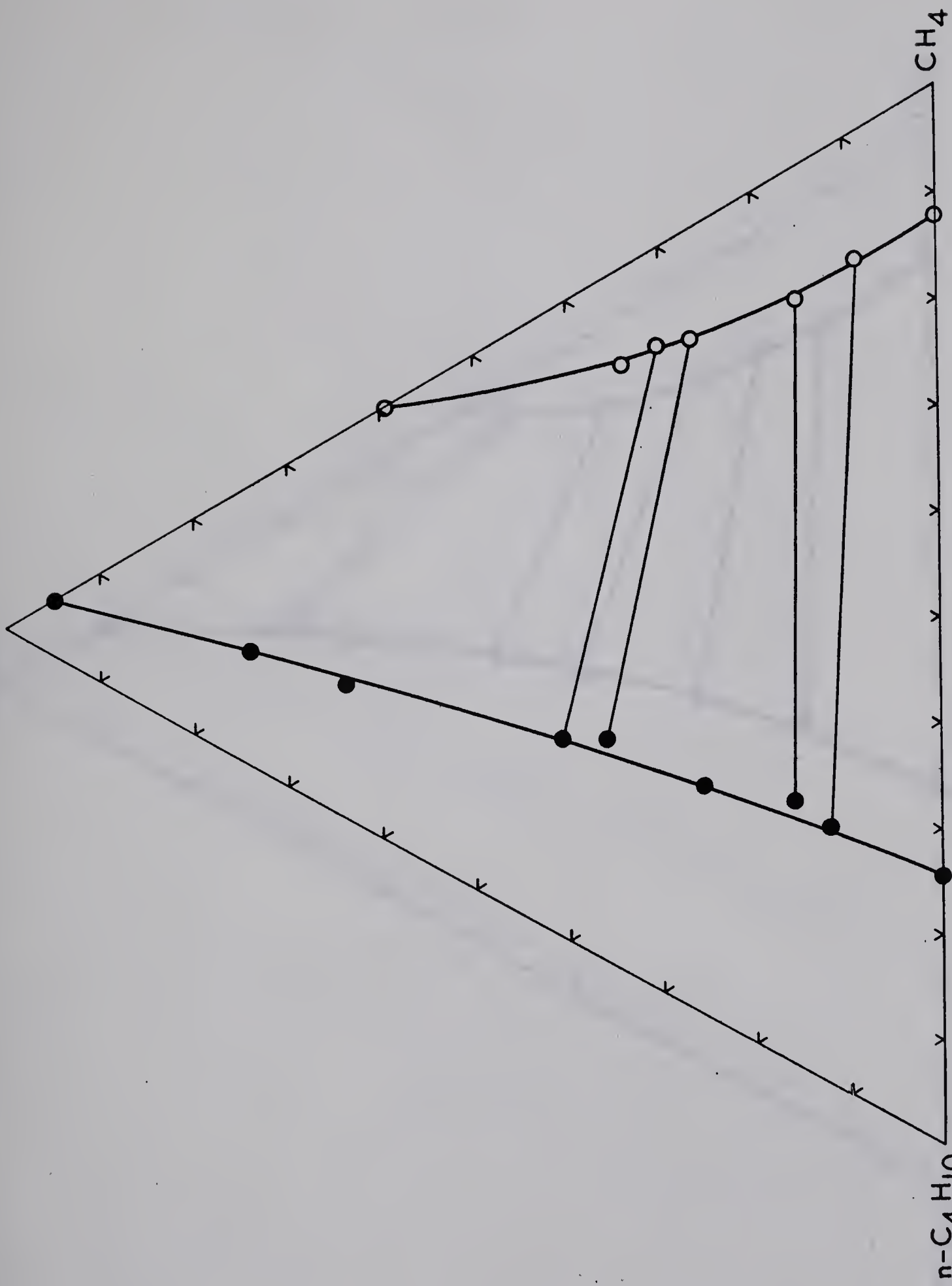

FIG. 5 Vapour-Liquid Equilibrium Data at 800 psia and 100°F for the Methane-Hydrogen Sulfide-n-Butane System

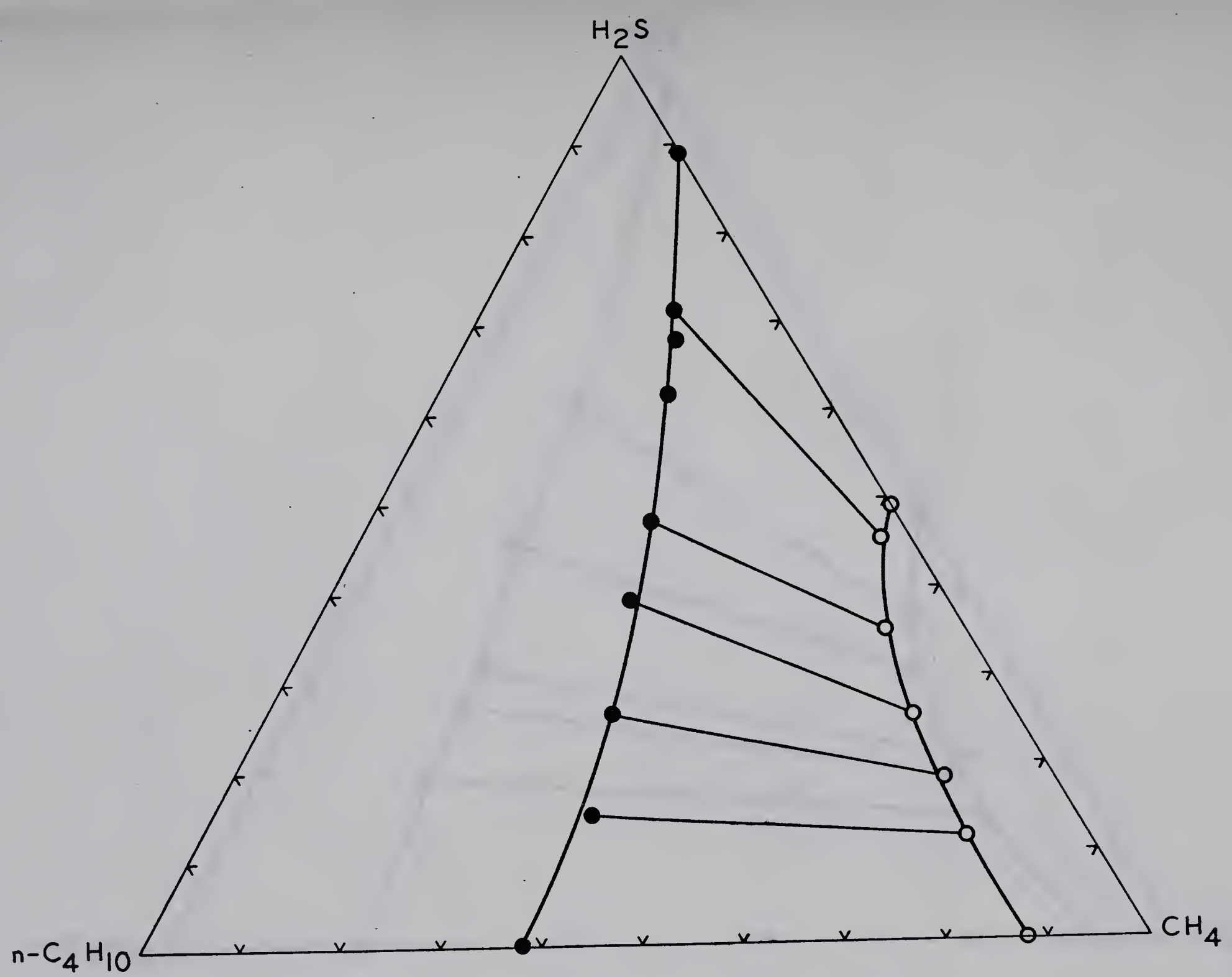

FIG. 6 Vapour-Liquid Equilibrium Data at 1200 psia and 100°F for the Methane-Hydrogen Sulfide-n-Butane System

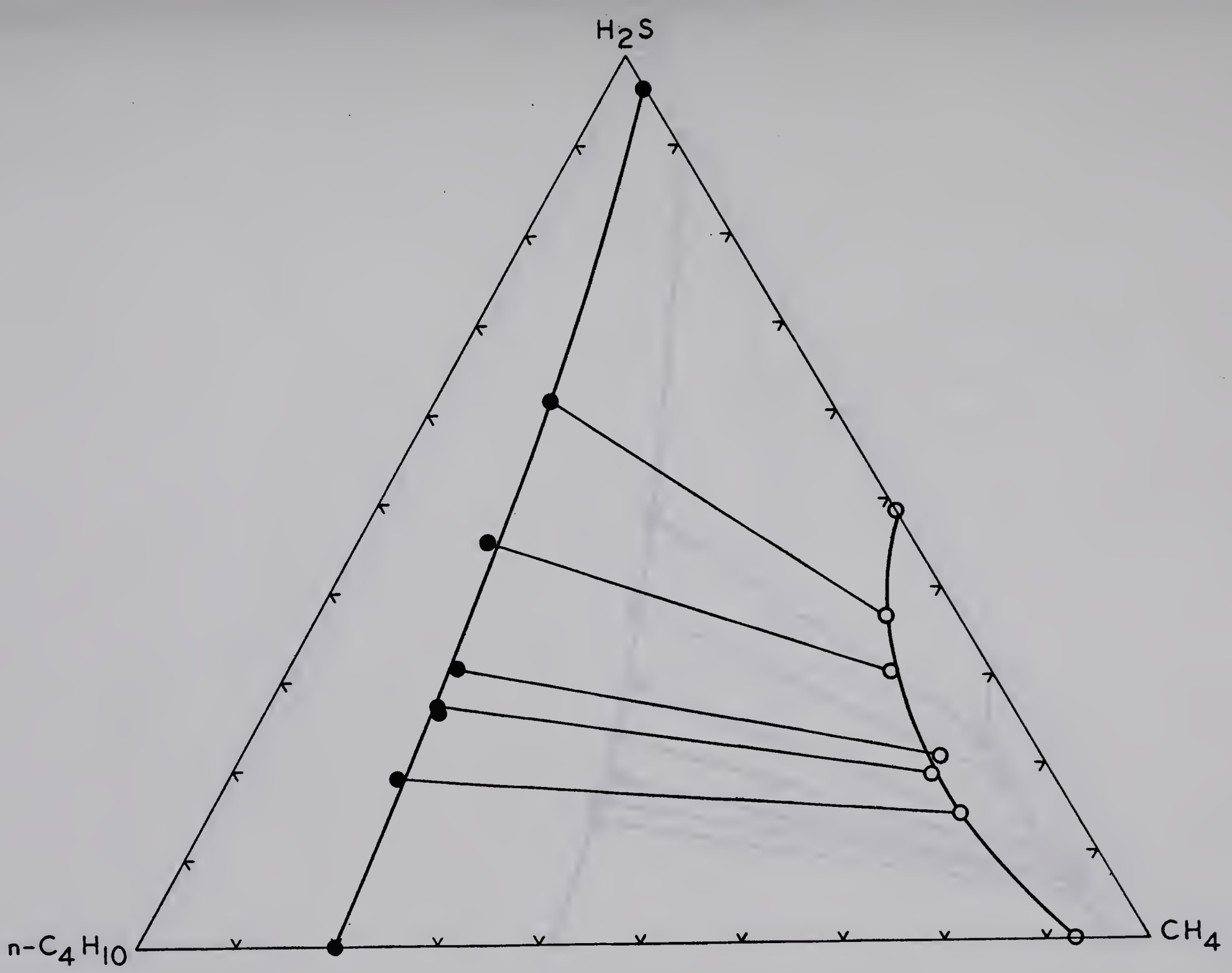

FIG. 7 Vapour-Liquid Equilibrium Data at 400 psia and 40°F for the Methane-Hydrogen Sulfide-n-Butane System

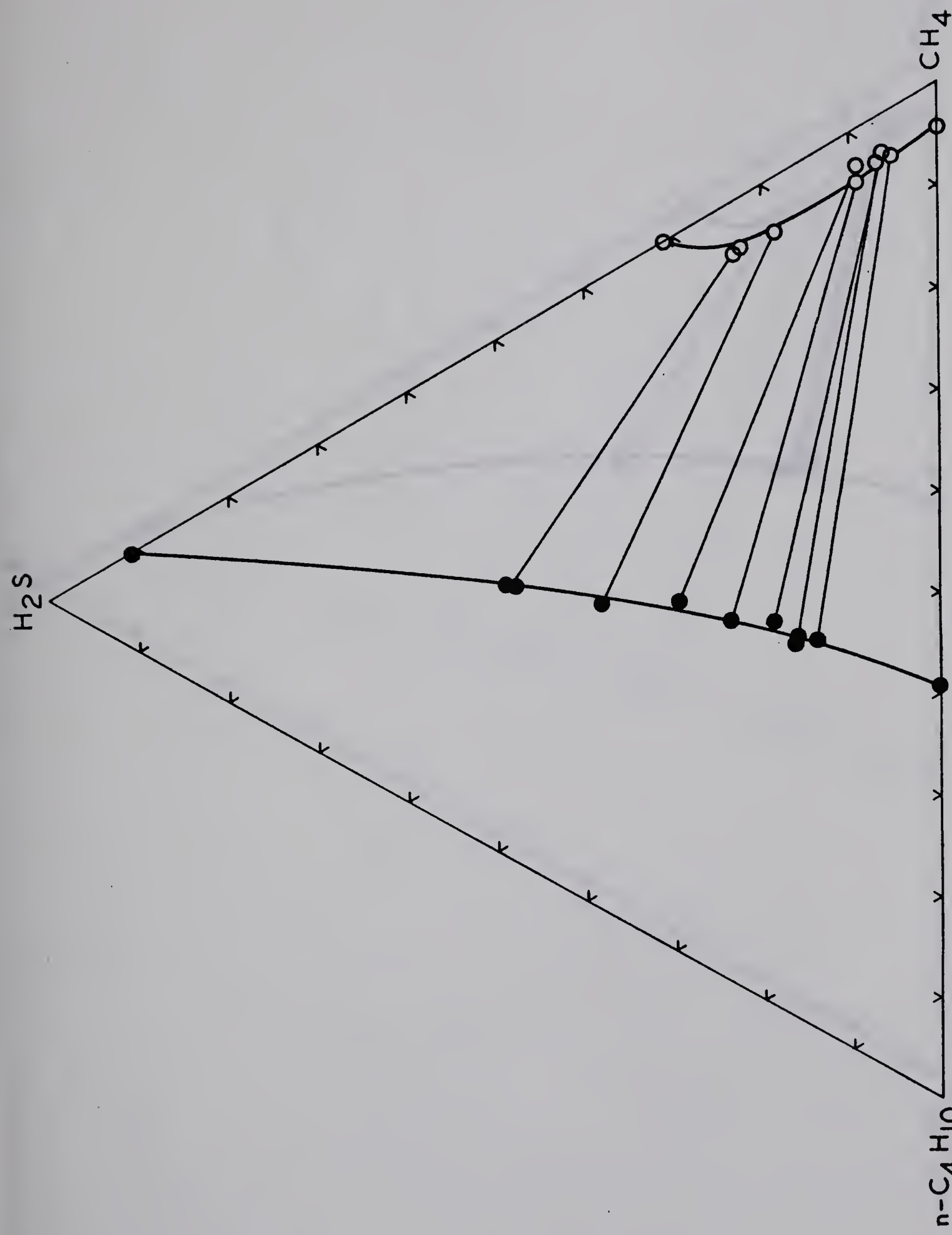

FIG. 8 Vapour-Liquid Equilibrium Data at 800 psia and 40°F for the Methane-Hydrogen Sulfide-n-Butane System

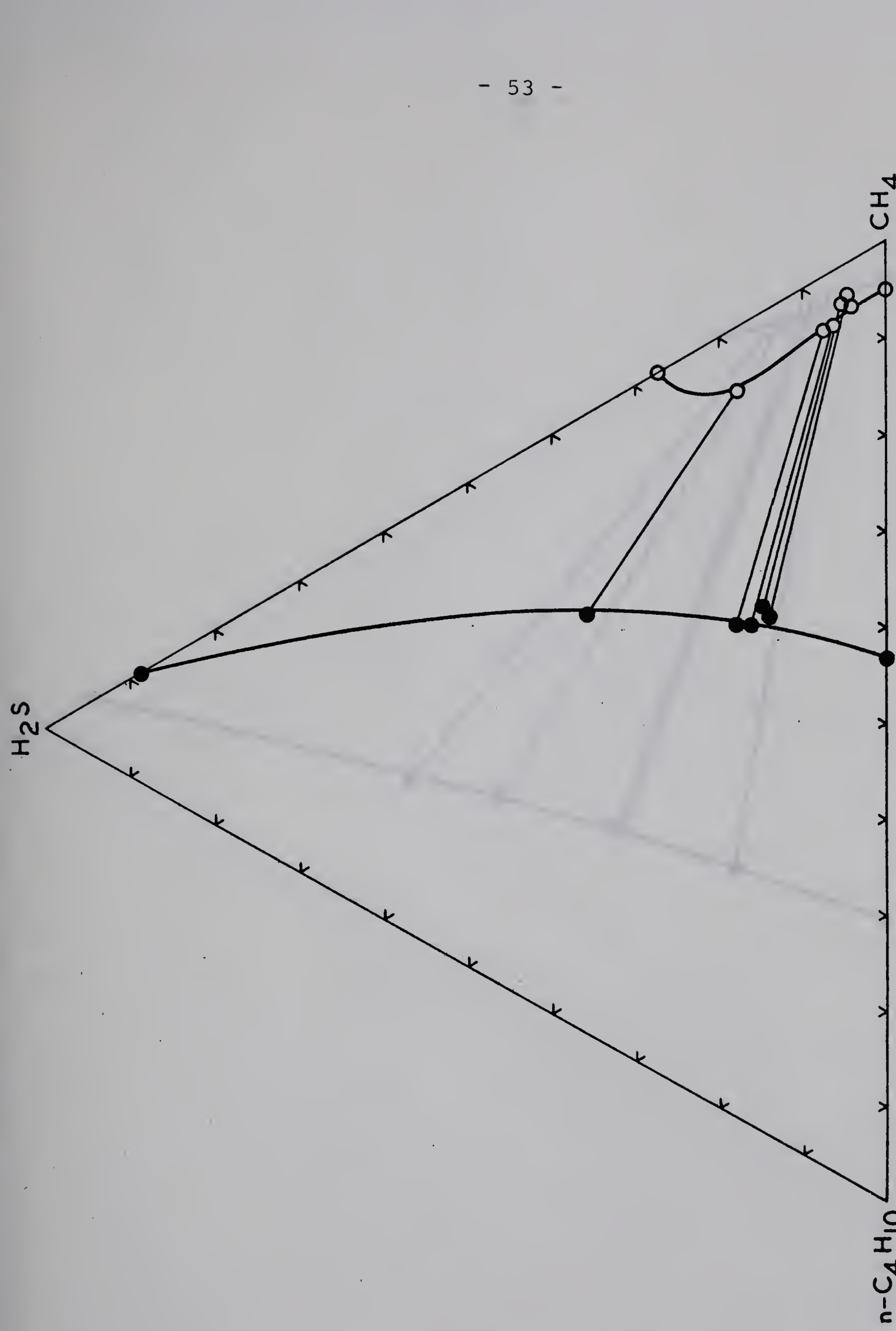

FIG. 9 Vapour-Liquid Equilibrium Data at 1200 psia and 40°F for the Methane-Hydrogen Sulfide-n-Butane System

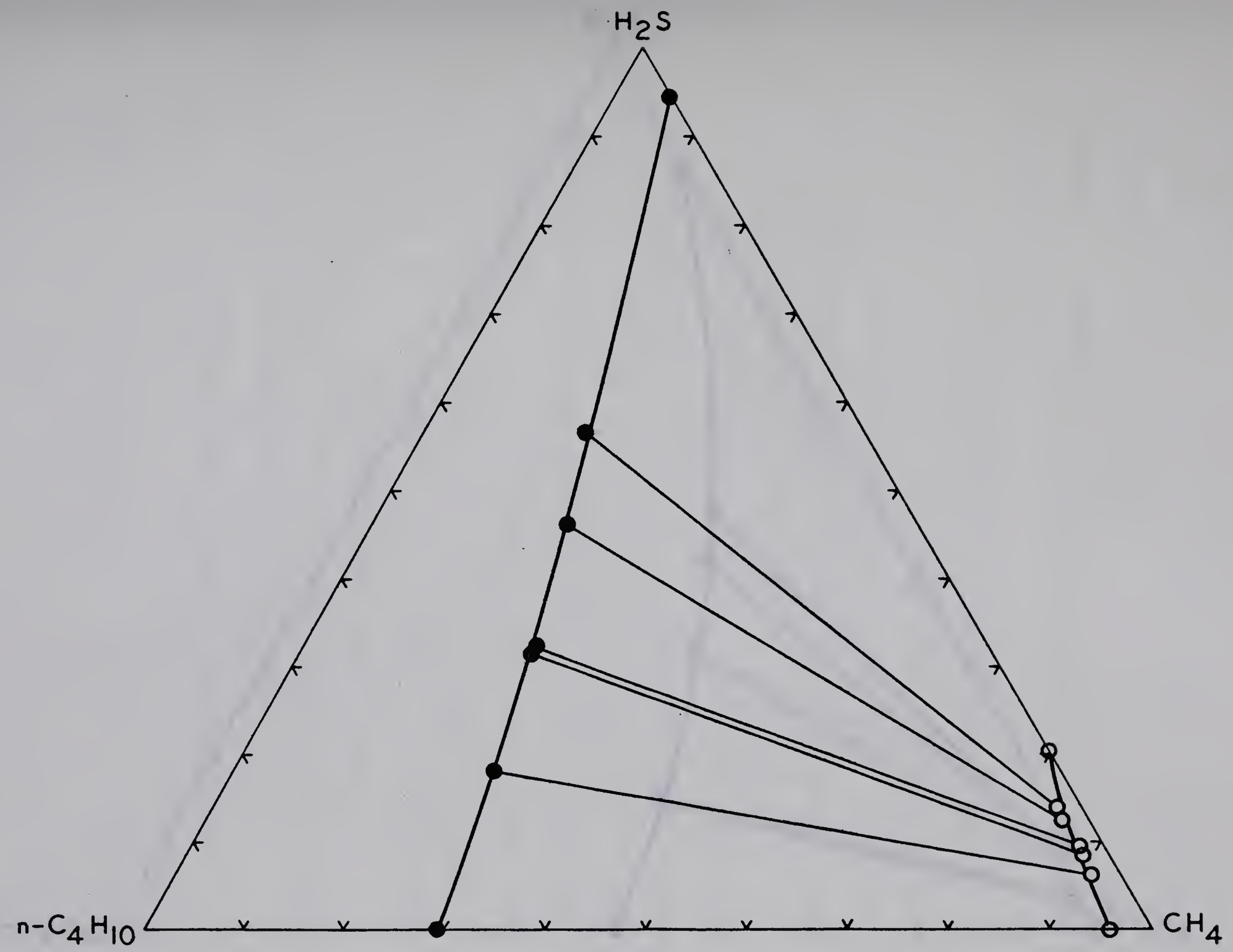

FIG. 10 Vapour-Liquid Equilibrium Data at 400 psia and -20°F for the Methane-Hydrogen Sulfide-n-Butane System

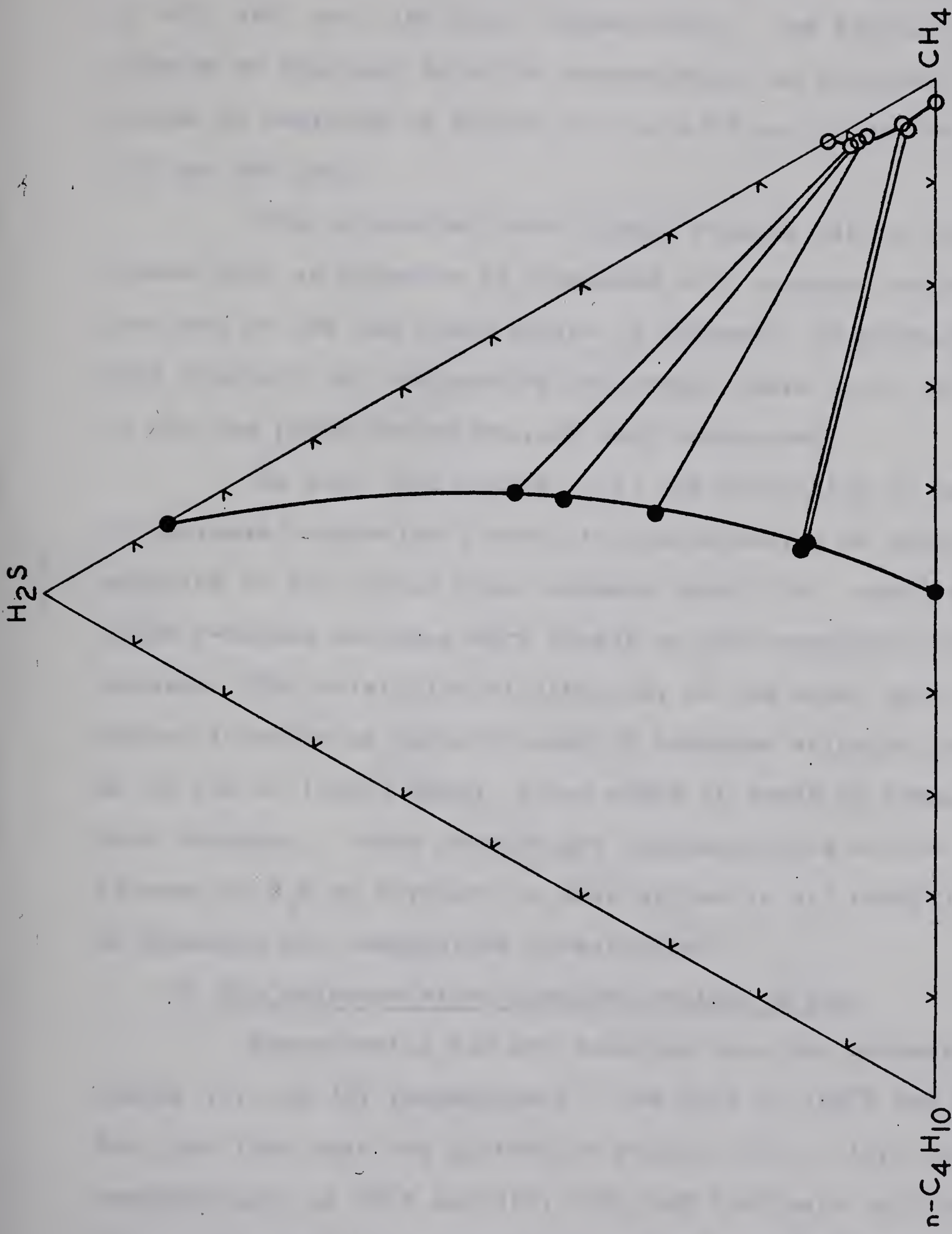

FIG. 11 Vapour-Liquid Equilibrium Data at 800 psia and -20°F for the Methane-Hydrogen Sulfide-n-Butane System

and (12) are plots of experimental data at -20°F and pressures of 400, 800, and 1200 psia, respectively. The typical influence of hydrogen sulphide concentration on K-values in this system is depicted in Figure (13) at 40°F and at pressures, 400 and 800 psia.

The triangular P-T-C plots, Figures (4) to (12), indicate that as pressure is increased at a constant temperature, the area of the two phase region is reduced. If pressure is kept constant and temperature increased, there is an increase in the two phase region but,not very pronounced.

As seen from Figure (13), the volatility of methane is increased appreciably when the concentration of hydrogen sulphide in the liquid phase exceeds about 50%. Hydrogen sulphide K-values decrease very slowly as its concentration increases. The volatility of n-butane, on the other hand, shows marked increase as concentration of hydrogen sulphide increases up to 50% in liquid phase, after which it tends to remain almost constant. These results are representative of the influence of H_2S on K-values in this system at all conditions of pressure and temperature investigated.

2) The Methane-Carbon Dioxide-n-Butane System

Experimental raw and smoothed data are presented in Tables (3) and (4) respectively. The data at 100°F and 400, 800, and 1200 psia are plotted in Figures (14), (15), and (16) respectively; at 40°F and 400, 800, and 1200 psia in Figures (17), (18), and (19) respectively; and at -20°F and 400, 800,

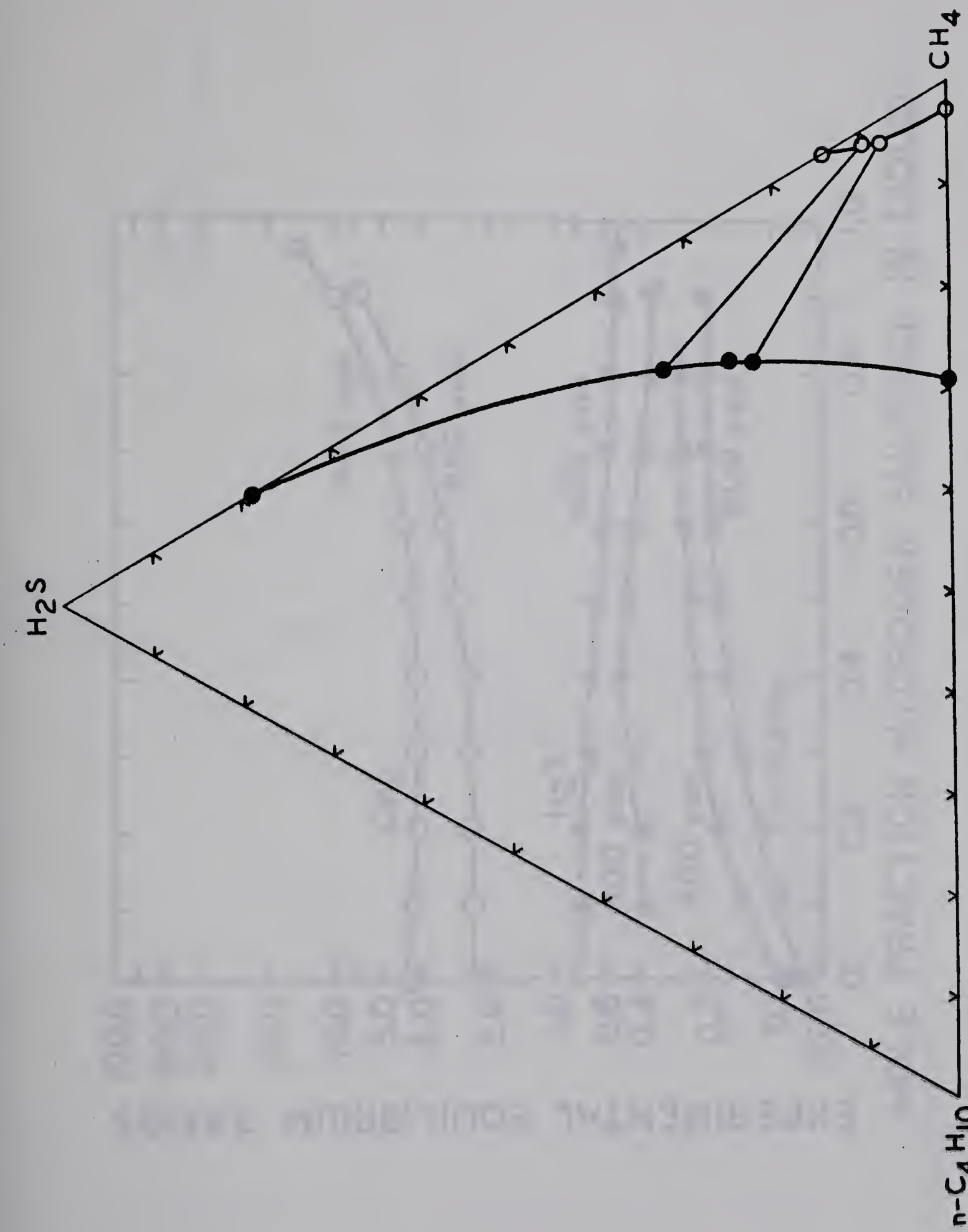

FIG. 12 Vapour-Liquid Equilibrium Data at 1400 psia and -20°F for the Methane-Hydrogen Sulfide-n-Butane System

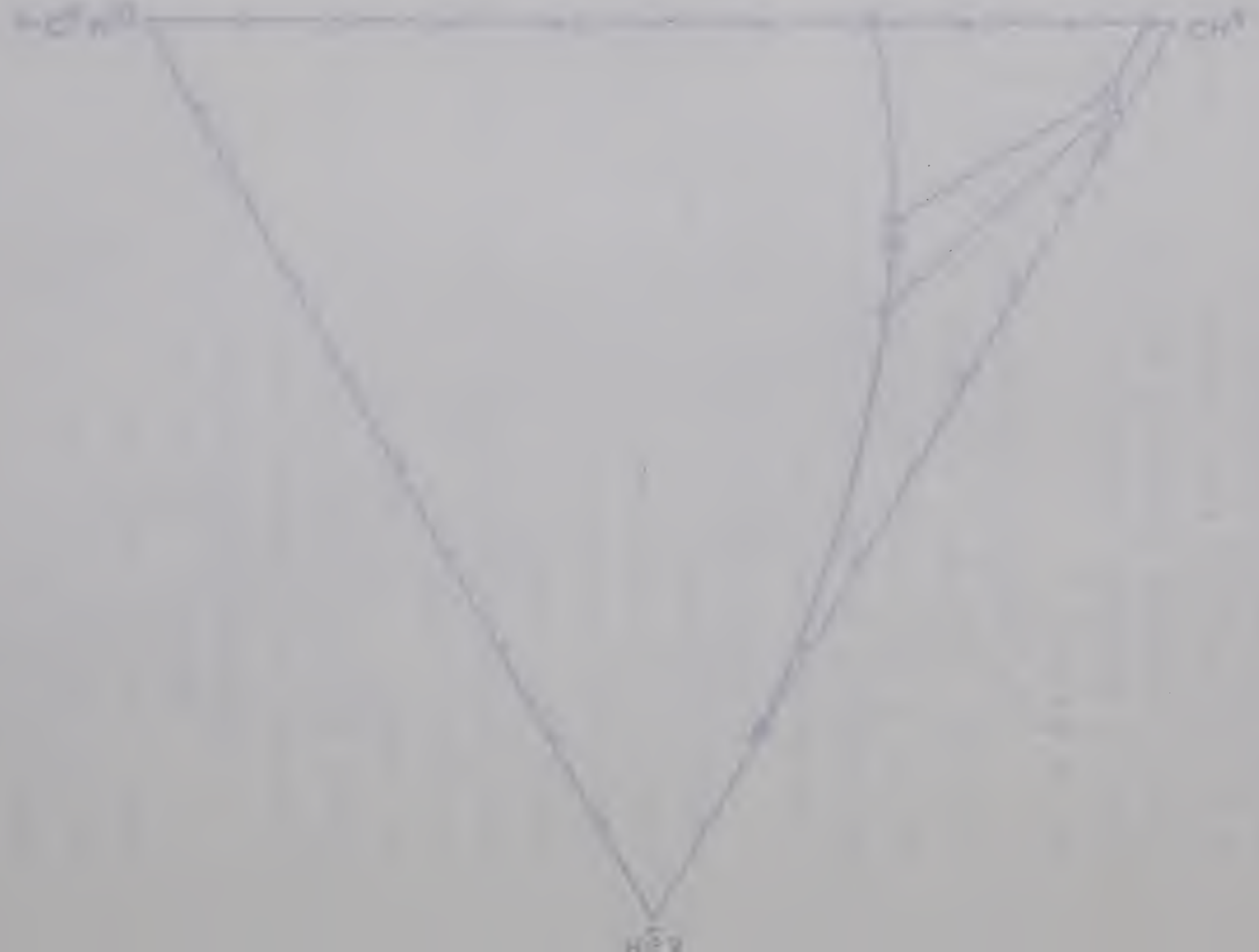

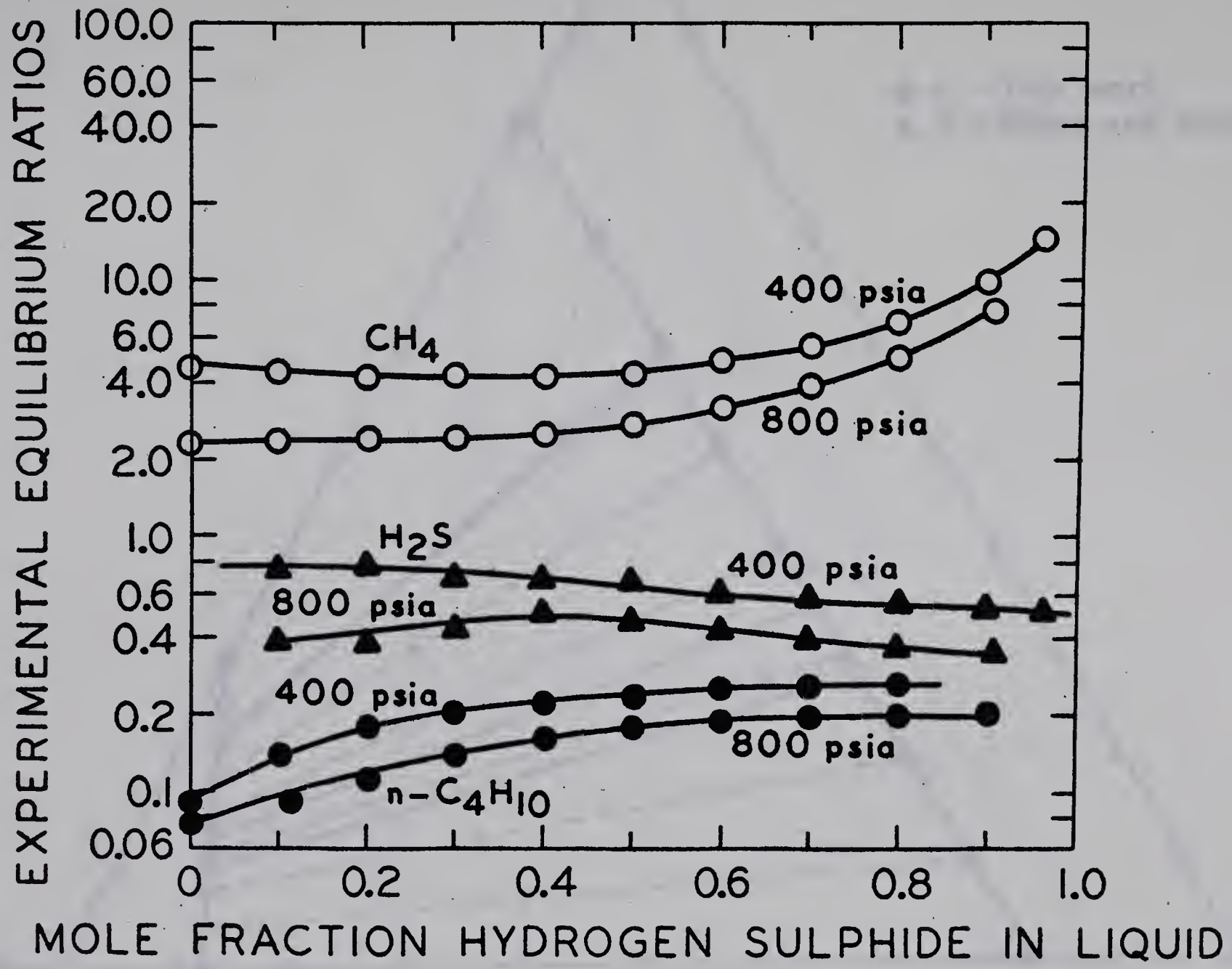

FIG. 13 Influence of Hydrogen Sulfide Concentration on K-factors in the Methane-Hydrogen Sulfide-n-Butane System at 40°F

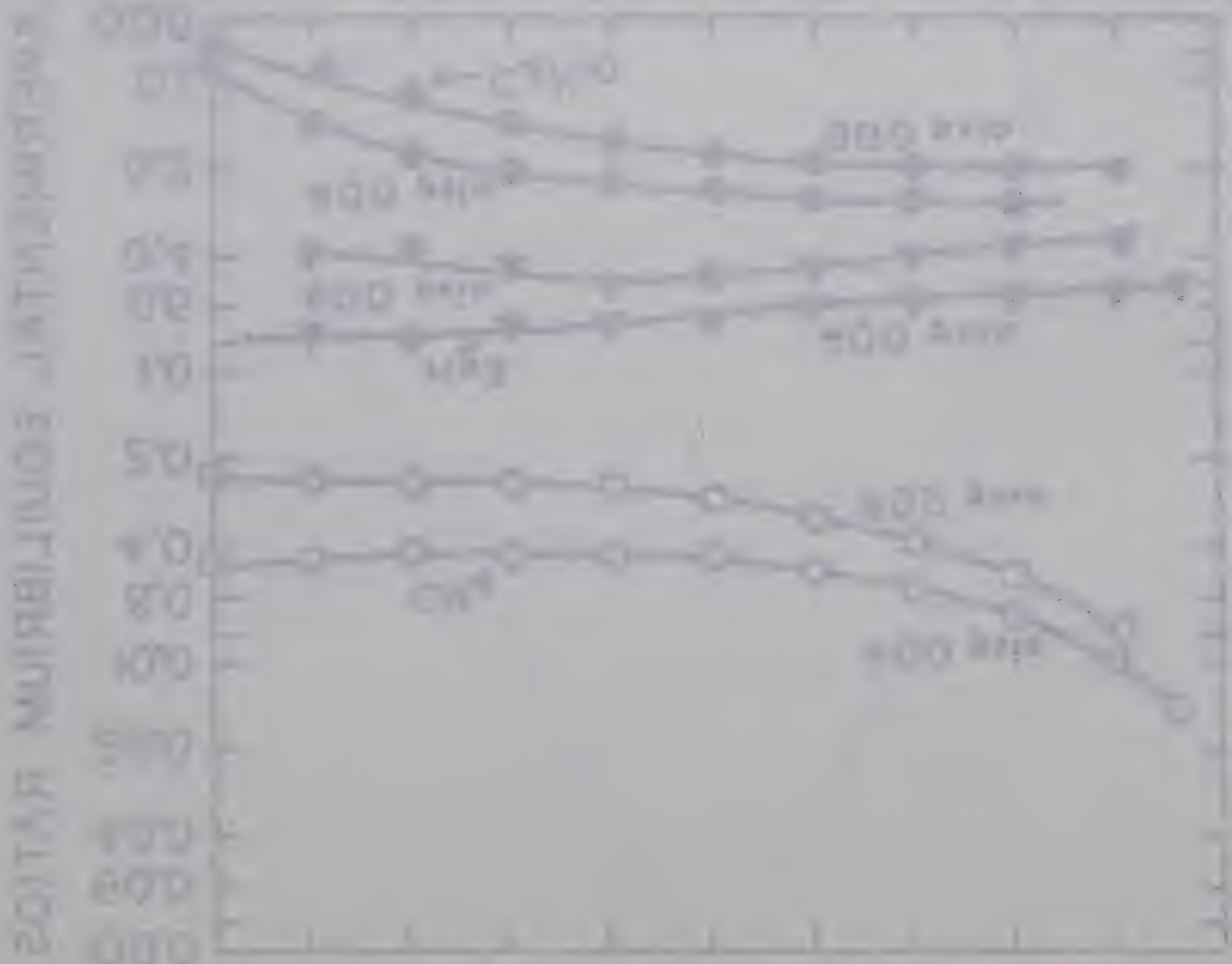

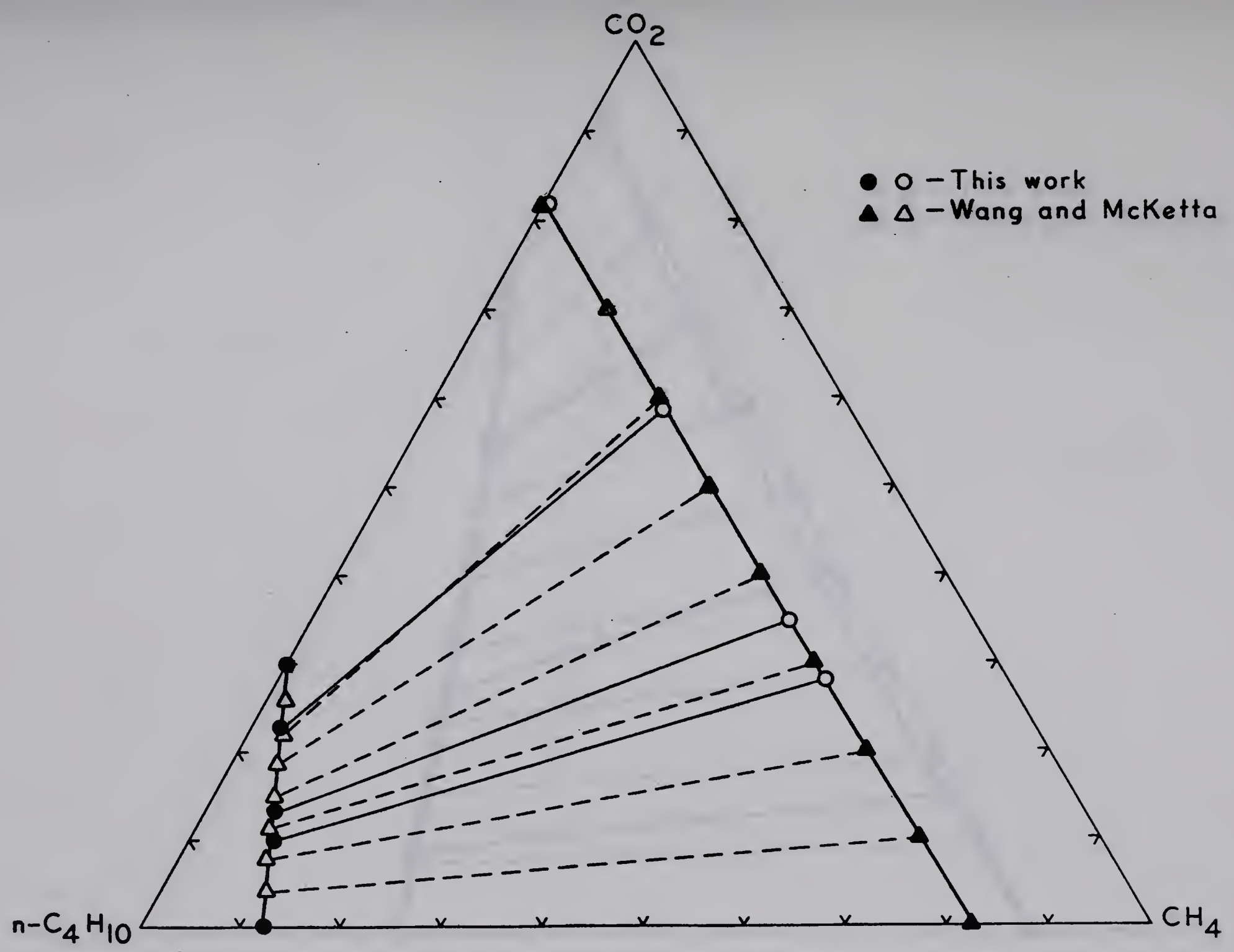

FIG. 14 Vapour-Liquid Equilibrium Data at 400 psia and 100°F for the Methane-Carbon Dioxide-n-Butane System

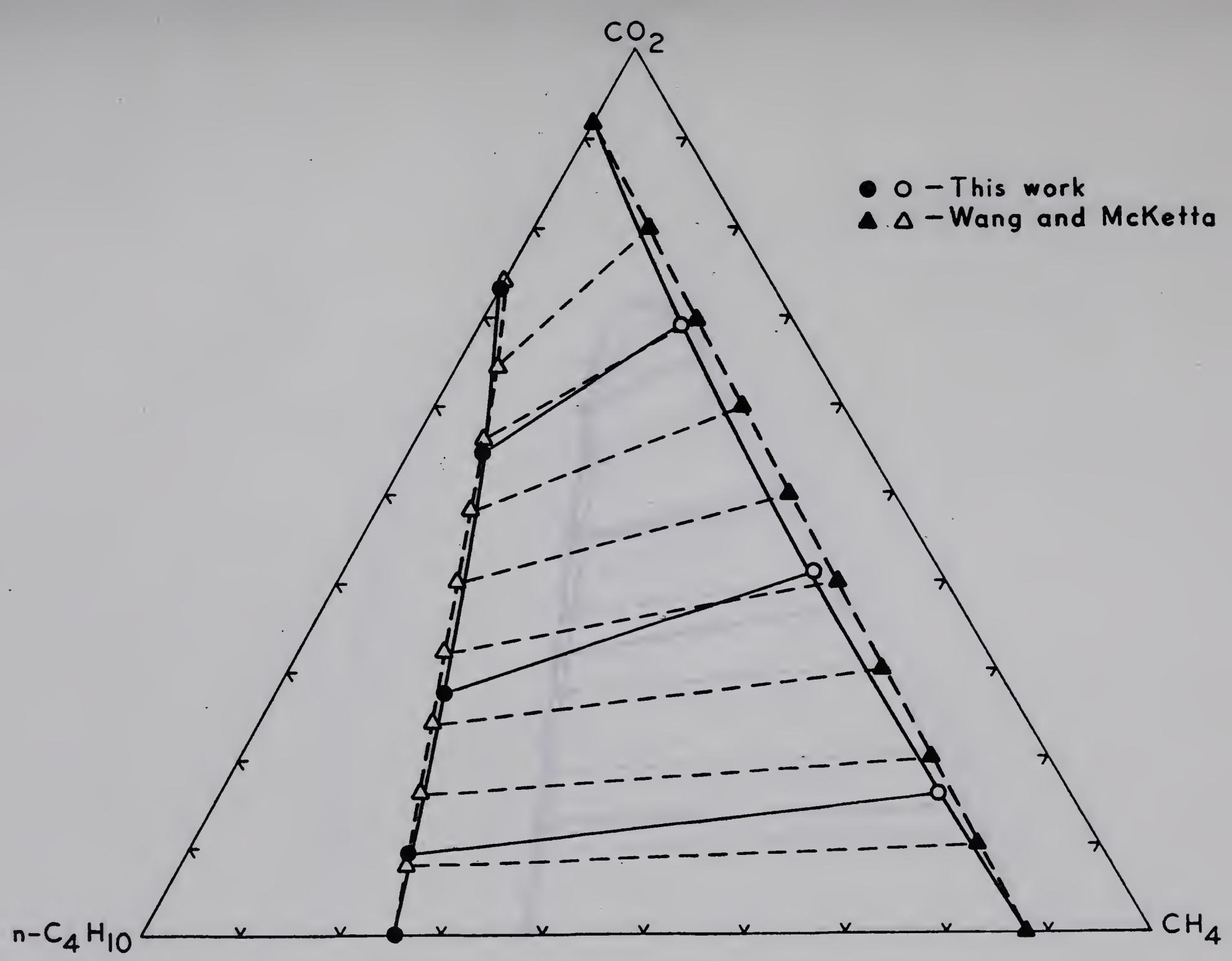

FIG. 15 Vapour-Liquid Equilibrium Data at 800 psia and 100°F for the Methane-Carbon Dioxide-n-Butane System

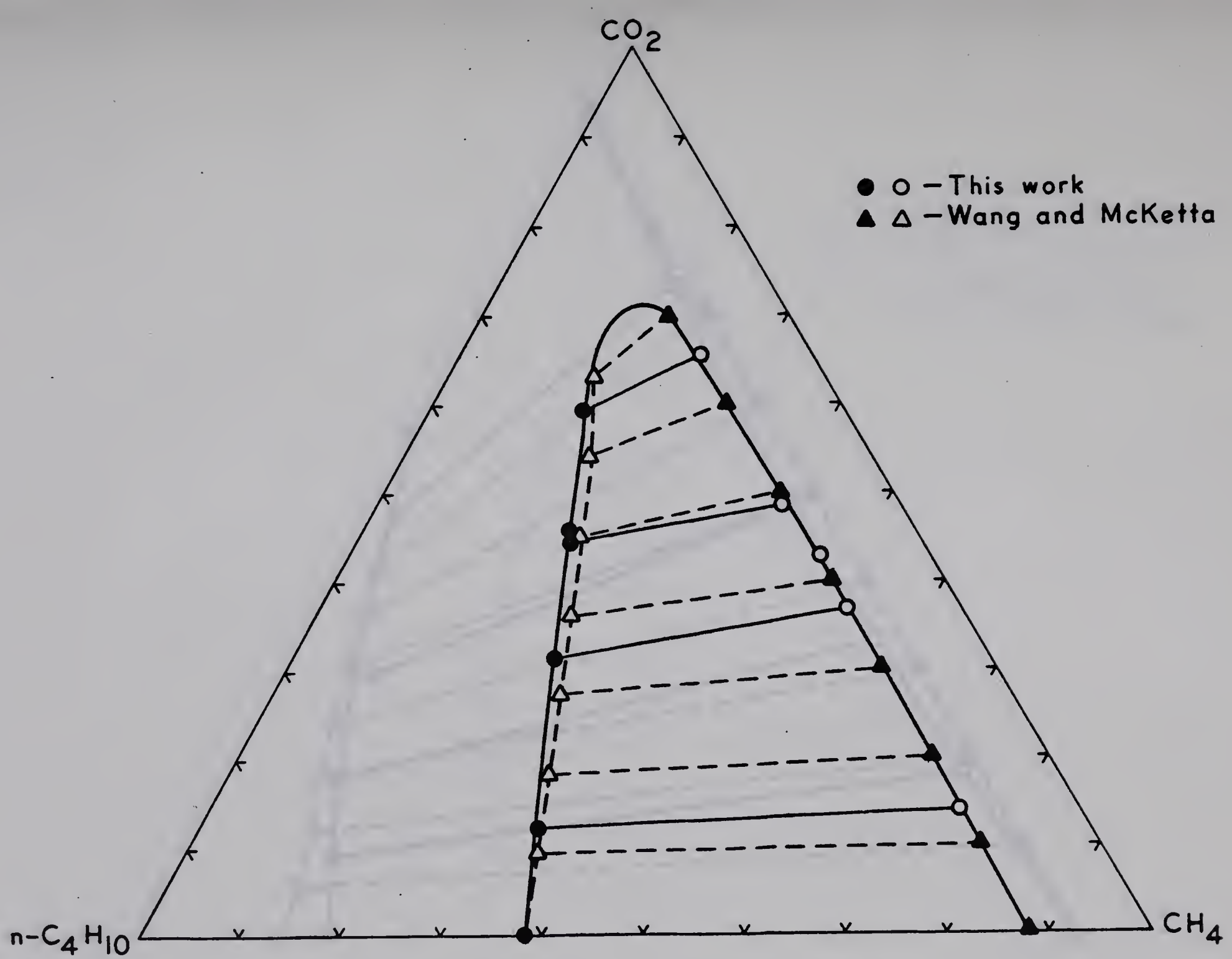

FIG. 16 Vapour-Liquid Equilibrium Data at 1200 psia and 100°F for the Methane-Carbon Dioxide-n-Butane System

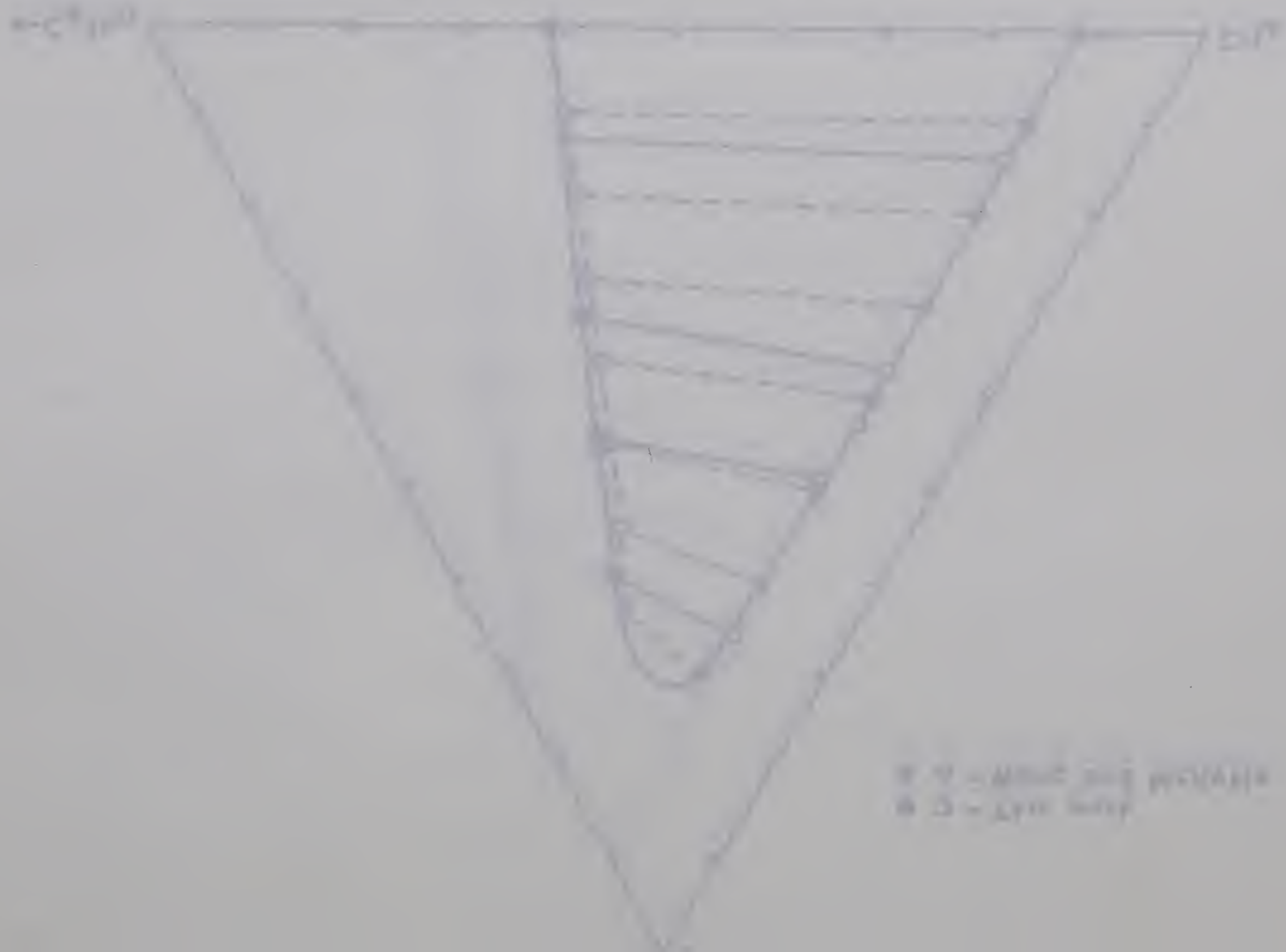

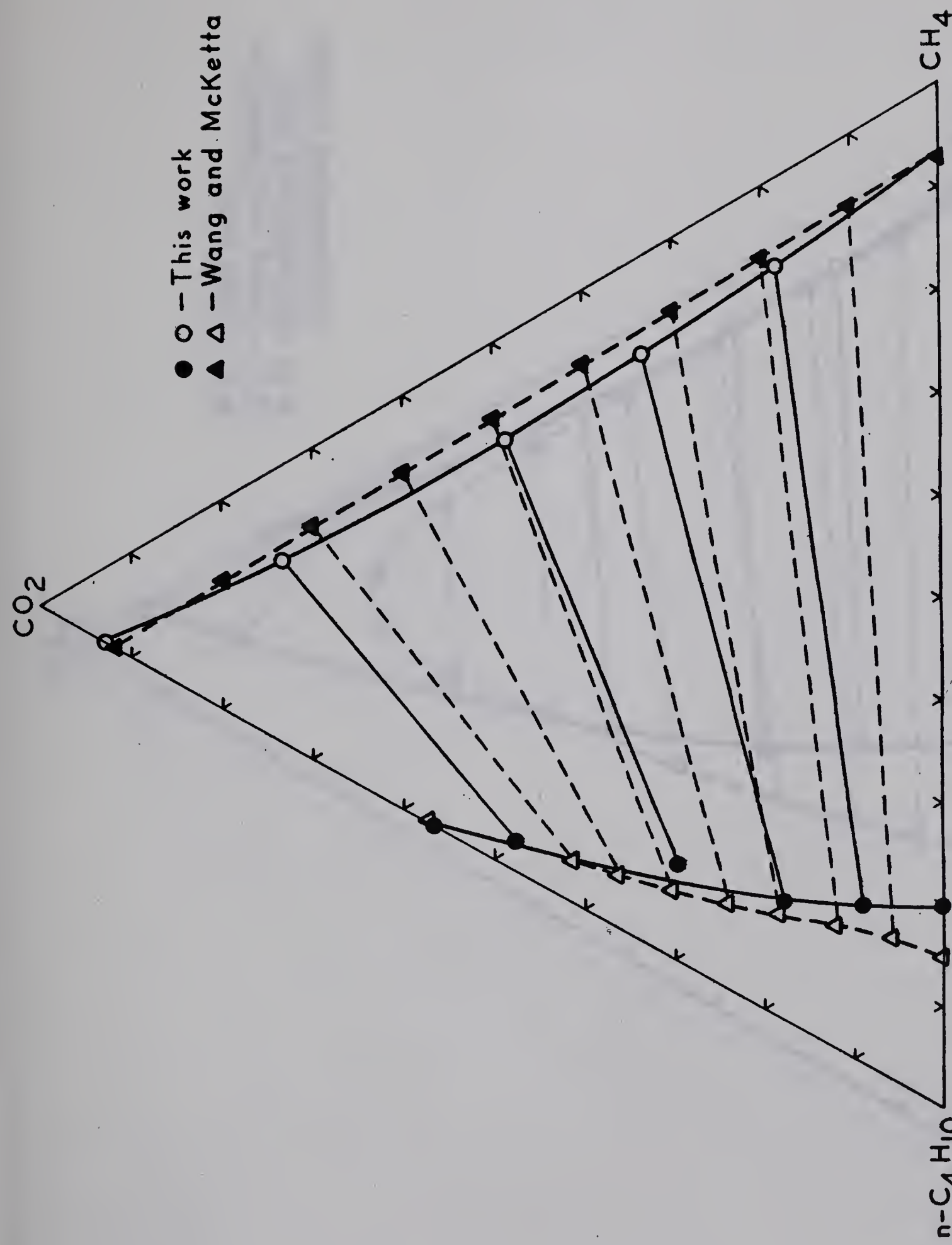

FIG. 17 Vapour-Liquid Equilibrium Data at 400 psia and 40°F for the Methane-Carbon Dioxide-n-Butane System

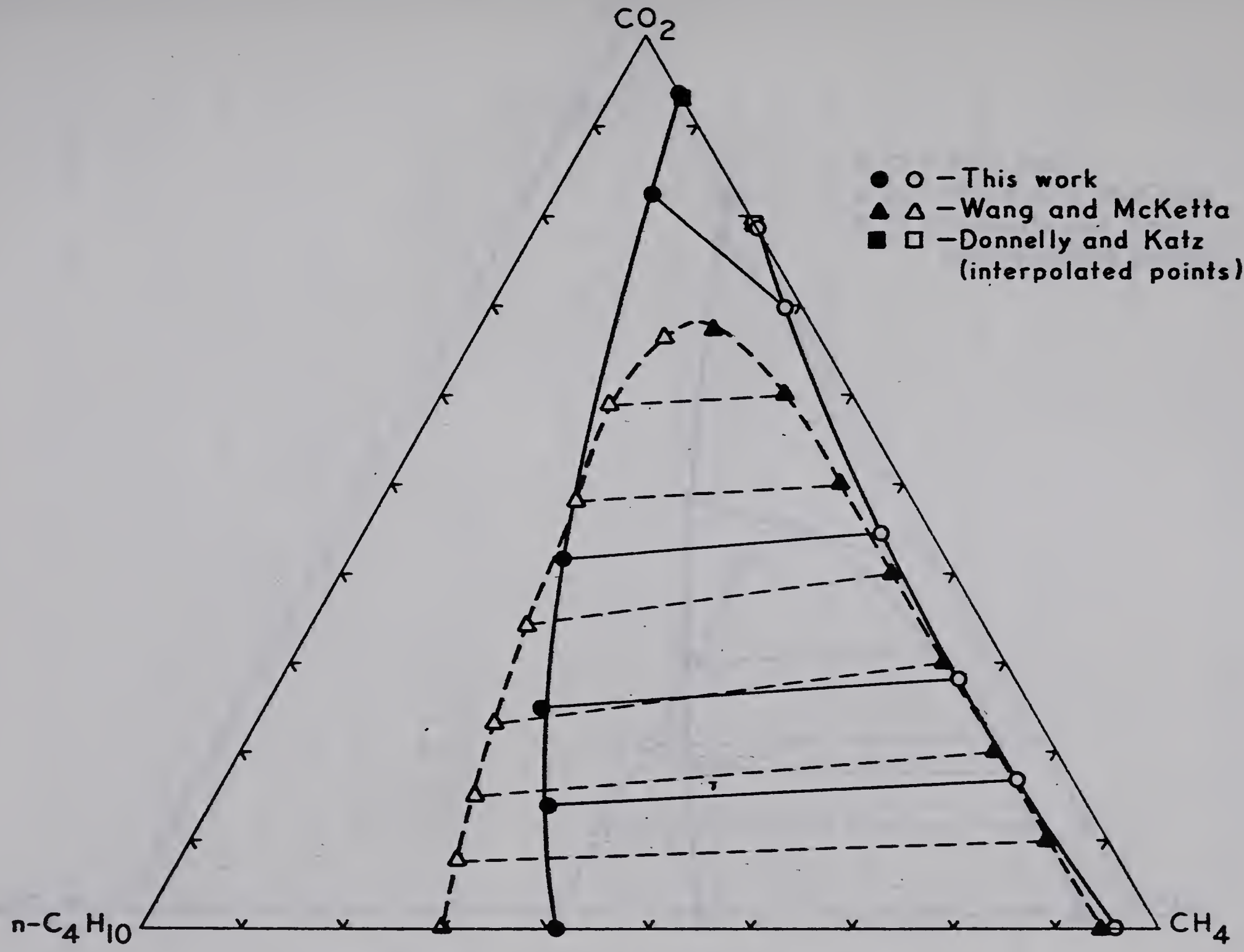

FIG. 18 Vapour-Liquid Equilibrium Data at 800 psia and 40°F for the Methane-Carbon Dioxide-n-Butane System

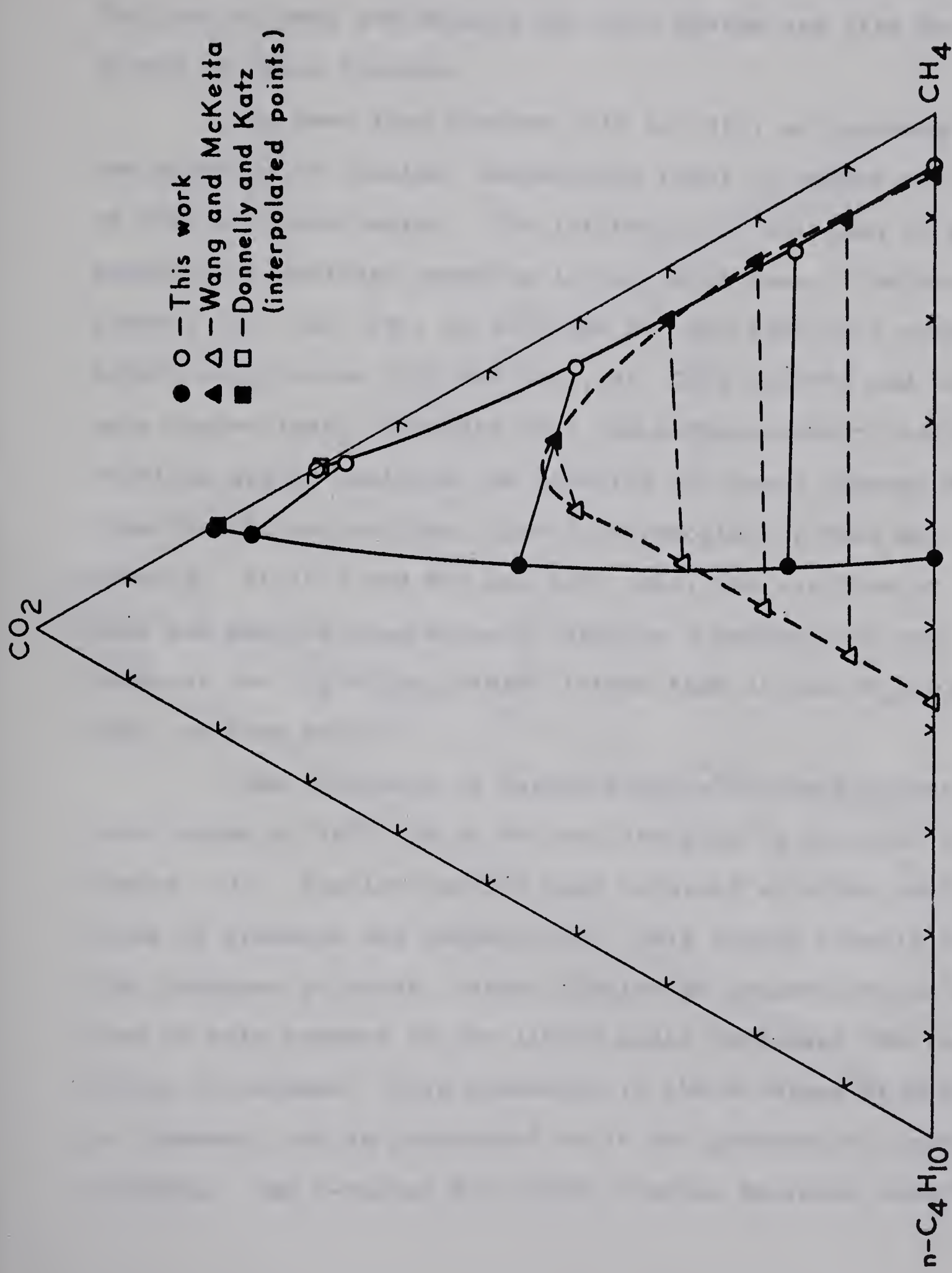

FIG. 19 Vapour-Liquid Equilibrium Data at 1200 psia and 40°F for the Methane-Carbon Dioxide-n-Butane System

and 1200 psia in Figures (20), (21), and (22) respectively. The data of Wang and McKetta for this system are also depicted on these figures.

As seen from Figures (14) to (22), an increase in the pressure at constant temperature tends to reduce the area of the two phase region. The influence of variation in temperature at constant pressure is not so obvious. The data of Figures (18) and (19), at 40°F and 800 and 1200 psia respectively,and Figures (20) and (21), at -20°F and 400 and 800 psia respectively, indicate that the methane-carbon dioxide-n-butane system exhibits the behavior of type 2 systems at these conditions and not type 1,as reported by Wang and McKetta. At 40°F and 800 and 1200 psia, the tie line of Wang and McKetta slope wrongly, showing a tendency to converge at the CO_2-nC_4H_{10} binary rather than at the CH_4-CO_2 binary, as they should.

The influence of carbon dioxide on the K-values in this system at 40°F and at 400 and 800 psia is depicted in Figure (23). Similar results were obtained at other conditions of pressure and temperature. This figure reveals that, like hydrogen sulphide, carbon dioxide at concentrations higher than 50 mole percent in the liquid phase increases the volatility of methane. This elevation in the K-values of methane is, however, not as pronounced as in the presence of hydrogen sulphide. The K-values for carbon dioxide decrease steadily

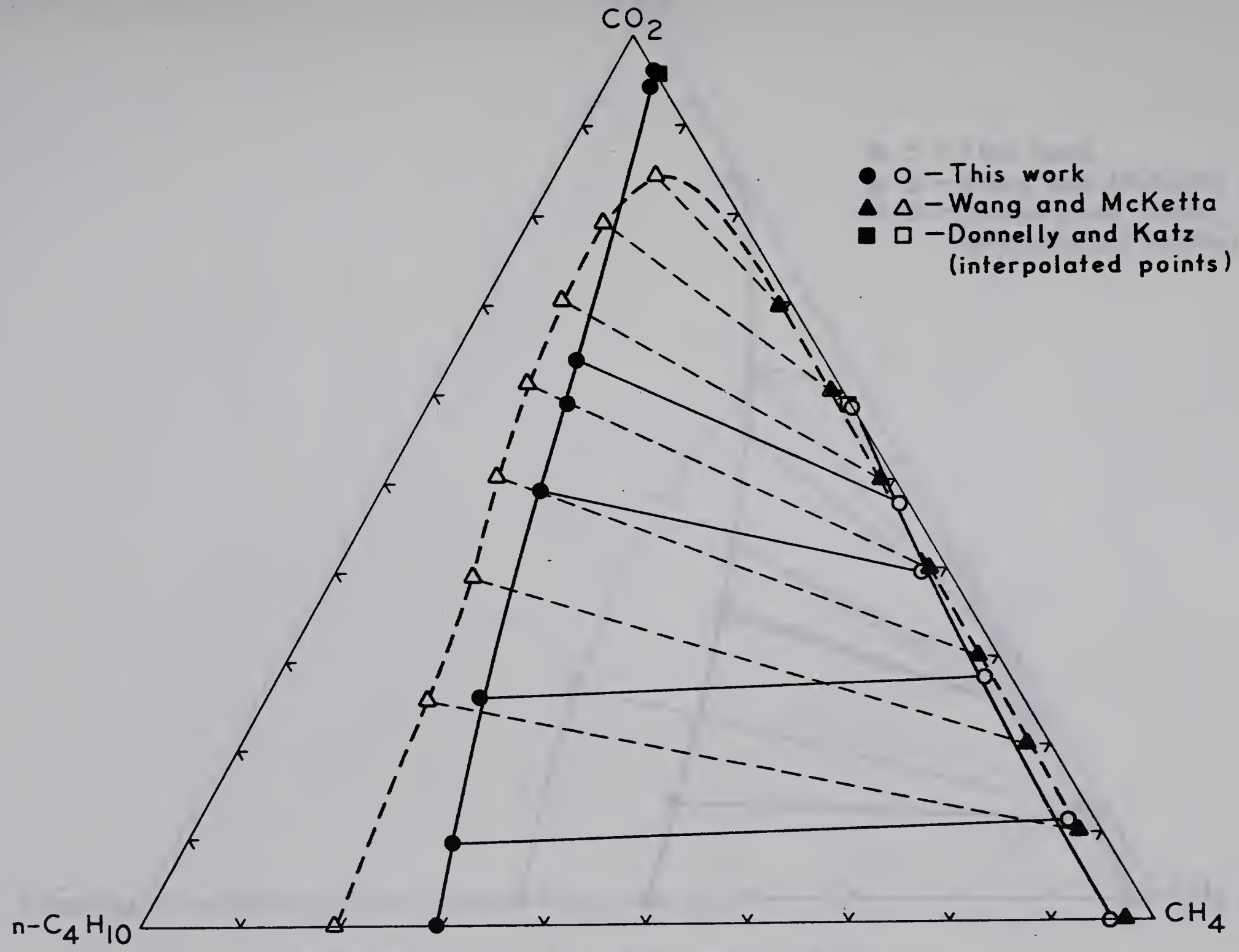

FIG.20 Vapour-Liquid Equilibrium Data at 400 psia and -20°F for the Methane-Carbon Dioxide-n-Butane System

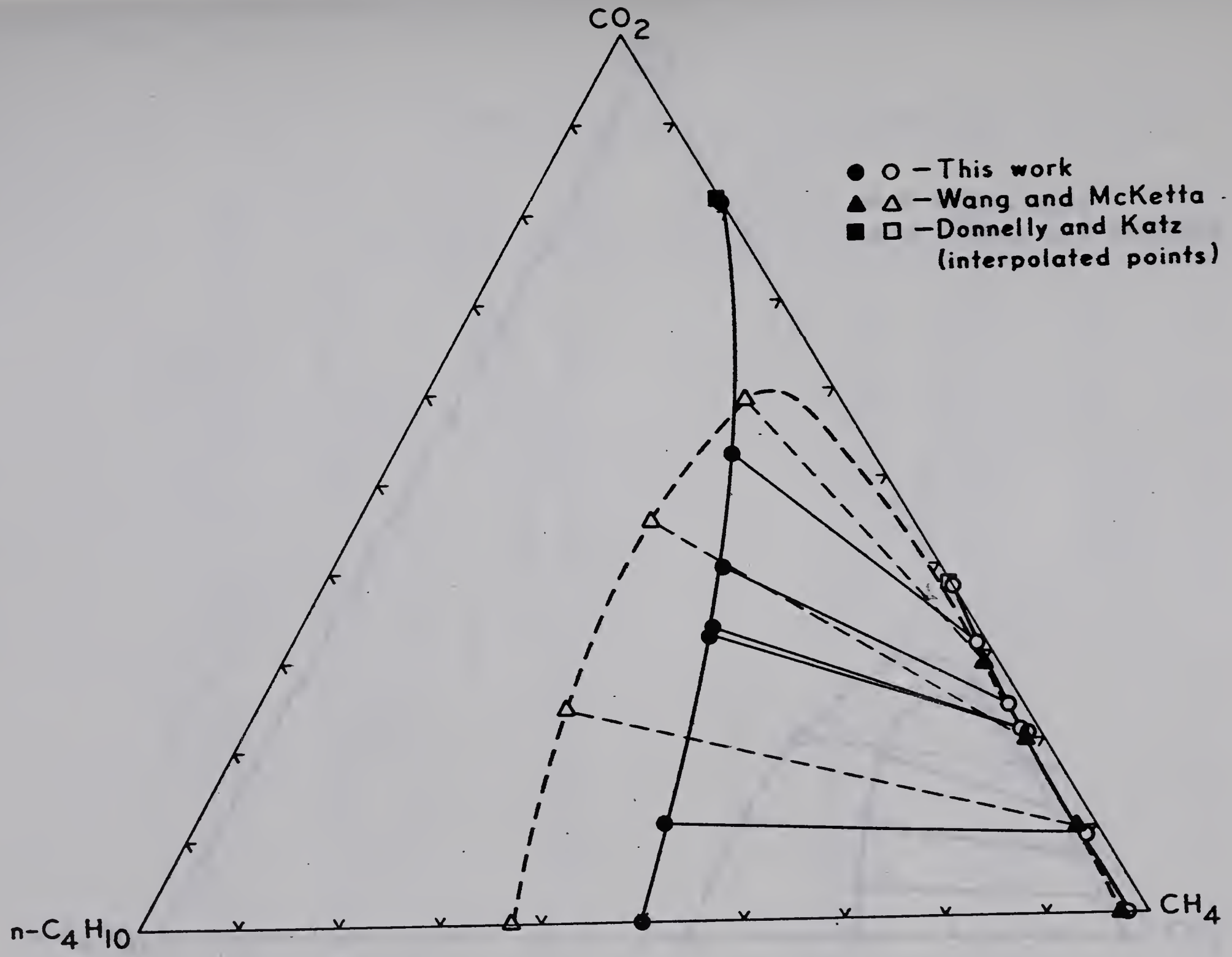

FIG. 21 Vapour-Liquid Equilibrium Data at 800 psia and -20°F for the Methane-Carbon Dioxide-n-Butane System

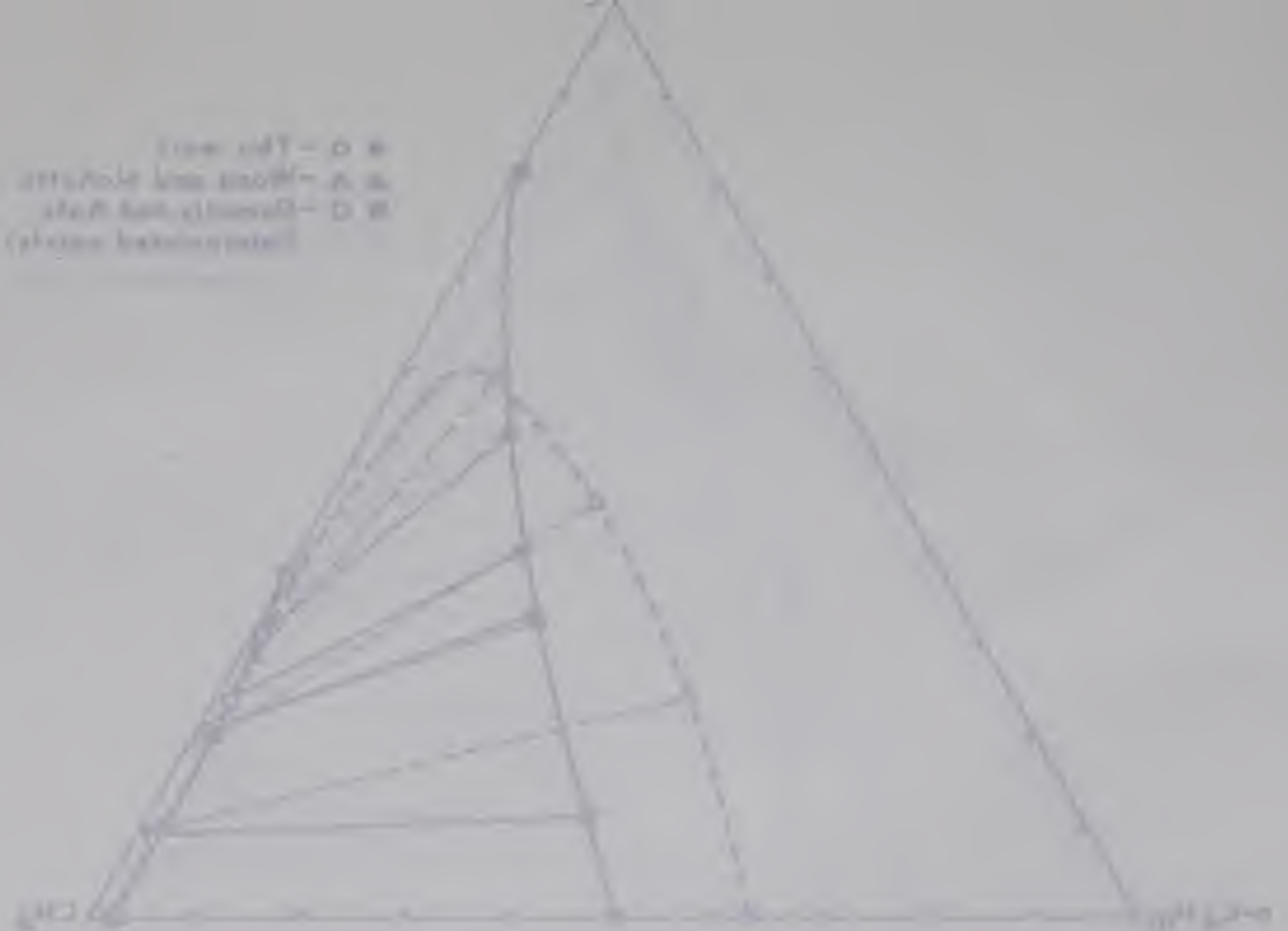

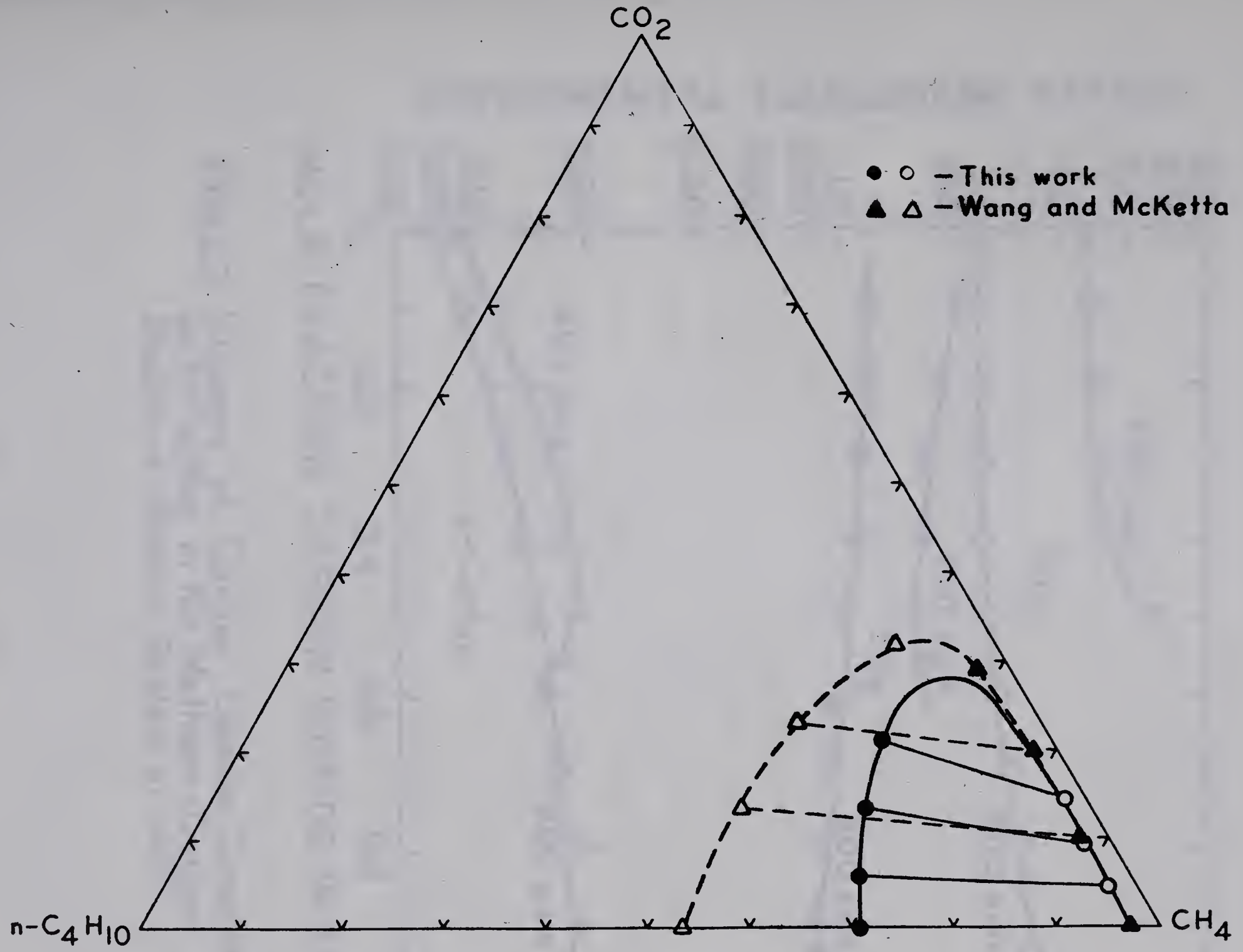

FIG. 22 Vapour-Liquid Equilibrium Data at 1200 psia and -20°F for the Methane-Carbon Dioxide-n-Butane System

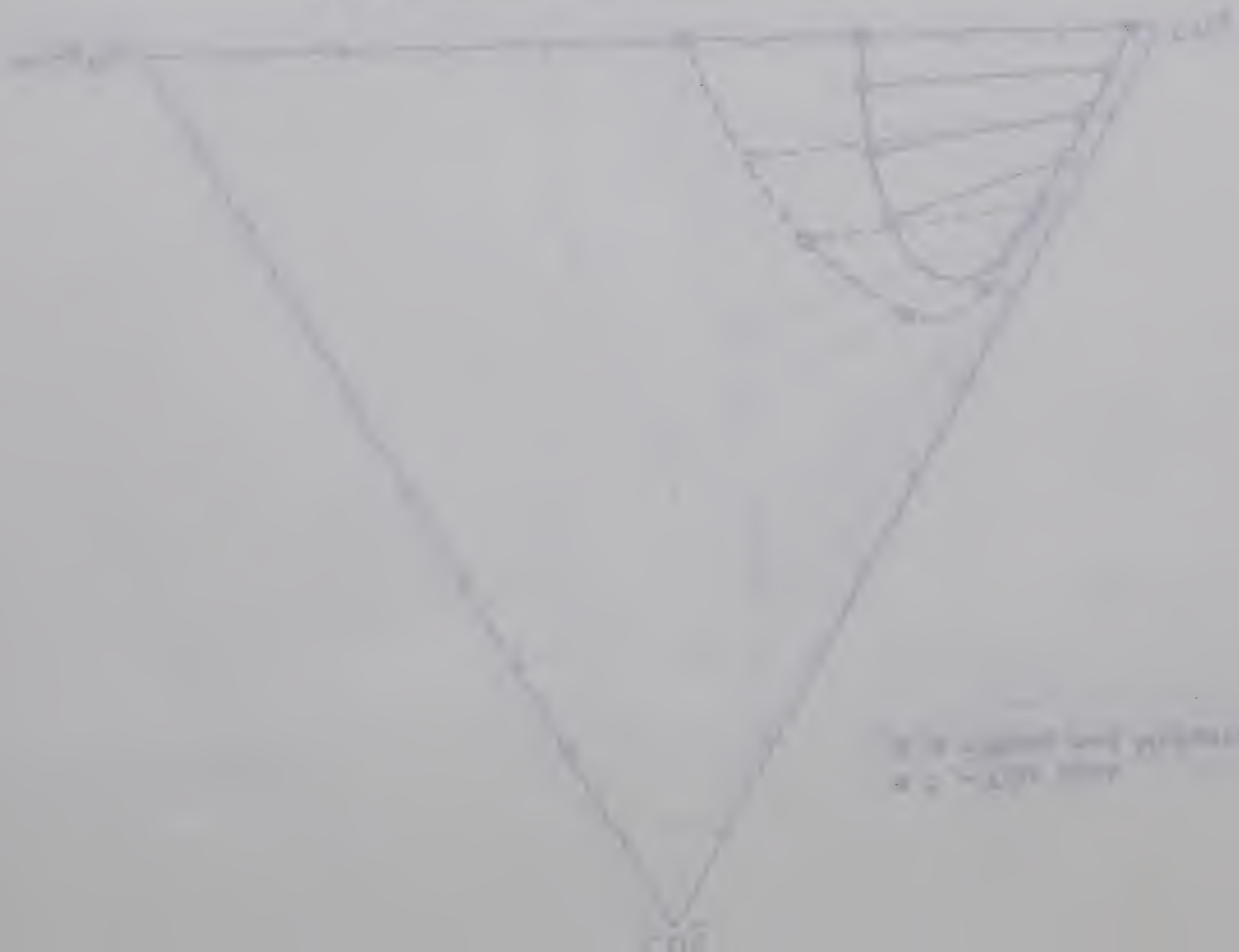

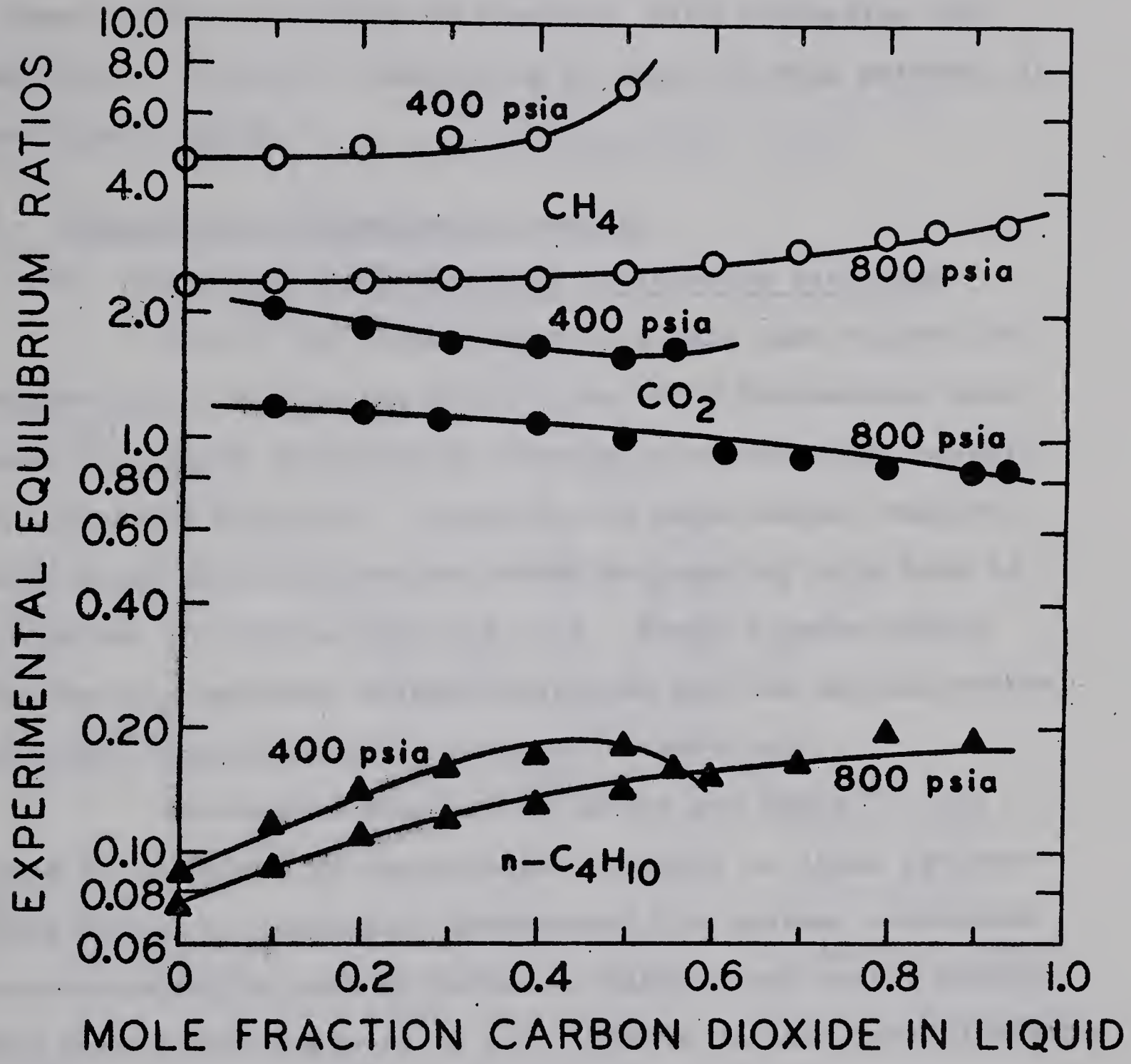

FIG.23 Influence of Carbon Dioxide Concentration on K-factors in the Methane-Carbon Dioxide-n-Butane System at 40°F

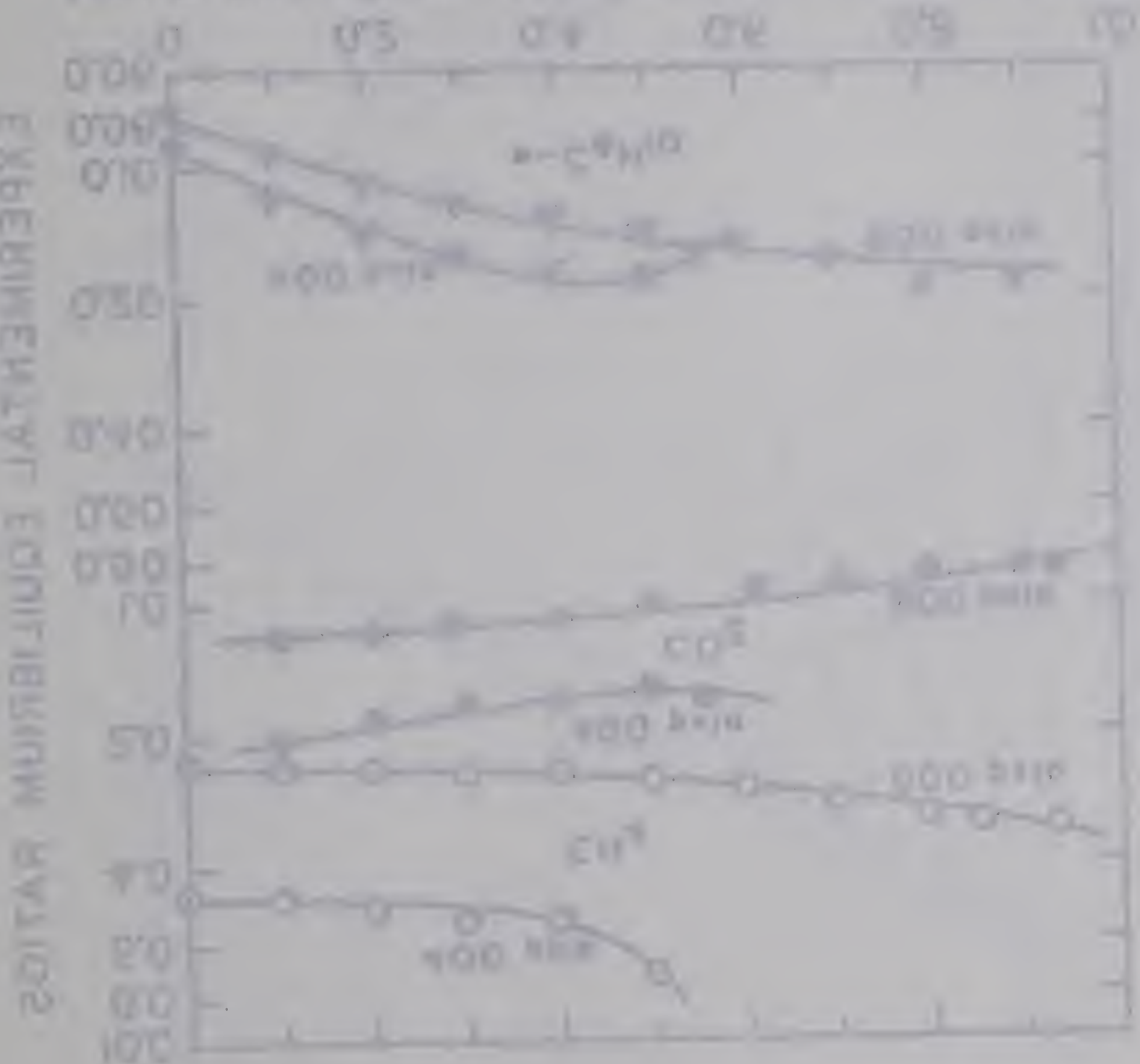
MOLE FRACTION CARBON DIOXIDE IN LIQUID
SOLAR MULTIBUBBLE JAR TEST
0
0.5
0.4
0.3
0.2
0.1
0.0
50
40
30
20
10
100 min
60 min
30 min
15 min
5 min

with increasing concentrations; while there is a marked increase in the volatility of n-butane, with increasing concentration of carbon dioxide, up to about 50 mole percent, in the liquid phase.

C. Comparison of Experimental Results

a) Comparison with the NGPSA Engineering Data Book

One of the oldest and most widely used sources of vapor-liquid equilibrium data is the NGPSA Engineering Data Book[73], which utilizes the concept of convergence pressure to correlate K-ratios. Comparison of experimental results with those obtained from the NGPSA Engineering Data Book is presented in Figures (24) and (25). These figures depict the methane-hydrogen sulphide-n-butane and the methane-carbon dioxide-n-butane systems, at 40°F, respectively.

The method proposed by Lenoir and White[57] was used to calculate the convergence pressure in these systems. This method is especially recommended for systems containing non-hydrocarbons such as hydrogen sulphide and carbon dioxide. The convergence pressure in all mixtures of this investigation was between 1000 and 2000 psia. The NGPSA Engineering Data Book K-values for methane and n-butane at convergence pressures of 1000 and 2000 psia are plotted in Figure (24) and (25). For hydrogen sulphide and carbon dioxide the NGPSA Engineering Data Book reports K-values at convergence pressures of 1000 and 4000 psia only. These comparisons are

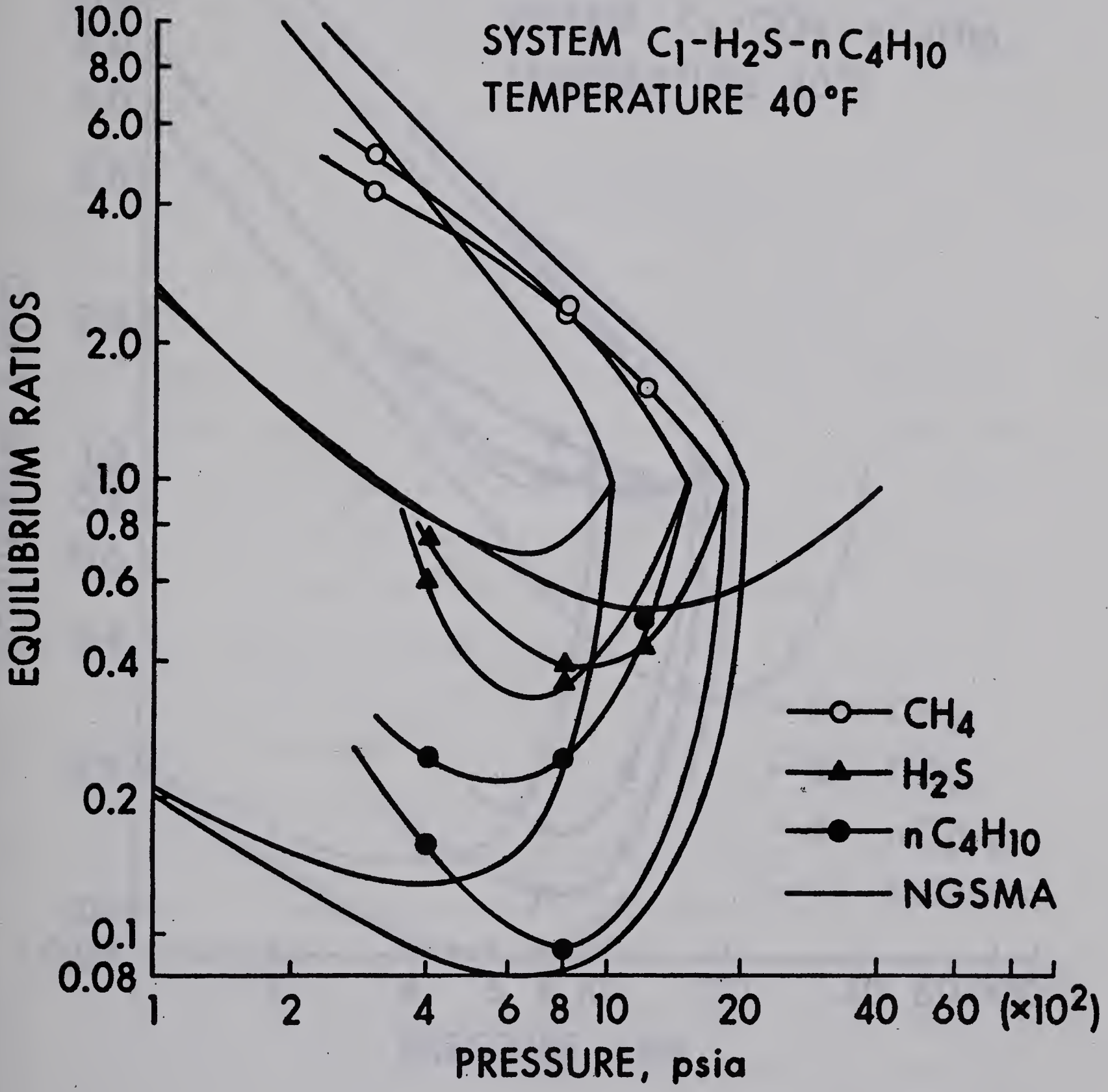

Figure 24 Comparison of Experimental and Predicted K-factors for Methane, Hydrogen Sulfide, and n-Butane at 40°F

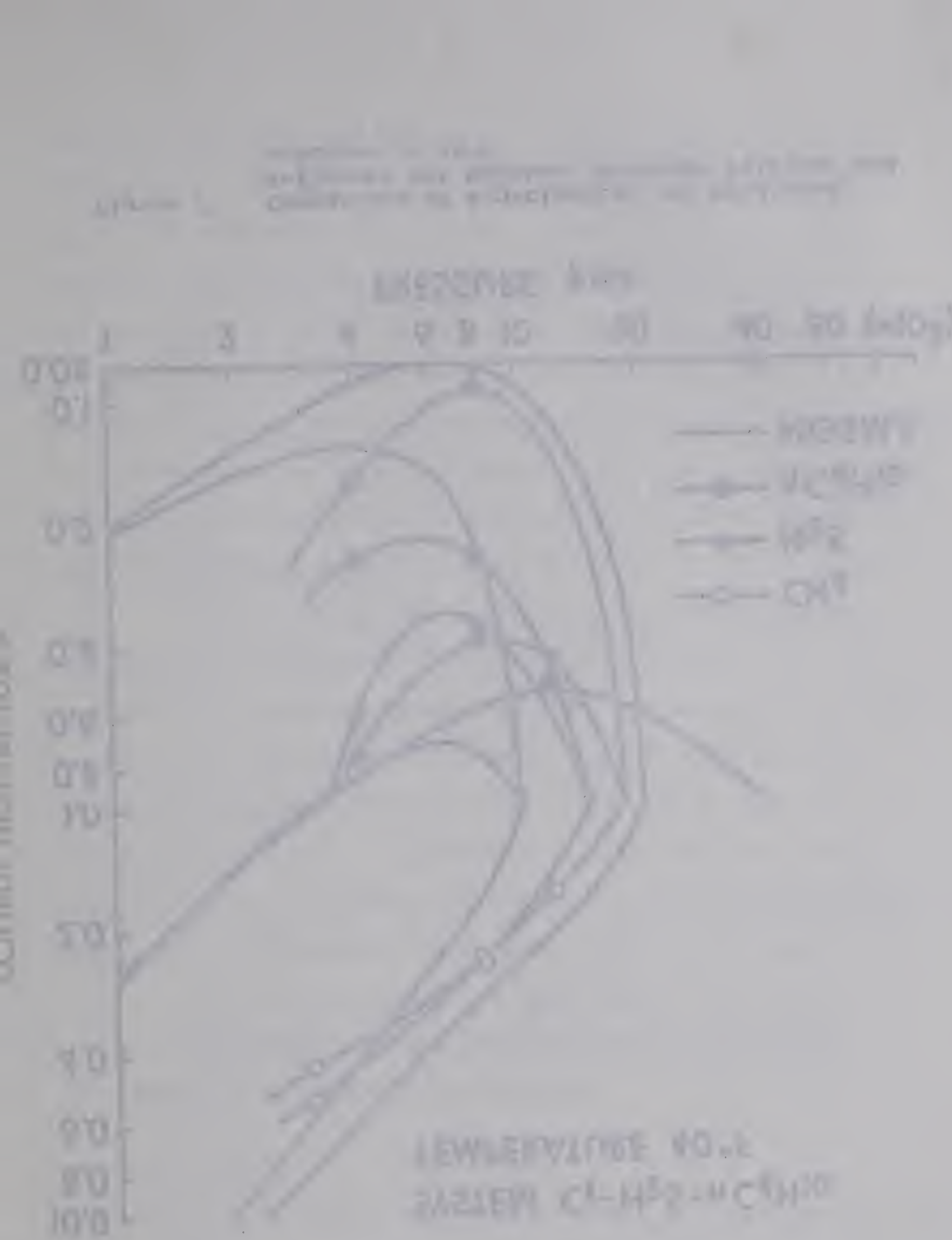

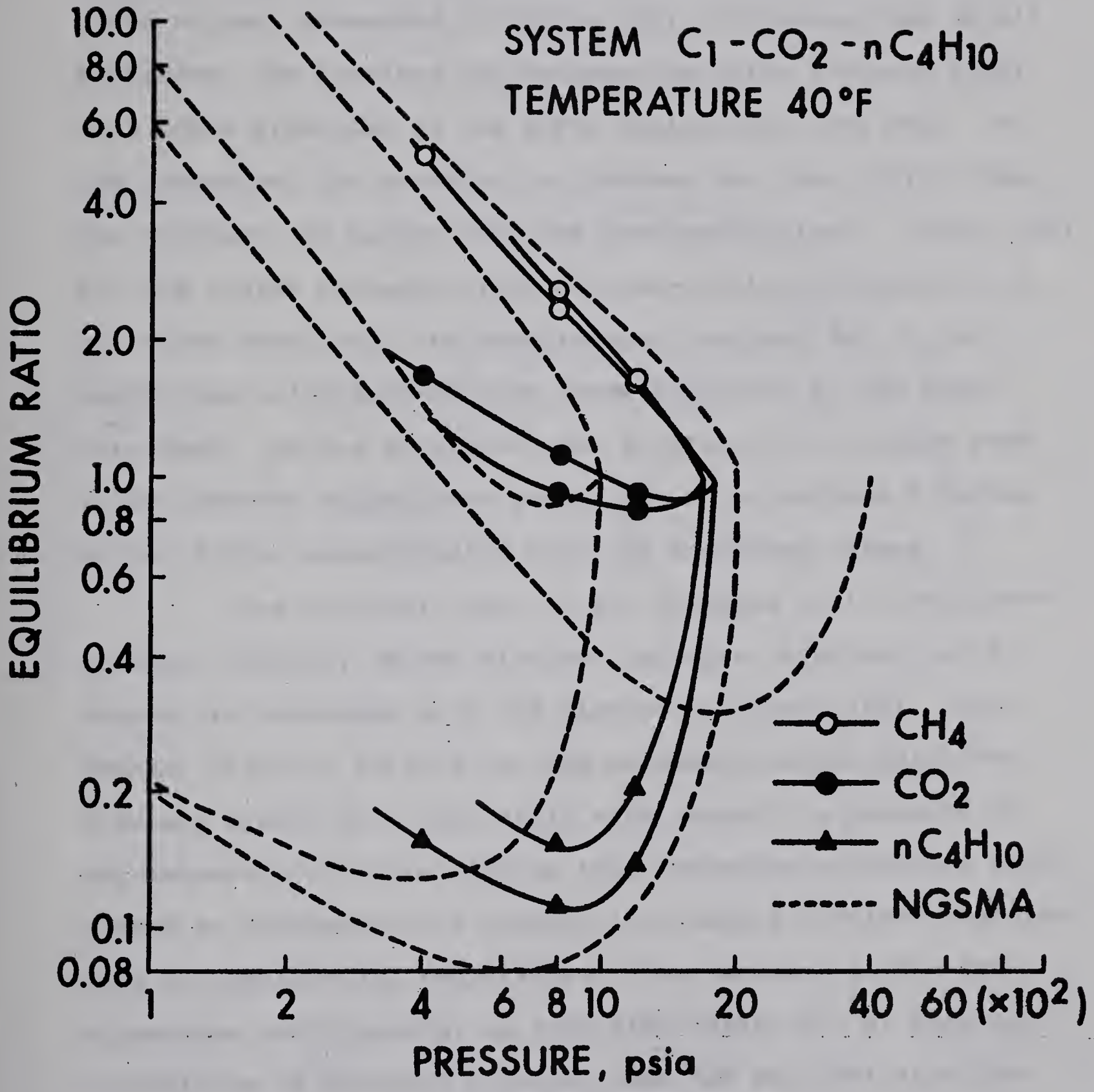

Figure 25 Comparison of Experimental and Predicted K-factors for Methane, Carbon Dioxide, and n-Butane at 40°F

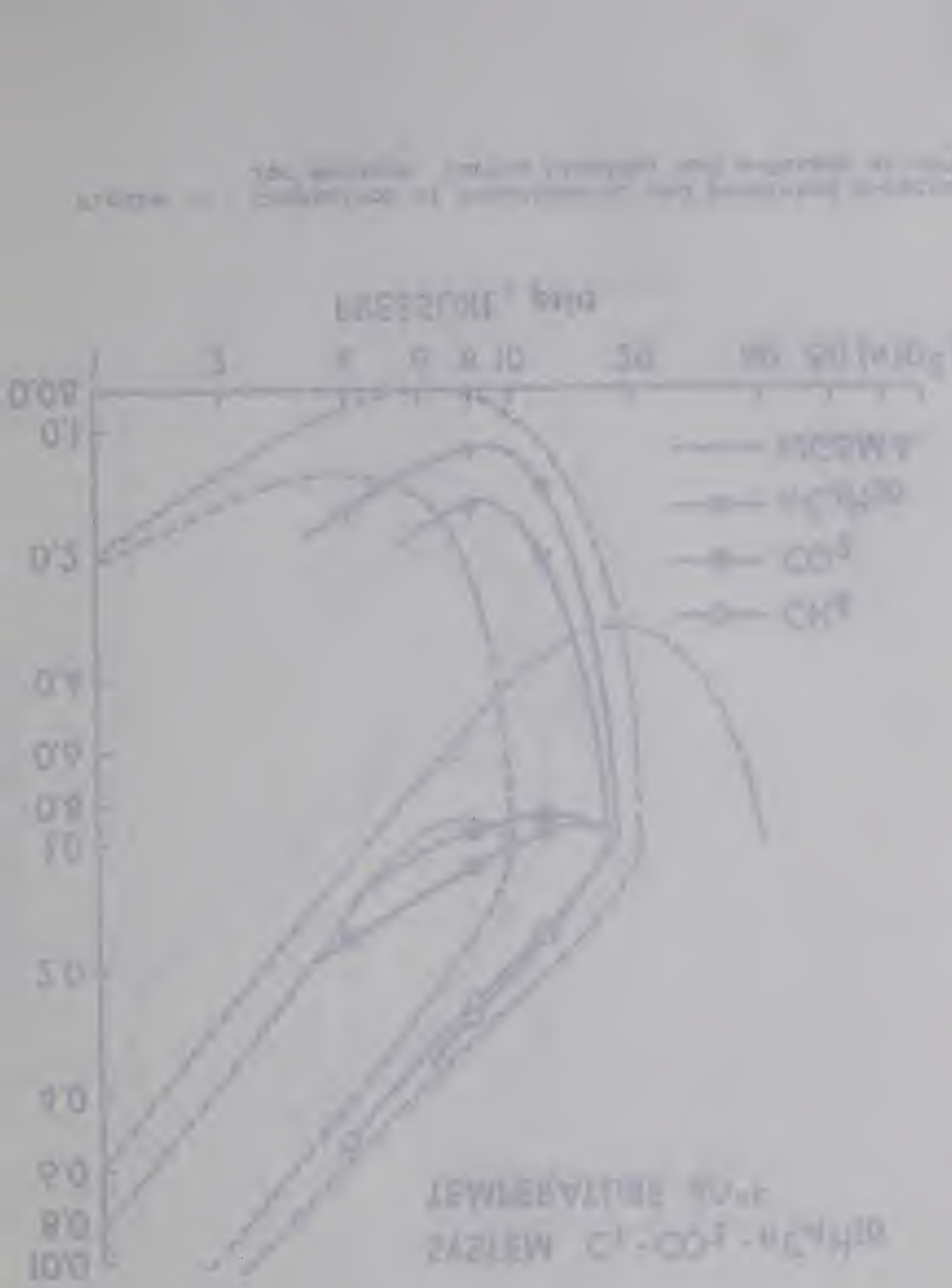

depicted in Figures (24) and (25) and tabulated in Table (9).

The comparison of experimental K-values with the NGPSA values, presented in Figure (24), indicates that at all pressures, the K-values for hydrogen sulphide are much lower than those predicted by the NGPSA Engineering Data Book. At low pressures, the K-values for methane are lower while those for n-butane are higher than the predicted values. Figure (25) for the system methane-carbon dioxide-n-butane indicates, on the other hand, that the experimental K-values for CO_2 are higher for all pressures than those predicted by the NGPSA Data Book. At low pressures, the K-values for n-butane seem to be somewhat higher than predicted, while methane K-values do not differ significantly from the predicted values.

The critical loci of all binaries of the four components, methane, carbon dioxide, hydrogen sulphide, and n-butane are presented on a P-T diagram in Figure (26). The ternary critical surface for the methane-hydrogen sulphide-n-butane system is a thin strip with respect to pressure at any temperature. This implies that convergence pressure would almost be independent of composition, making K-values functions only of pressure and temperature. The increase in K-values of methane and n-butane, as seen from Table (2), at high concentrations of hydrogen sulphide does not bear out this prediction. In the methane-carbon dioxide-n-butane system, on the other hand, the ternary critical surface predicts strong dependence of K-factors on convergence pressure. Experimental

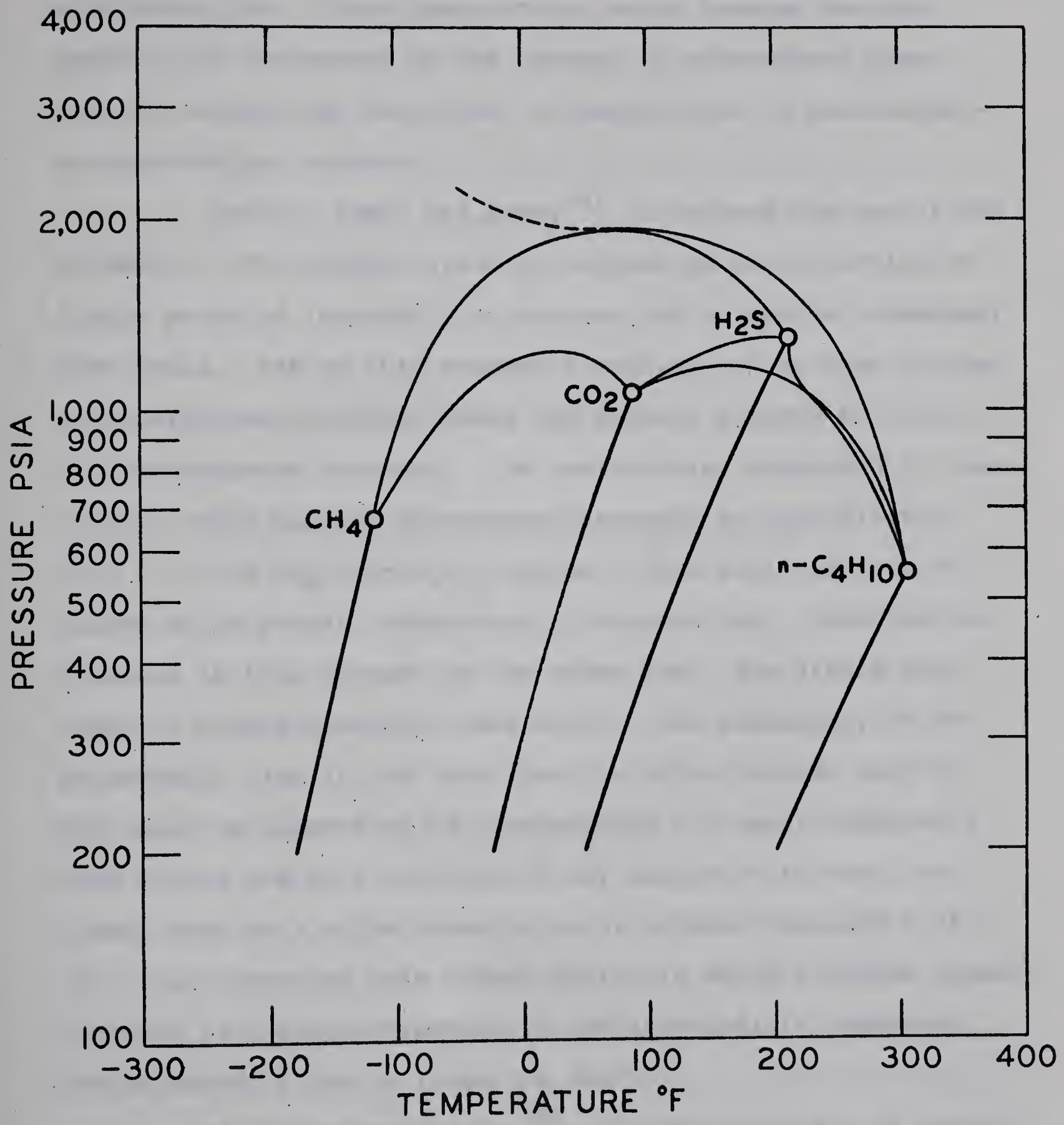

FIG. 26 Critical Loci of Binary Systems

K-values,presented in Table (4), are not such strong functions of composition. These observations point towards the probability of inadequacy of the concept of convergence pressure to account for the effect of composition in hydrocarbon-non-hydrocarbon systems.

Carter, Sage, and Lacey[8] introduced the use of the parameter C for ternary systems, defined as mole fraction in liquid phase of intermediate component on a lightest component free basis. Use of this parameter enables one to draw a hypothetical-binary critical locus for ternary systems to calculate convergence pressure. The construction suggested by these authors would predict convergence pressure to vary slightly with C in the CH_4-H_2S-nC_4H_{10} system. This would require K-values to be almost independent of composition. Experimental K-values in this system, on the other hand, are strong functions of composition and therefore C. The inadequacy of the parameter C lies in the fact that its value depends only on the relative proportion of intermediate and heavy components. This allows the mole fraction of any component to vary from almost zero to a value close to unity without changing C at all. In systems of this investigation in which K-values depend strongly on the mole fraction of the intermediate component, the parameter C can no longer be useful.

Robinson and Saxena[99], in their analysis of several hydrocarbon-hydrogen sulphide binaries have concluded that the

presence of hydrogen sulphide tends to elevate K-values for methane and ethane, as compared to K-values reported for these components in the NGPSA Engineering Data Book. The K-values for propane and heavier components are, however, not affected. The data in the CH_4-H_2S-nC_4H_{10} system, presented in Figure (24), are not consistent with this observation. The K-values for methane are not affected appreciably, while n-butane K-values increase significantly at low pressures. The presence of a third component evidently has a significant bearing on the influence of H_2S on the vaporization characteristics of hydrocarbons.

b) Comparison with the Chao-Seader Correlation

The Chao-Seader correlation was used to predict the relative amount of the two phases and the K-values of all components, corresponding to an experimental liquid to vapor ratio of unity. Three sets of constants were employed: the Chao-Seader constants[9], the Grayson-Streed constants[32], and the revised Chao-Seader constants[72]. The results of predictions using the Chao-Seader correlation for the methane-hydrogen sulphide-n-butane and methane-carbon dioxide-n-butane systems are presented in Table (5), together with similar comparisons for the methane-propane-n-butane system. Detailed values are included only for the set of constants which provided the best predictions, as seen from the sum of standard deviations in K-values and percent liquid value. A summary

of deviations using all three sets of constants is also presented in Table (5). The concentration of the non-hydrocarbon component in the liquid phase varied from 0 to 30% in the data points, included in this comparison.

Various deviations from experimental data, reported in Table (5), are defined as follows:

$$\text{Percent deviation} = \frac{\text{Predicted value - Experimental value}}{\text{Experimental value}} \times 100 \qquad (63)$$

$$\text{Average deviation} = \frac{1}{N}\left(\sum_{k=1}^{N} \text{Percent deviation}\right) \qquad (64)$$

$$\text{Standard deviation} = \frac{1}{N-1}\left[\left(\sum_{k=1}^{N} (\text{Percent deviation})^2\right)\right]^{\frac{1}{2}} \qquad (65)$$

where, N = number of data points.

The order of deviations was much the same for all conditions of pressure and temperature. Results of predictions for the methane-propane-n-pentane system[8] are included to offer a direct comparison with the usefulness of the Chao-Seader correlation in a system of only hydrocarbons.

A comparison of the experimental K-values with those predicted using the Chao-Seader correlation and the NGPSA Engineering Data Book is presented in Figures (27) and (28), for the methane-hydrogen sulphide-n-butane and the methane-carbon dioxide-n-butane system respectively.

In Figure (29), predicted K-values in the methane-hydrogen sulphide-n-butane system are plotted against mole

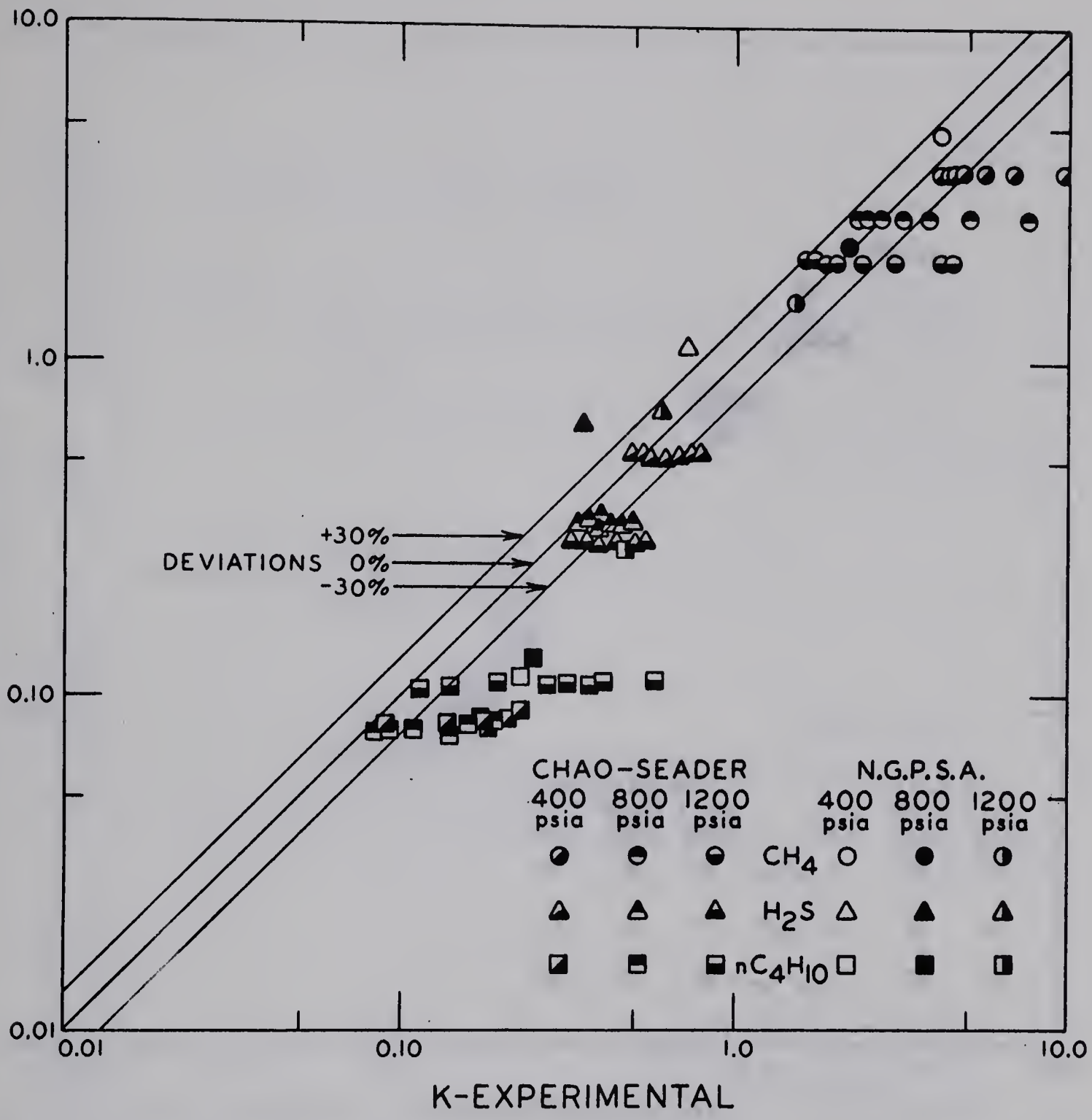

FIG. 27 Comparison of Experimental K-Values with those predicted using the Chao-Seader Correlation and the N.G.P.S.A. Engineering Data Book, for the Methane-Hydrogen Sulfide-n-Butane System at 40°F.

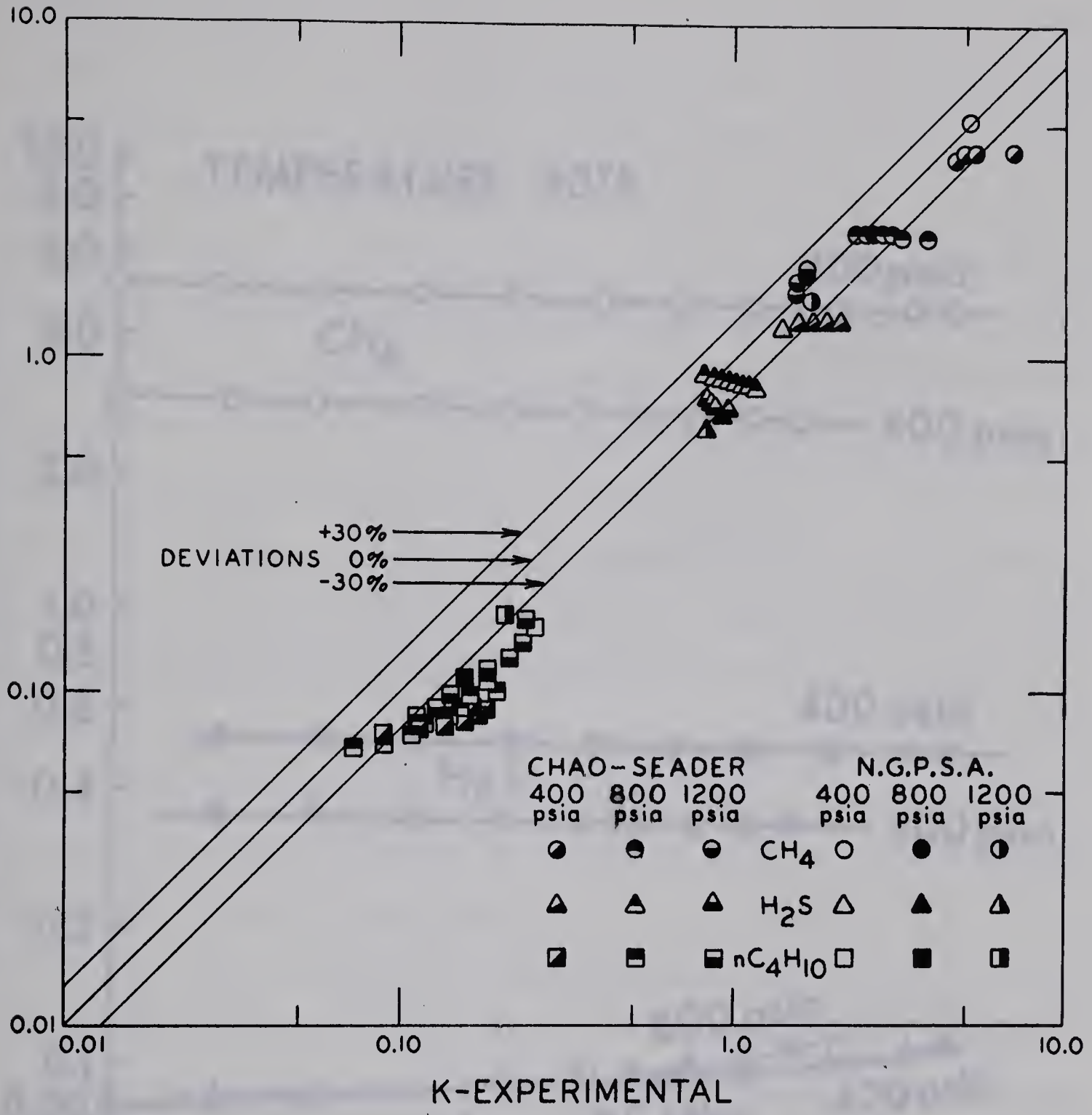

FIG. 28 Comparison of Experimental K-Values with those predicted using the Chao-Seader Correlation and the N.G.P.S.A. Engineering Data Book, for the Methane-Carbon Dioxide-n-Butane System at 40°F.

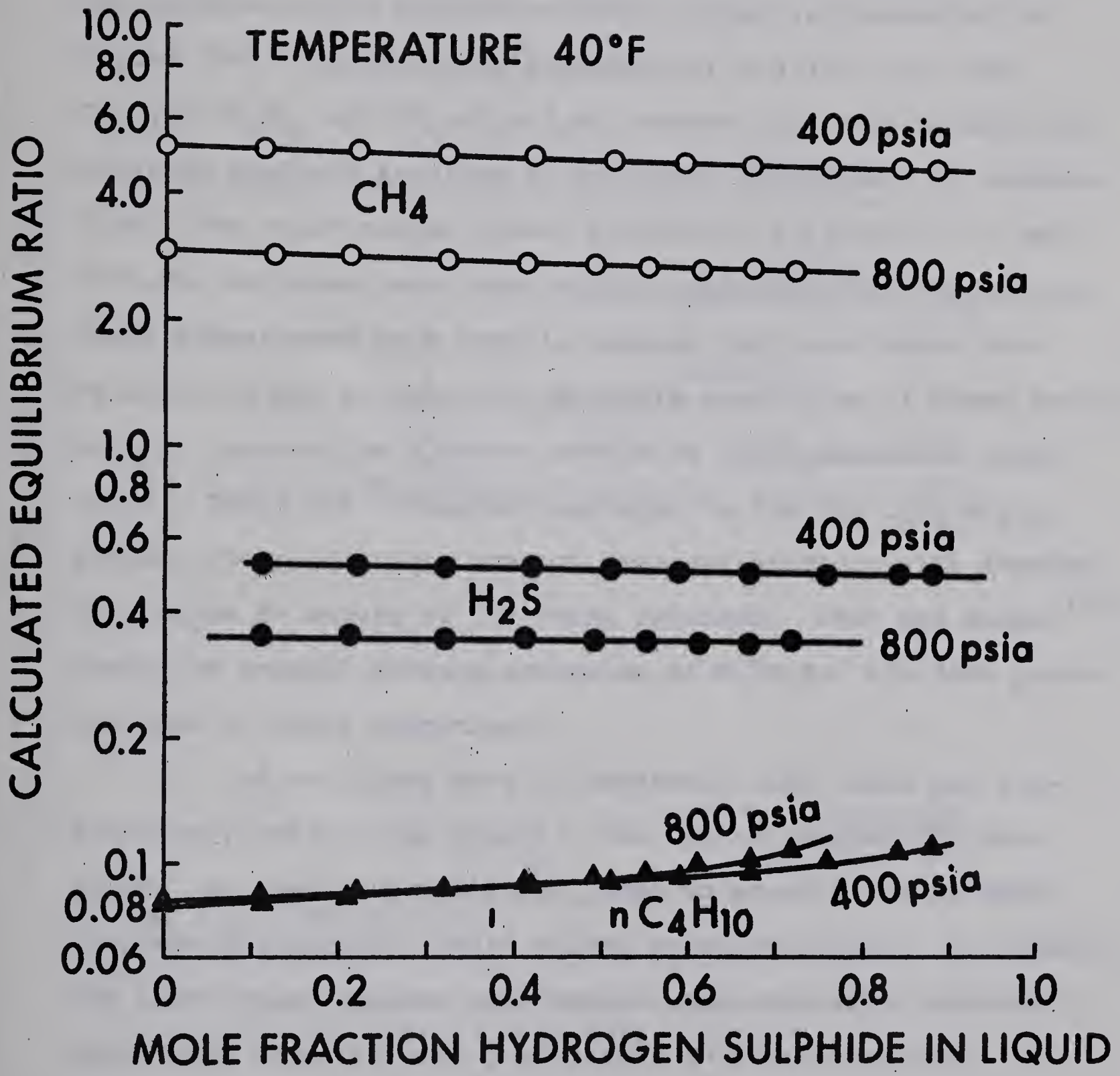

FIGURE 29 INFLUENCE OF HYDROGEN SULPHIDE CONCENTRATION ON K-FACTORS IN THE METHANE-HYDROGEN SULPHIDE-N-BUTANE SYSTEM AT 40°F, PREDICTED BY CHAO-SEADER CORRELATION

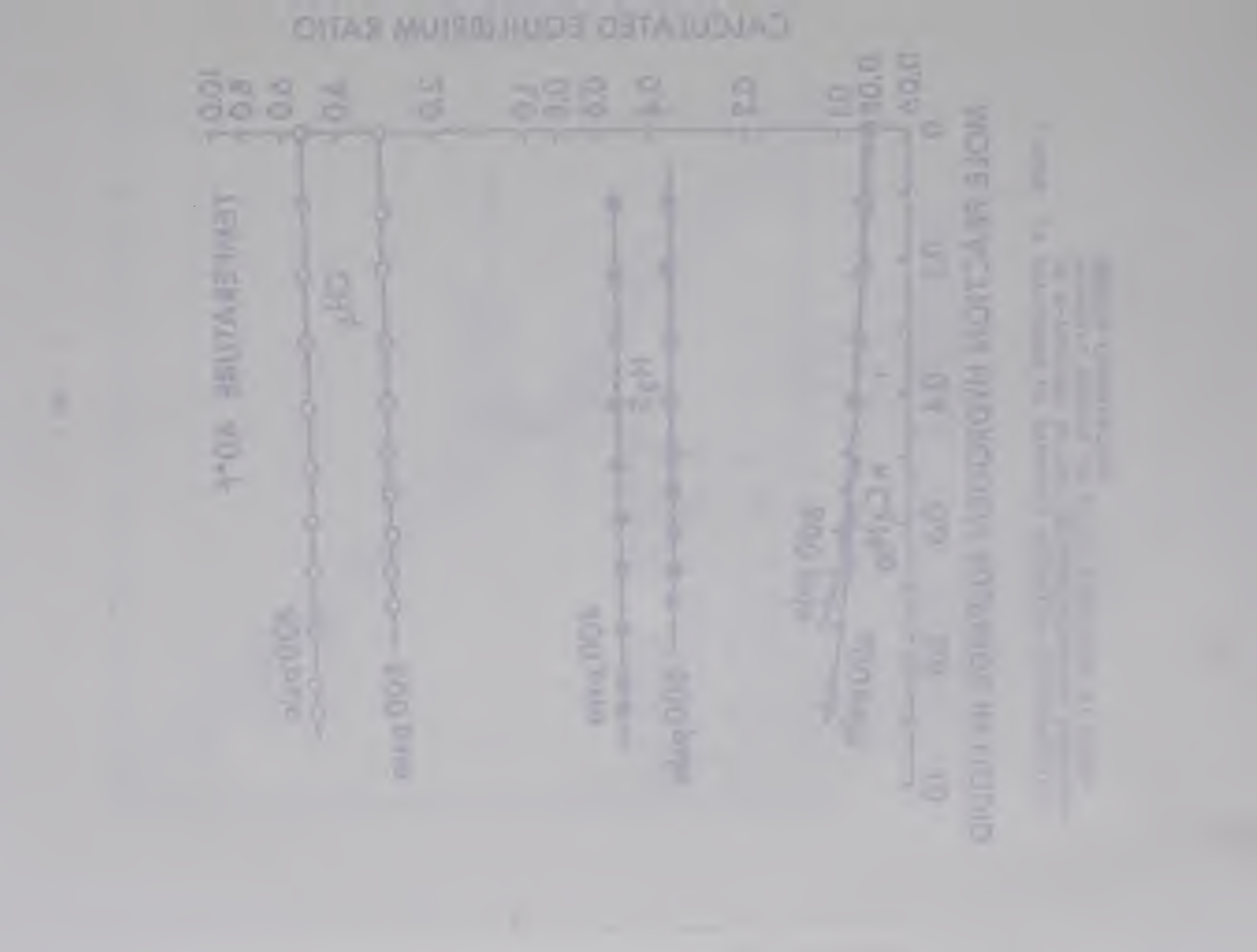

fraction of hydrogen sulphide in the liquid phase, at a temperature of 40°F and at 400 and 800 psia. Similar plots for the methane-carbon dioxide-n-butane system are presented in Figure (30). As seen from Figures (29) and (30), for the CH_4-H_2S-nC_4H_{10} and CH_4-CO_2-nC_4H_{10} system, the Chao-Seader correlation predicts K-values to be almost independent of composition. The experimental values presented in Figures (13) and (23),on the other hand, show strong dependence on composition. These comparisons show that in general the Chao-Seader correlation is not suitable for accurate prediction of phase equilibria in hydrocarbon systems containing non-hydrocarbon components. Table (5) indicates that even in the CH_4-C_3H_8-nC_5H_{12} system, the predictions are not very satisfactory with average deviations in excess of 20% being obtained. Chao and Seader[10] report an overall average deviation of 8.7% for the 2696 points included in their comparison.

Of the three sets of constants used, none was significantly better than others. The Grayson-Streed[32] constants, as seen from Table (5), seem to predict the methane K-values and percent liquid values somewhat better. In general, the Chao-Seader program made better predictions for ternary systems as compared with predictions in binary systems.

In order to better understand the failure of the Chao-Seader correlation to predict high pressure vapor-liquid equilibria, a review of all assumptions associated with this

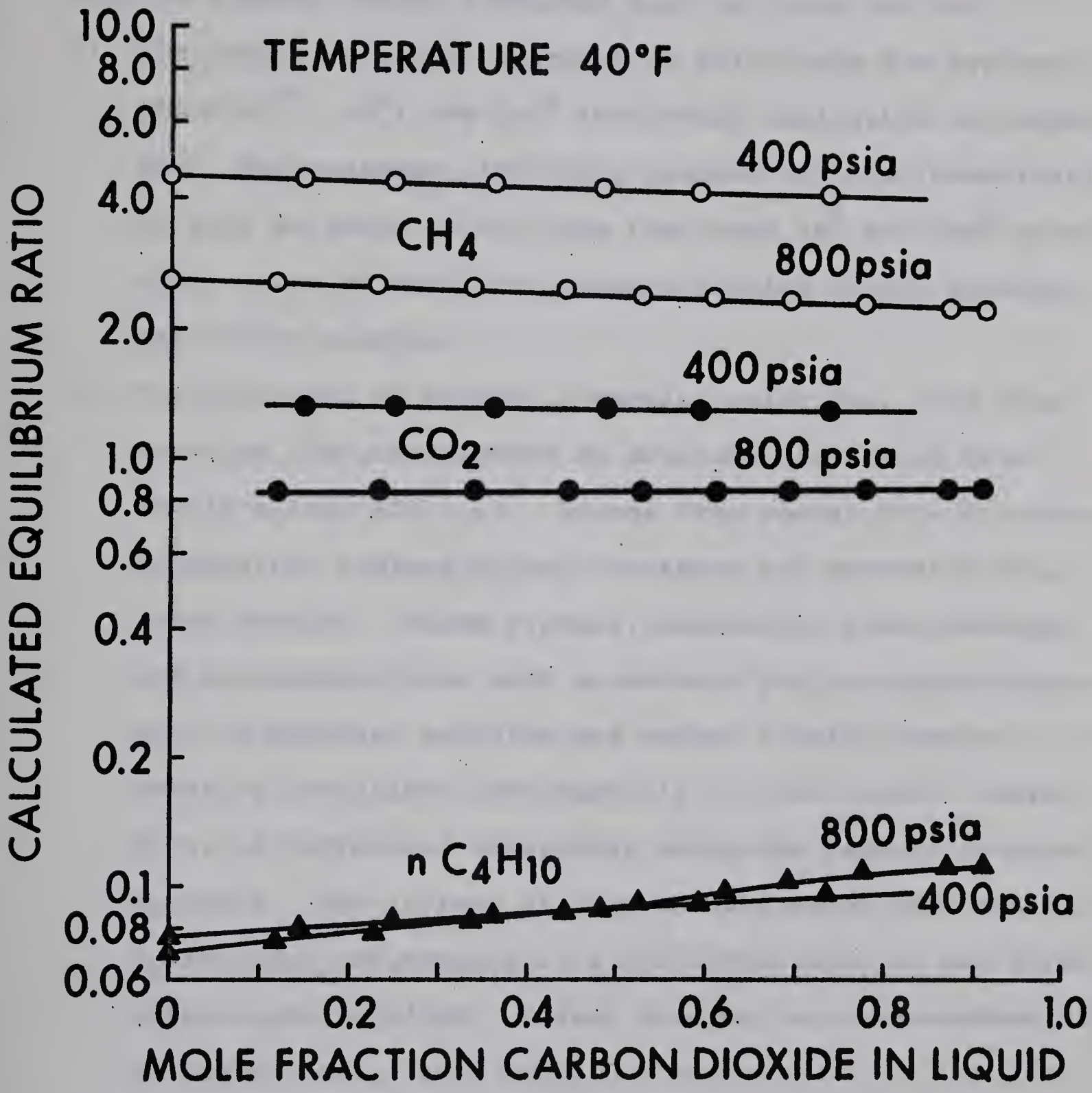

FIGURE 30 INFLUENCE OF CARBON DIOXIDE CONCENTRATION ON K-FACTORS IN THE METHANE-CARBON DIOXIDE-N-BUTANE SYSTEM AT 40°F, PREDICTED BY THE CHAO-SEADER CORRELATION

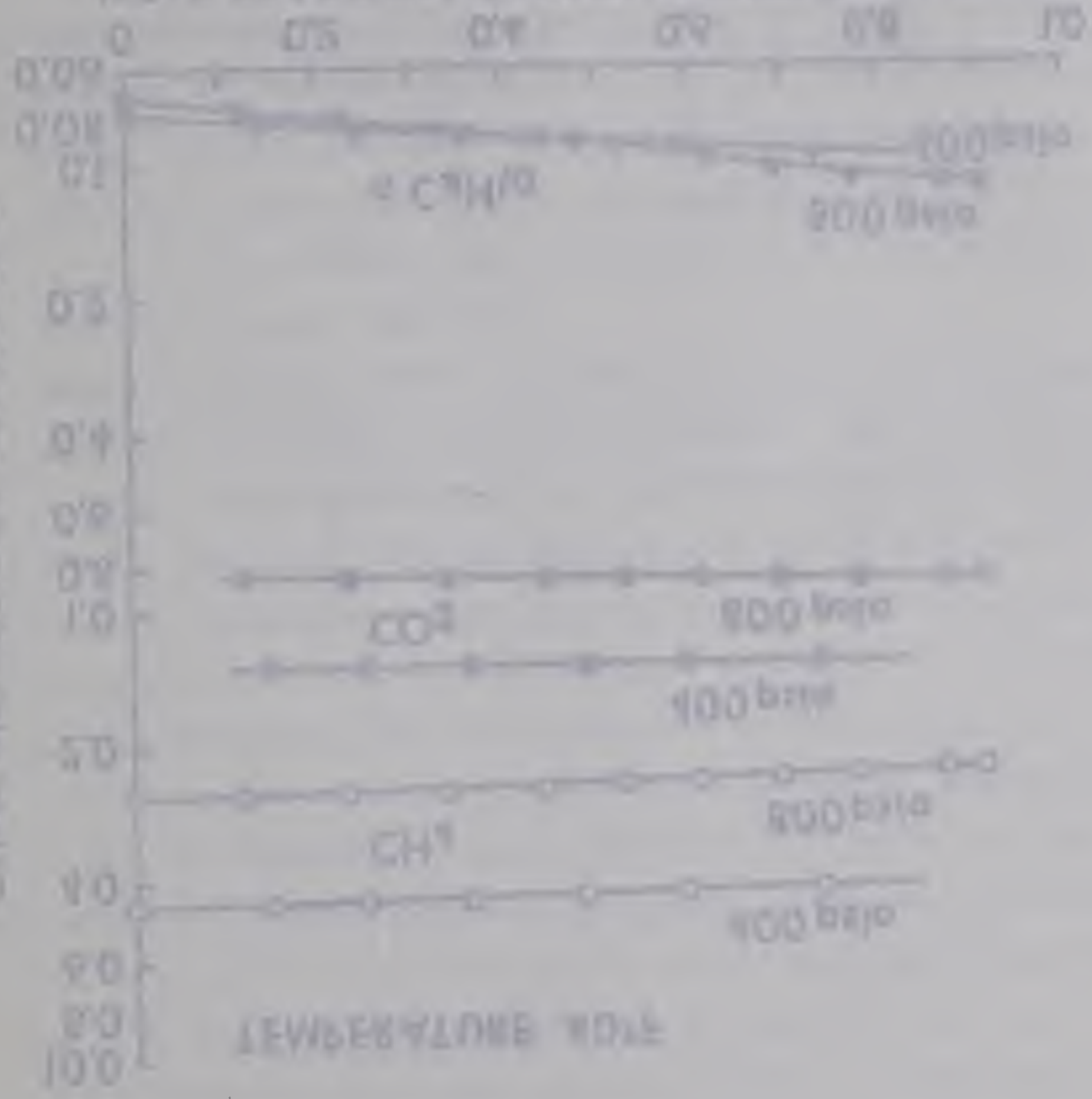
MOLE FRACTION CARBON DIOXIDE IN LIQUID
0
0.25
0.5
0.75
1.0
0.001
0.01
0.1
0.5
1.0
EQUILIBRIUM FUGACITY
CO2
CH4
100 bars
200 bars
400 bars
600 bars
800 bars
1000 bars
TEMPERATURE 10°C

approach and an assessment of how far these are satisfied by systems of this investigation is presented here. Hildebrand[41] has, in general terms, discussed most of these earlier.

1) The regular solution approach is valid only for systems in which $\Delta F^E \simeq \Delta H^E$; the $T\Delta S^E$ term being negligible in comparison. Many systems, including systems of this investigation as will be shown later, have the terms ΔH^E and $T\Delta S^E$ of an equal order of magnitude, when a regular liquid solution may not be assumed.

2) Positive heat of mixing in regular solutions, seen from Equation (38),corresponds to positive deviations from Raoult's law; all $\gamma_i > 1$. Excess free energy data for many hydrocarbon systems at high pressure are presented in a later section. These systems, especially those containing non-condensibles such as methane and non-hydrocarbons such as hydrogen sulphide and carbon dioxide, depict negative deviations from Raoult's law and cannot, therefore, be correlated adequately using the regular solution approach. The systems of this investigation have one non-hydrocarbon and methane is a non-condensible at all three temperatures studied. Carbon dioxide is a non-condensible at $100^{\circ}F$.

3) The intermolecular forces are assumed to be short range dispersion forces; for molecules which possess dipoles the assumption of strict additivity is no longer valid.

The anisotropic force centers of dipole interactions give rise to non-regular solution behavior. In the case of some large molecules possessing long,extended electronic oscillators, it is necessary to account for the spacial extension of these oscillators. An attempt has been made to break up these molecular forces into certain smaller units but this makes the forces non-additive. Polar components such as hydrogen sulphide and carbon dioxide would, therefore, tend to form solutions deviating from regular solution behavior.

4) The intermolecular forces are considered to be radial and of similar form, which is an oversimplification for polar molecules and for molecules such as paraffins which are far from being spherical. The deviations from regularity obviously depend upon the magnitude and location of dipoles. Large and exposed rather than buried dipoles cause greater deviations from regularity.

5) Repulsive forces are simplified by assuming them to be uniform, radial, and of high inverse power type. This simplification has proved adequate only for spherical, non-polar molecules. Both hydrogen sulphide and carbon dioxide are non-spherical molecules and the former has a large dipole moment while the latter, a large quadruple moment.

6) The constants of attraction between unlike molecules are assumed to be the geometric mean of these between like

molecules (Berthelot Relation). This assumption may no longer be valid in the presence of polar components and non-condensible components, which exist as a hypothetical liquid.

7) The segregating effect of unequal attractive forces is assumed to be completely overcome by thermal agitation. This assumption may not be fulfilled for paraffin solutions at high pressures, in the presence of non-condensible and non-hydrocarbon components.

8) The change of volume on mixing is assumed negligible, a serious assumption in the presence of non-condensible components. If the volume change on mixing is positive, it will be accompanied by increased entropy of mixing and vice versa.

9) The effect of temperature on the solubility parameter is neglected, and one constant value for each component is used for all conditions of pressure and temperature. This might, very easily, be an oversimplification, especially in characterization of non-condensible components in different solvents. A knowledge of the difference between the heat capacities of liquid and vapor is necessary for an extrapolation of solubility parameter data. There are very few systems, however, for which these properties are predictable or have been determined experimentally. In cases where one constant value for the solubility parameter of a component is calculated from best fit of the

experimental vapor-liquid equilibrium data on a variety of systems containing this component, the results are too approximate to be expected to apply in the presence of all solvents, of different molecular structures.

10) A knowledge of liquid volumes of pure components is essential for application of Equation (40). Hypothetical liquids offer the greatest uncertainties in this regard and their liquid volume is a strong function of solvent characteristics. There are very few experimental data reported on partial molar liquid volumes as functions of solvent properties, pressure, and temperature. A constant value of liquid volume for all components can hardly be expected to yield more than qualitative agreement with actual solution behavior.

11) To account for the effect of pressure on activity coefficients, as pointed out previously, a knowledge of partial molar liquid volumes is essential. In the case of hypothetical liquids the problem is even more difficult. Extrapolation of liquid volumes and other physical properties to temperatures beyond the critical point of the component introduces additional uncertainties.

c) Comparison with the Wilson Equation

An attempt was made to use the Wilson equation[122] to predict vapor-liquid equilibria in the methane-hydrogen sulphide-n-butane and methane-carbon dioxide-n-butane systems.

A knowledge of binary Wilson constants is essential to predict ternary and multicomponent phase equilibria. These are calculated by a simultaneous solution of Equations (51), for known values of γ_1, γ_2, x_1, and x_2. Negative values were obtained for Wilson constants in all the component binaries of the systems of this investigation at almost all conditions of pressure and temperature. Typical results for the methane-hydrogen sulphide system are presented in Table (6). Negative Wilson constants, as seen from Equations (49) and (50), are not in accordance with the Wilson model and yield, sometimes, imaginary values of excess free energy of solution in ternary and multicomponent systems. This happens due to the logarithmic term in the expression for excess free energy of solution.

Binary activity coefficients were calculated using several methods. These were by direct calculation of the integral $\frac{1}{RT}\int_{P}^{P^V} VdP$, using extrapolated values of vapor pressure for hypothetical components; by assuming, the liquid phase obeys Raoult's law and the vapor, Dalton's law; by neglecting non-idealities of vapor solution and calculating K_{ideal} using Pitzer's modified form of the principle of corresponding states, as embodied in the Chao-Seader correlation; and by accounting for the non-idealities of vapor solution in the previous method, utilizing the Redlich and Kwong equation of state. Negative Wilson constants were obtained with all of the above methods

for calculating γ_i^1. An attempt was made to predict ternary phase equilibria by setting negative binary Wilson constants equal to zero or unity, but it was of no avail and imaginary values of ΔF^E were still encountered. Considering Wilson constants as purely empirical parameters and using their negative values as obtained also yielded imaginary values of excess free energy of solution.

Prausnitz et al[79] have found binary interaction energies to be independent of temperature, over small ranges of temperature, for many systems containing organic solvents, at low pressures. In the case of a very few binaries for which meaningful Wilson constants could be calculated, the effect of pressure and temperature on the Wilson constants was studied. It was found that both pressure and temperature affect binary interaction energies and therefore Wilson constants significantly. The results of the calculation of the Wilson constants and binary interaction energies for the methane-hydrogen sulphide system are presented in Table (6).

It is believed that negative Wilson constants are encountered due to the presence of non-condensible components. In the case of hydrocarbon systems at high pressures, for most conditions of interest, at least one of the components exists as a hypothetical liquid. Methane, for instance, at temperatures above -116.7°F, its critical temperature, is a non-condensible. An adequate characterization of the behavior of such non-condensible components, as noted previously, has not

been possible.

Eckert, Prausnitz, Orye, and O'Connell[20], in their treatment of hypothetical liquids, have utilized the Henry's law constant as the reference state for non-condensible components. The activity coefficient equations are accordingly modified to accommodate this unsymmetrical reference system. This reference state requires a knowledge of dilute solution properties of the hypothetical liquid in the solvent, which are rarely, if ever, available. These authors attempted to extrapolate the behavior of a hypothetical liquid in one solvent to its behavior in a different solvent. Experimental data on the behavior of the non-condensible component in one solvent, when it exists in a hypothetical liquid state, are still necessary. The expression presented by them for the unsymmetrical activity coefficient for non-condensible components requires a knowledge of constants in two solvents. The derivation of this equation is not very clear.

It is felt that the behavior of a non-condensible component is such a strong function of the solvent properties that no generalization of this behavior in all solvents is possible, at the present stage of understanding of the behavior of hypothetical liquids. A change in reference state, it should be remembered, is not a complete solution of the problem of hypothetical components. To account for the effect of pressure on activity coefficients, the lower limit of the

integral $\int_{p}^{P} V dP$ is hypothetical, because the system temperature is beyond the critical temperature of the component.

A review of all assumptions and sources of error involved in the use of the Wilson equation to predict vapor-liquid equilibria will be instructive at this stage. These are discussed below:

1) It is assumed that $\Delta H^E \simeq 0$, which means that all non-idealities are due to non-ideal entropy of mixing, making $\Delta F^E \simeq -T\Delta S^E$. Whether or not the term ΔH^E is actually negligible in comparison with the $-T\Delta S^E$ term for hydrocarbon systems at high pressures, in the presence of one or more non-condensible components, would dictate the usefulness of this approach to predict vapor-liquid equilibria in these systems. A comparison of these terms, presented in a later section, indicates that these terms are of an equal order of magnitude in most systems with non-condensible components. It is well to remember that the Flory-Huggins expression for excess entropy of mixing, of which the Wilson equation is an extension, was found to be useful only for solutions of chain molecules having molecular weights many times the molecular weight of the solvent.

2) Both the Wilson equation and Chao-Seader correlation have some common sources of error. These are uncertainties regarding liquid volumes, accounting for the effect of

pressure on activity coefficients, and the problem of hypothetical liquids.

3) It is not possible to find values of Wilson constants which reproduce maxima and minima in activity coefficients. The data of Robinson et al[97,98] and Hensel and Massoth[39] for the methane-carbon dioxide-hydrogen sulphide system indicate that under many conditions of pressure and temperature maxima and minima in activity coefficients are observed. The systems of the present investigation also exhibit extrema in activity coefficients which cannot be predicted using the Wilson approach. Data on the methane-hydrogen sulphide system, presented in Appendix (C), offer an example of a system which shows extrema in activity coefficients with respect to composition.

D. Excess Functions in Hydrocarbon Systems

A search through the literature has revealed that excess enthalpy for hydrocarbon systems containing non-condensible components has never been determined experimentally or calculated from data on activity coefficients. No information is available about the relative magnitude of excess properties in such systems and systems without non-condensible components. Most systems which have been satisfactorily represented assuming ideal, regular, or athermal solutions exhibit small deviations from ideality, as seen by the magnitude of excess properties. There is no reason to believe that the

systems of non-condensible components also depict small deviations from ideality and can be correlated assuming ideal enthalpy, entropy, or free energy of mixing. Since non-condensible components exist in a hypothetical state in a liquid solution,their presence may be expected to cause very much larger deviations from ideality.

In the absence of experimental data on the enthalpy of mixing, this quantity may be calculated from the temperature dependence of activity coefficients. Calorimetric measurements, if available, are undoubtedly more reliable. The calculated values, as will be shown later, may be used as an order of magnitude estimate of excess properties. The relative magnitudes of ΔH^E and $T\Delta S^E$ terms, determined from such a calculation, would enable one to see whether or not the assumption of an ideal, regular, or athermal solution is justified. This would, therefore, indicate the degree of accuracy that may be expected from the Chao-Seader correlation and the Wilson equation to predict high pressure hydrocarbon vapor-liquid equilibria.

The derivation of equations which are necessary for the calculation of the excess free energy, the excess entropy, and the excess enthalpy of mixing is outlined below. Only the expressions for binary solutions are presented. Equation (19) gives

$$\Delta F^E = RT(x_1 \ln \gamma_1 + x_2 \ln \gamma_2) \qquad (66)$$

a) Excess Entropy

Excess entropy, from equation (36) is given by,

$$\Delta S^E = -\frac{\partial}{\partial T}(\Delta F^E) \tag{67}$$

Therefore,

$$\Delta S^E = -RT\left(x_1 \frac{\partial \ln \gamma_1}{\partial T} + x_2 \frac{\partial \ln \gamma_2}{\partial T}\right)$$

$$- R(x_1 \ln \gamma_1 + x_2 \ln \gamma_2) \tag{68}$$

b) Excess Enthalpy

From equation (36),

$$\Delta H^E = -T^2 \frac{\partial}{\partial T}\left(\frac{\Delta F^E}{T}\right) \tag{69}$$

Therefore,

$$\Delta H^E = -RT^2\left(x_1 \frac{\partial \ln \gamma_1}{\partial T} + x_2 \frac{\partial \ln \gamma_2}{\partial T}\right) \tag{70}$$

The excess free energy, the excess enthalpy, and the excess entropy in a few binary hydrocarbon systems have been calculated. The procedure employed in the calculation of the excess functions from constant pressure data consisted of the following steps.

1) The activity coefficients for both components and the equilibrium temperature were plotted as a function of the liquid composition.
2) At the desired liquid composition, the values of the activity coefficients and the temperature were read off

from the above plots.

3) The activity coefficients were then plotted as a function of temperature.

4) The slope of these plots at the temperature obtained in step (2), gave the partial derivatives of the activity coefficients with respect to temperature.

5) Next, the partial derivatives $\frac{\partial \ln \gamma_i}{\partial T}$ $(= \frac{1}{\gamma_i} \frac{\partial \gamma_i}{\partial T})$ were calculated.

6) Equations (66) and (68) were then used to calculate ΔF^E and ΔH^E, respectively. According to equation (36), $T\Delta S^E$ was obtained from the difference $(\Delta H^E - \Delta F^E)$.

A sample calculation of the excess functions in the methane-hydrogen sulphide system is presented in Appendix (C). Table (7) presents the results of the calculation of excess functions for a few hydrocarbon systems at high pressures, and, for the carbon tetrachloride-benzene system at a pressure of one atmosphere. The activity coefficients were calculated using the Cavett[9] program which utilizes Pitzer's modified form of the principle of corresponding states for the liquid phase. The non-idealities of the vapor phase are accounted for using the Redlich-Kwong equation of state. For systems at atmospheric and lower pressures, the activity coefficients were calculated using Raoult's law for the liquid phase and Dalton's law for the vapor phase. Table (8) presents the excess functions obtained from the literature for a number of systems without non-condensible components. With the exceptions of the

carbon tetrachloride-benzene system and the n-pentane-n-heptane system at 147 psia, all systems of Table (7) have one non-condensible component, which exists in a hypothetical liquid state at the system temperature.

The calculated value of the excess enthalpy for the carbon tetrachloride-benzene system from Table (7) was compared with the experimental value which is presented in system (10) of Table (8). Reasonable agreement between the two sets of values is apparent. Williamson and coworkers[121] have compared the calorimetrically determined values of the enthalpy of mixing for the iso-octane-perfluoroheptane system with the values calculated from the temperature dependence of the excess free energy of mixing. For an equimolar mixture at $50^{o}F$, the experimental heat of mixing was found to be 500 cal/gm.mole. This compares reasonably well with the value 497 cal/gm.mole calculated for the heat of mixing from the temperature dependence of the free energy of mixing. The later quantity was calculated from vapor-liquid equilibrium measurements on this system. These results show that the calculation of excess function from the temperature dependence of excess free energy of mixing or of the activity coefficients yields results which are at least semi-quantitatively correct.

The following deductions can be made from the results of Table (7) and Table (8).

1) Comparison of the results of Table (8) with those of

Table (7) shows that the systems for which the magnitude of the excess functions is not very large can and have been represented fairly well using at least one of the three approaches; ideal solution, regular solution or athermal solution.

2) In systems without non-condensibles the deviations from ideality are small, as seen from the magnitude of the ΔF^E terms in Table (8). The presence of a non-condensible component results in very much larger deviations from ideality. The deviations from ideality in systems of non-condensible components increase greatly with pressure. Non-hydrocarbon components such as hydrogen sulphide and carbon dioxide also cause greater deviations.

3) For most hydrocarbon systems when one of the components is a non-condensible and the system pressure high, Table (7) indicates that the order of magnitude of the ΔH^E and the $T\Delta S^E$ terms is equal. This explains why both the Chao-Seader correlation and the Wilson equation failed to correlate vapor-liquid equilibria in these systems. Negative values of ΔF^E in Table (7) correspond to negative deviations from ideality which the Chao-Seader correlation, according to Equation (40), is totally inadequate to account for. The square term in this equation predicts all γ_i's ≥ 1.

4) A knowledge of excess functions, calculated from temperature dependence of activity coefficients or from calorimetric

measurements of the excess enthalpy of mixing, provides additional information about a system. This is the case because of the basic nature of excess functions and their easier physical interpretation. The activity coefficient is a useful function for thermodynamic consistency tests of experimental vapor-liquid equilibrium data. However, the activity coefficient by itself does not tell as much about a system as the excess functions would if they were available. To know that the activity coefficient is smaller than unity does indicate a negative deviation from ideality and thus prominence of the $T\Delta S^E$ term over the ΔH^E term. A knowledge of the actual magnitudes of these functions would, however, provide better insight into the magnitude and nature of the non-idealities. An activity coefficient of unity, $\Delta F^E = 0$, as another example, does not necessarily mean ideal solution behavior. Cancellation of non-zero ΔH^E and $T\Delta S^E$ terms might lead to this erroneous interpretation.

The above considerations point out that correlations which express ΔH^E and $T\Delta S^E$, rather than the activity coefficient, as functions of state variables would be more desirable. The ΔH^E values required for the development of such a correlation may be obtained from the temperature dependence of the activity coefficients, whenever the more reliable calorimetric measurements are not available.

A knowledge of the individual magnitude of ΔH^E and $T\Delta S^E$ terms might enable an extension of the regular and athermal solution approaches. Such extensions will be useful not for the prediction of ΔF^E, which is a measure of overall deviations from ideality, but for the calculation of the ΔH^E and $T\Delta S^E$ terms separately. Such an approach does not make assumptions of an ideal enthalpy or entropy of mixing, and for this reason, should be useful for components of many different molecular types and states.

It may also be possible to develop a general expression for ΔF^E which includes both the ΔH^E and the $T\Delta S^E$ terms. A combination of Scatchard-Hildebrand equation for ΔH^E and the Wilson equation for ΔS^E, is one possible approach. The constants for this complete expression may be calculated from experimental vapor-liquid data on component binaries and from pure component properties.

VI. CONCLUSIONS

1. An internal valve has been developed for use in experimental vapor-liquid equilibrium equipment. In conjunction with a double acting mercury pump, it can be used effectively to bring about equilibrium conditions between the two phases. The simple, inexpensive design and absence of moving parts make it a very useful mechanism. The presence of corrosive materials such as hydrogen sulphide does not influence the performance of this device.
2. Experimental vapor-liquid equilibrium data in the methane-hydrogen sulphide-n-butane system have been obtained. The investigations were conducted at pressures of 400, 800 and 1200 psia and at -20°, 40°, and 100°F at each pressure. These data cover the full range of two phase compositions.
3. Experimental vapor-liquid equilibrium compositions in the methane-carbon dioxide-n-butane system have been determined. The investigations were conducted at pressures of 400, 800, and 1200 psia and at -20°, 40°, and 100°F at each pressure; and cover the full range of two phase equilibria. A comparison with previously reported results for this same system has revealed some serious inconsistencies in the earlier work at temperatures of -20° and 40°F.

4. Hydrogen sulphide and carbon dioxide significantly influence the K-values of hydrocarbon components in vapor-liquid systems. As the concentration of H_2S or CO_2 increases from 0 to 100%, there is a significant increase in the K-values of methane and n-butane, at all conditions of pressure and temperature of this investigation.
5. The Chao-Seader correlation failed to adequately correlate the data for the systems of this investigation. The predicted K-values were not as strong functions of composition as the experimental values. In a number of binary systems for which experimental vapor-liquid equilibrium data were previously available, negative deviations from ideality ($\Delta F^E < 0$) were obtained. The Chao-Seader correlation is useful only for systems which display positive deviations from ideality. In all of these systems one of the components was a non-condensible at the system temperature.
6. The Wilson model failed to correlate binary vapor-liquid equilibrium data in the presence of a non-condensible component. The ΔH^E and the $T\Delta S^E$ terms are of an equal order of magnitude for all of the hydrocarbon systems in the presence of non-condensible components. These systems, it is reasonable to expect therefore, cannot be correlated utilizing the concepts of regular or athermal solutions.
7. The convergence pressure does not seem to be a satisfactory parameter to account for the influence of com-

position on K-values in hydrocarbon-non-hydrocarbon systems. The parameter C, being a function only of relative amounts of intermediate and heavy component in a ternary system, is not suitable for calculating the convergence pressures in the systems investigated here.

8. A comparison of excess properties in systems with non-condensible components, with simpler systems which have components which are all condensible has been made. This has indicated that the main problem of correlating vapor-liquid equilibrium data lies in the characterization of the behavior of a non-condensible component. A non-condensible component, looking from a physical point of view, is made to exist in the liquid phase due to the presence of solvent components. The behavior of such hypothetical liquids should, therefore, be strongly dependent on the structure of solvent molecules. All attempts to correlate the behavior of non-condensible components do not account for the influence of the solvent on the behavior of such hypothetical liquids.

This investigation has revealed that the present understanding of the nature of vapor-liquid equilibrium is inadequate. Before a general, comprehensive theory may be developed, a large amount of experimental data on systems of different types is essential. A knowledge of partial molar volumes of hypothetical liquids, as functions of pressure,

temperature, and composition is necessary to account for the influence of pressure on activity coefficients. This knowledge will also shed some light on the behavior of non-condensible components. The use of the Henry's law constant as the reference fugacity for non-condensible components circumvents the problem of using a hypothetical standard state. Before this approach can be useful, however, a knowledge of the Henry's law constant in the solvent of interest is essential.

The excess properties such as excess enthalpy and excess entropy of mixing appear to be useful functions for interpretation of experimental vapor-liquid equilibrium data. Two approaches for developing a correlation for the excess functions in terms of state variables have been suggested.

NOMENCLATURE

A	van Laar constant
B	van Laar constant
E	molal energy
F	molal free-energy
H	molal enthalpy
K	equilibrium ratio
L	percent liquid in the system
N	number of components in a mixture or number of data points
P	total pressure of system
P(i/j)	probability of finding a molecule of type i, compared to finding a molecule of type j
R	gas constant
S	molal entropy
T	temperature of system
V	liquid molal volume
Z	effective volume fraction
a	constant of interaction
$\bar{a}$	activity of a component
f	fugacity of a component
f',f",f"'	denotes a function of variables
n	number of moles of a component
p	partial pressure of a component
p^V	vapor pressure of a component
q	effective molal volume

v	molal volume of liquid or vapor
x	mole fraction in liquid phase
y	mole fraction in vapor phase

Greek Letters

Δ	denotes a small increment or difference
Λ	Wilson constant
Σ	denotes summation over a variable
α	relative volatility
γ	activity coefficient
δ	solubility parameter
λ	binary interaction energy
ν	fugacity coefficient in pure liquid state
ξ	local volume fraction
ϕ	volume fraction
ϕ'	fugacity coefficient in vapor mixture

Superscripts

v	vapor phase
l	liquid phase
E	excess property
V	vaporization
*	indicates that the unsymmetrical reference system has been used
o	standard state

Subscripts

i	i^{th} component
j	j^{th} component, etc.
cv	convergence pressure
mix	mixing property
ideal	ideal solution property
-	a bar at top denotes value of property in a mixture

BIBLIOGRAPHY

1. Adler, S.B., Friend, L., and Pigford, R.L.; A.I.Ch.E.J. 12, No. 4, 629 (1966).

2. Barker, J.A.; Australian J. Chem. 6, 207 (1953).

3. Benedict, M., Webb, G.B., Rubin, L.C.; J. Chem. Phys. Part I, 8, 334 (1940); Part II, 10, 747 (1942); Chem. Eng. Prog., Part III, 47 419 (1951); Part IV, 47, 449 (1951); Part V, 47, 571 (1951); and Part VI, 47, 609 (1951).

4. Bierlin, J.A. and Kay, W.B.; Ind. Eng. Chem. 45, 618 (1953).

5. Black, K.; Ind. Eng. Chem. 50, 403 (1958); 50, 391 (1958); 51, 211 (1959).

6. Cajander, B.C., Hipkin, H.G., and Lenoir, J.M.; J. Chem. Eng. Data, 5, 251 (1960).

7. Carlson, H.C. and Colburn, A.P.; Ind. Eng. Chem. 34, 581 (1942).

8. Carter, R.T., Sage, B.H., and Lacey, W.N.; Am. Inst. Mining Met. Engrs. Tech. Pub. 1250 (Oct. 1940).

9. Cavett, R.H.; Proc. Am. Pet. Inst. 42, No. 3, 351 (1962).

10. Chao, K.C. and Seader, J.D.; A.I.Ch.E.J. 7, 598 (1961).

11. Chueh, P.L., Muirbrook, N.K., and Prausnitz, J.M.; A.I. Ch.E.J. 11, 1097 (1965).

12. Clark, A.M.; Trans. Faraday Soc. 41, 718 (1945).

13. Clark, A.M. and Din., F.; Discussions Faraday Soc. 15, 202 (1953).

14. Curl, R.F. and Pitzer, K.S.; Ind. Eng. Chem. 50, 265 (1958).

15. Dalton, J.P.; Mem. Literary Phil. Soc. Manchester, 1, (1805).

16. Davis, J.A., Rodewald, N., and Kurata, F.; A.I.Ch.E.J. 8, 537 (1962).

17. Deal, C.H., Derr, E.L., and Papadopoulos, M.N.; I. and E.C. Fundamentals, 1 (1), 17 (1962).

18. DePriester, C.L.; Chem. Eng. Prog. Sym. Ser. 49, No. 7, 1 (1953).

19. Donnelly, H.G. and Katz, D.L.; Ind. Eng. Chem. 46, 511 (1954).

20. Eckert, C.A., Prausnitz, J.M., Orye , R.V. and O'Connell, J.P.; "Advances in Separation Techniques", A.I. Ch.E. - I. Chem. E. Joint Meeting, London, 1, No. 7, 58 (1965).

21. Edmister, W.C.; "Applied Hydrocarbon Thermodynamics", Gulf Publishing Company, Houston, Texas (1961).

22. Edmister, W.C. and Ruby, C.L.; Chem. Eng. Prog. 51, No. 2, 95-F (1955).

23. Edwards, B.S., Hashmall, F., Gilmont, R. and Othmer, D.F.; Ind. Eng. Chem. 46, 194 (1954).

24. Erdős, E.; Chem. Listy 50, 503 (1956); Coll. Czech Chem. Comm. 21, 1528 (1956).

25. Ewell, R.H., Harrison, J.M. and Berg, L.; Ind. Chem. Eng. 36, 871 (1944).

26. Flory, P.J.; J. Phys. Chem. 10, 51 (1942).

27. Francis, A.W.; Ind. Eng. Chem. 36, 764 (1944).

28. Gilmont, R.; Ind. Eng. Chem. 42, 1607 (1950).

29. Gilmont, R.; Ind. Eng. Chem. 44, 1450 (1952).

30. Gilmont,R. and Othmer, D.F., Ind. Eng. Chem. 36, 1061 (1944).

31. Gilmont, R., Weinman, E.A., Miller, E., Hashmall, F., and Othmer, D.F., Ind.Eng.Chem. 42, 120 (1950).

32. Grayson, H.G. and Streed, C.W.; "Vapor-Liquid Equilibria for High Temperature, High Pressure Hydrogen-Hydrocarbon Systems", Sixth World Petroleum Congress, Frankfurt/Main, June 19-26, 1963.

33. Guggenheim, E.A.; "Mixtures", Oxford University Press (1952).

34. Guggenheim, E.A.; "Thermodynamics", North Holland Publishing Co., Amsterdam (1957).

35. Hadden, S.T.; Chem. Eng. Prog. Sym. Ser. 49, No. 7, 53 (1953).

36. Hadden, S.T. and Grayson, H.C.; Petroleum Refiner, 40, 207 (1961).

37. Hala, E., Fried, V., Pick, J., and Vilim, O.; Chem. Listy., 50, 343 (1956); Coll. Czech, Chem. Communn. 21, 1381 (1956).

38. Hala, E., Pick, J., Fried V., and Vilim, O.; "Vapor-Liquid Equilibrium", Permagon Press, New York (1958).

39. Hensel, W.E., Jr. and Massoth, F.E.; J. Chem. & Eng. Data; 9, 352 (1964).

40. Hildebrand, J.H.; J. Am. Chem. Soc., 51, 66 (1929).

41. Hildebrand, J.H.; Chem. Revs. 44, 37 (1949).

42. Hildebrand, J.H. and Scott, R.L., "Regular Solutions", Prentice-Hall, Inc., New Jersey (1962).

43. Hirata, M.; Chem. Eng. (Japan) 13, 138 (1949).

44. Hirata, M.,; Japan Sci Rev. Ser. I. 2, No. 3, 265, (1952).

45. Holland, C.D.; "Multicomponent Distillation", Prentice-Hall Inc. New Jersey (1963).

46. Hougen, O.A., Watson, K.M., and Ragatz, R.A.; "Chemical Process Principles", Asia Publishing House, Bombay (1962).

47. Huggins, M.L.; Ann. N.Y. Acad. Sci., 43, 1 (1942).

48. Hughes, R.E.; "Vapor-Liquid Equilibria in Hydrogen Sulphide-n-Butane Systems", M.Sc. thesis, Library, University of Alberta, Edmonton (1963).

49. Ju Chin Chu; "Distillation Equilibrium Data", Reinhold, New York (1950).

50. Katz, D.L. and Hackmuth, K.H.; Ind. Eng. Chem. 29, 1072 (1937).

51. Kohn, J.P. and Kurata, F.; A.I.Ch.E. Journal, 4, 211 (1958).

52. Kretschmer, C.B. and Wiebe, R., J. Am. Chem. Soc. 71, 1743 and 3176 (1949).

53. Kuo Tsung Ju and Coull, J.; Chem. Eng. Prog. Symp. Ser. 48, No. 2, 38 (1952).

54. Kurata, F. and Sobocinski, D.P.; A.I.Ch.E.J., 5, 545 (1959).

55. Leland, T.W., Chappelear, P.A., and Gamson, B.W.; A.I.Ch.E.J. 8, 489 (1962).

56. Leland, T.W. and Mueller, W.H.; Ind. Eng. Chem. 51, 597 (1959).

57. Lenoir, J.M.; A.I.Ch.E.J. 4, 263 (1958).

58. Lenoir, J.M. and White, G.A.; 32, 115 and 121 (1953) Pet. Refiner.

59. Lenoir, J.M. and White, G.A.; Pet.Ref., 37, 173 (1958).

60. Levy, R.M.; Ind. Eng. Chem. 33, 928 (1941).

61. Lewis, G.N. and Randall, M., Pitzer, K.S. and Brewer, L.; "Thermodynamics", Second Edition, McGraw-Hill, New York (1961).

62. Lewis, W.K. and Kay, W.C.; Oil and Gas J., p. 40 (March 27, 1934).

63. Li, Y.M. and Coull, J.J.; Inst. Petrol. 34, 692 (1948).

64. Longuet-Higgins, H.C.; Proc. Roy. Soc. A205, 247 (1951).

65. Lu, B.C.Y., Li, J.C.M., and Ting, T.W.; Ind. Eng. Chem. 51, 219 (1959).

66. Lydersen, A.L., Greenkorn, R.A. and Hougen, O.A.; University of Wisconsin Engineering Experimental Station, Report No. 4, Madison, Wisconsin (1955).

67. Mayo, F.R. and Lewis, F.H.; J. Am. Chem. Soc. 66, 1594 (1944).

68. Margules, M.; S.B. Akad. Wiss. Wien. Math. Naturw. Kl. II, 104, 1243 (1895).

69. Musil, A. and Schramke, E.; Acta Phys. Austr. 3, 137 and 309 (1949).

70. Muskat, M.; "Physical Principles of Oil Production", McGraw-Hill Book Co., New York (1949).

71. Myers, H.S. and Lenoir, J.M.; Pet. Refiner, 36, 167 (1957).

72. Natural Gas Processors' Association,"New Constants for Chao-Seader Correlation for N_2, H_2S and CO_2", Tulsa, Oklahoma (1965).

73. "Natural Gasoline Producers' and Suppliers' Association Engineering Data Book", Tulsa, Oklahoma (1958).

74. Neberbraght, G.W.; Ind. Eng. Chem. 30, 587 (1938).

75. Nord, M.; Chem. Eng. Prog. Sym. Ser. 48, No. 3, 55 (1952).

76. Norrish, R.S. and Twigg, G.H.; Ind. Eng. Chem. 46, 201 (1954).

77. O'Connell, J.P. and Prausnitz, J.M.; I. and E.C. Fundamentals, 3, 347 (1964).

78. Olds, R.H., Reamer, H.H., Sage, B.H. and Lacey, W.N.; Ind. Eng. Chem. 41, 475 (1949).

79. Orye, R.V. and Prausnitz, J.M.; Ind. Eng. Chem. 57, 18 (1965).

80. Othmer, D.F. and Gilmont, R.; Ind. Eng. Chem. 36, 858 (1944); 40, 2118 (1948).

81. Pierotti, G.J., Deal, C.H., and Derr, E.L.; Ind. Eng. Chem. 51, 95 (1959).

82. Pitzer, K.S.; J. Am. Chem. Soc. 77, 3427 (1955); 79 2369 (1957).

83. Poettmann, F.H. and Katz, D.L.; Ind. Eng. Chem. 37, 847 (1945).

84. Prahl, W.H.; Ind. Eng. Chem. 43, 1767 (1951).

85. Prausnitz, J.M.; Chem. Eng. Sci. 18, 613 (1963).

86. Prigogine, I.; "Molecular Theory of Solutions", North Holland Publishing Co. (1957).

87. Prigogine, I. and Defay, R.; "Chemical Thermodynamics", Longmans Green and Co. London (1950).

88. Raoult, F.M.; Compt. Rend. 104, 1430 (1887).

89. Reamer, H.H.; Korpi, K.J., Sage, B.H., and Lacey, W.N.; Ind. Eng. Chem. 59, 206 (1947).

90. Reamer, H.H., Sage, B.H. and Lacey, W.N.; Ind. Eng. Chem. 43, 976 (1951).

91. Redlich, O.; Chem. Rev. 44, 1 (1949).

92. Redlich, O. and Kister, A.T.; Ind. Eng. Chem. 40, 345 (1948).

93. Redlich, O. and Kister, A.T.; J. Amer. Chem. Soc. 71, 505 (1949).

94. Redlich, O., Kister, A.T. and Turnquist, C.E., Chem. Eng. Prog. Symp. Seri, 48, No. 2, 49 (1952).

95. Redlich, O. and Kwong, J.N.W.; Chem. Rev. 44, 233 (1949).

96. Rigas, D.F., Mason, D.F., and Thodos, G.; Ind. Eng. Chem. 50, 1297 (1958).

97. Robinson, D.B. and Bailey, J.A.; Can. J. Chem. Eng. 35, 151 (1957).

98. Robinson, D.B., Lorenzo, A.P. and Macrygeorgos, C.A.; Can. J. Chem. Eng. 37, 212 (1959).

99. Robinson, D.B. and Saxena, A.C., "Hydrocarbon K-Ratios in the Presence of Hydrogen Sulphide and Carbon Dioxide", paper presented at the C.I.C. Conference, Saskatoon, June (1966).

100. Sage, B.H., Budenholzer, R.A., and Lacey, W.N.; Ind. Eng. Chem. 32, 1262 (1940).

101. Sage, B.H., Hicks, B.L., and Lacey, W.N.; Ind. Eng. Chem. 32, 1085 (1940).

102. Sandercock, J.A.W.; "Equipment for Phase Behavior Studies: The Hydrogen Sulphide -n-Butane System at 100°F" M.Sc. Thesis, Library, University of Alberta, Edmonton, (1962).

103. Saxena, A.C.; "Phase Equilibria in a Quaternary Natural Gas System", Unpublished M.Sc. Thesis, Library, University of Alberta, Edmonton, (1964).

104. Scatchard, G.; Trans. Faraday Soc. 33, 160 (1937).

105. Scatchard, G.; Ann. Rev. Phys. Chem. 3, 269 (1952).

106. Scatchard, G.; Chem. Rev. 8, 321 (1931); J. Am. Chem. Soc. 56, 995 (1934); and Trans. Faraday Soc. 33, 160 (1937).

107. Scatchard, G. and Hamer, W.G.; J. Am. Chem. Soc. 57, 1805 (1935).

108. Scheibel, E.G. and Friedland, N.; Ind. Eng. Chem. 39, 1329 (1947).

109. Scott, R.L.; Chem. Phys. 25, 193 (1956).

110. Smith, K.A. and Smith, R.B.; Petroleum Processing 4, Dec. 1949.

111. Souders, M., Selheimer, C.W. and Brown G.G.; Ind. Eng. Chem. 24, 517 (1932).

112. Spinner, I.H., Lu, B.C.Y., and Graydon, W.F., Ind. Eng. Chem. 48, 147 (1956).

113. Steckel, F.; Svensk, Kem. Tid. 57, 209 (1945).

114. Sweeney, R.F. and Rose, A.; A.I.Ch.E.J. 9, 390, (1963).

115. Thiel, A. and Schultz, E.; Univ. Marburg Z. Physik. Chem. 96, 312 (1920).

116. van Laar, J.J.; Z. Phys. Chem. 72, 723 (1910).

117. van Laar, J.J.; Z. Phys. Chem. 185, 35 (1929).

118. Wall, F.T.; J. Am. Chem. Soc., 66, 2050 (1944).

119. Wang. R.H. and McKetta, J.J.; J. Chem. and Eng. Data, 9, 30 (1964).

120. White, R.R.; Trans. Am. Inst. Chem. Engrs., 41, 546, (1945).

121. Williamson, A.G., Scott, R.L. and Dunlap, R.D.; J. Chem. Phys. 30, 325 (1959); Williamson, A.G. and Scott, R.L.; J. Phys. Chem. 65, 275 (1961).

122. Wilson, G.M.; J. Am. Chem. Soc. 86, 127 (1964).

123. Wilson, G.M. and Deal, C.H.; I. and E.C. Fundamentals, 1, 20 (1962).

124. Winn, F.W.; Chem. Eng. Prog. Symp. Ser. 48, No. 2, 121 (1952).

125. Wohl, K.; Trans. Am. Inst. Chem. Engrs., 42, 215 (1946).

126. Wohl, K.; Chem. Eng. Prog., 49, 218 (1953).

APPENDIX A

TABULATIONS

Table 1

Experimental Data in the CH_4-H_2S-nC_4H_{10} System

(all compositions are in mole fractions)

Run No.	Vapor Phase			Liquid Phase		
	CH_4	H_2S	$n\text{-}C_4H_{10}$	CH_4	H_2S	$n\text{-}C_4H_{10}$
		100°F			400 psia	
A-1	0.8240	-	0.1760	0.1220	-	0.8780
A-2	0.0120	0.988	-	0.0010	0.9990	-
A-3	0.3992	0.4907	0.1101	0.0738	0.5212	0.4050
A-4	0.3523	0.5479	0.0998	0.0690	0.6307	0.3003
A-5	-	-	-	0.1189	0.1411	0.7400
A-6	-	-	-	0.0745	0.5726	0.3529
A-7	0.2141	0.7280	0.0579	0.0392	0.7808	0.1800
A-8	0.4940	0.3809	0.1251	-	-	-
A-9	0.6751	0.1487	0.1762	-	-	-
A-10	0.7465	0.0840	0.1695	0.1236	0.0885	0.7878
A-11	0.5955	0.2543	0.1502	0.1086	0.2692	0.6222
A-12	-	-	-	0.1401	0.1055	0.7544
		100°F			800 psia	
A-13	0.8770	-	0.1230	0.2540	-	0.7460
A-14	0.4050	0.5950	-	0.0510	0.9490	-
A-15	-	-	-	0.1053	0.7413	0.1534
A-16	-	-	-	0.1247	0.6392	0.2361
A-17	0.5700	0.3400	0.0900	-	-	-
A-18	-	-	-	0.2155	0.2545	0.5300
A-19	0.6061	0.3016	0.0923	0.1867	0.4073	0.4060
A-20	0.7240	0.1530	0.1230	0.2503	0.1569	0.5928
A-21	0.7926	0.0877	0.1196	0.2442	0.1184	0.6374
A-22	0.6309	0.2655	0.1035	0.2093	0.3584	0.4323
		100°F			1200 psia	
A-23	0.8800	-	0.1200	0.3810	-	0.6190
A-24	0.5080	0.4910	-	0.1100	0.8900	-
A-25	0.7084	0.1834	0.1082	0.3471	0.2599	0.3930
A-26	0.6450	0.2550	0.1000	0.3022	0.3887	0.3091
A-27	0.5160	0.4559	0.0281	0.1909	0.7136	0.0955
A-28	-	-	-	0.2068	0.6826	0.1106
A-29	0.5720	0.3508	0.0772	0.2810	0.4780	0.2401
A-30	-	-	-	0.2290	0.6208	0.1502
A-31	0.7640	0.1170	0.1191	0.3810	0.1463	0.4727

Table 1 (continued)

Run No.	Vapor Phase CH_4	Vapor Phase H_2S	Vapor Phase $n\text{-}C_4H_{10}$	Liquid Phase CH_4	Liquid Phase H_2S	Liquid Phase $n\text{-}C_4H_{10}$
		40°F			400 psia	
B-1	0.9278	-	0.0722	0.1977	-	0.8023
B-2	0.5130	0.4870	-	0.0350	0.9650	-
B-3	0.5979	0.3049	0.0972	0.1286	0.4574	0.4140
B-4	0.6932	0.2087	0.0982	0.1663	0.3153	0.5184
B-5	0.7461	0.1436	0.1103	0.1685	0.1900	0.6415
B-6	0.5620	0.3678	0.0702	0.1131	0.6153	0.2716
B-7	0.6962	0.1887	0.1151	0.1688	0.2717	0.5596
B-8	-	-	-	0.1726	0.2653	0.5621
		40°F			800 psia	
B-9	0.9560	-	0.0440	0.4070	-	0.5930
B-10	0.6900	0.3100	-	0.0900	0.9100	-
B-11	0.7610	0.1861	0.0529	0.3002	0.3826	0.3172
B-12	0.7260	0.2240	0.0500	-	-	-
B-13	0.7168	0.2321	0.0511	0.2694	0.4781	0.2525
B-14	-	-	-	0.2576	0.4849	0.2576
B-15	0.8708	0.0930	0.0362	0.3449	0.2460	0.4092
B-16	0.8558	0.0933	0.0509	0.3549	0.2368	0.4083
B-17	0.8870	0.0683	0.0447	0.3688	0.1639	0.4673
B-18	0.8986	0.0635	0.0379	0.3790	0.1878	0.4332
B-19	-	-	-	0.3756	0.1616	0.4629
B-20	0.9015	0.0543	0.0442	0.3845	0.1402	0.4753
		40°F			1200 psia	
B-21	0.9496	-	0.0504	0.5670	-	0.4330
B-22	0.7270	0.2730	-	0.1620	0.8380	-
B-23	0.7555	0.1793	0.0452	0.4350	0.3588	0.2062
B-24	0.8706	0.0747	0.0547	0.5145	0.1797	0.3058
B-25	0.8810	0.0638	0.0550	0.5210	0.1634	0.3156
B-26	0.9074	0.0526	0.0400	0.5479	0.1482	0.3039
B-27	0.9110	0.0412	0.0477	-	-	-
B-28	0.9217	0.0455	0.0328	0.5406	0.1419	0.3175

Table 1 (continued)

Run No.	Vapor Phase CH_4	Vapor Phase H_2S	Vapor Phase $n\text{-}C_4H_{10}$	Liquid Phase CH_4	Liquid Phase H_2S	Liquid Phase $n\text{-}C_4H_{10}$
		$-20^{\circ}F$			400 psia	
C-1	0.9566	-	0.0434	0.2935	-	0.7065
C-2	0.7970	0.2030	-	0.0535	0.9465	-
C-3	0.8808	0.0959	0.0233	0.2305	0.3202	0.4493
C-4	0.9090	0.0620	0.0290	0.2592	0.1814	0.5594
C-5	0.8490	0.1255	0.0255	0.1925	0.4635	0.3440
C-6	0.8365	0.1404	0.0232	0.1589	0.5677	0.2733
C-7	0.8879	0.0853	0.0268	0.2297	0.3186	0.4516
		$-20^{\circ}F$			800 psia	
C-8	0.9783	-	0.0217	0.4991	-	0.5009
C-9	0.8786	0.1214	-	0.1371	0.8629	-
C-10	0.9392	0.0390	0.0218	0.4673	0.1512	0.3815
C-11	0.9367	0.0325	0.0308	0.4740	0.1464	0.3796
C-12	0.9070	0.0777	0.0153	0.4215	0.3150	0.2635
C-13	0.8888	0.0963	0.0149	0.3623	0.4739	0.1638
C-14	0.8968	0.0896	0.0135	0.3816	0.4199	0.1985
		$-20^{\circ}F$			1200 psia	
C-15	0.9721	-	0.0279	0.7078	-	0.2922
C-16	0.8580	0.1420	-	0.2110	0.7890	-
C-17	-	-	-	0.6029	0.2494	0.1476
C-18	0.9019	0.0749	0.0232	0.6146	0.2232	0.1622
C-19	0.8914	0.0944	0.0142	0.5580	0.3232	0.1188

Table 2

Smoothed Data in the CH_4-H_2S-nC_4H_{10} System

(all compositions are in mole fractions)

Vapor Phase			Liquid Phase			Equilibrium Ratios		
CH_4	H_2S	$n\text{-}C_4H_{10}$	CH_4	H_2S	$n\text{-}C_4H_{10}$	CH_4	H_2S	$n\text{-}C_4H_{10}$
			100°F and 400 psia					
0.737	0.096	0.167	0.120	0.100	0.780	6.142	0.960	0.214
0.670	0.171	0.159	0.112	0.200	0.688	5.982	0.855	0.231
0.575	0.280	0.145	0.105	0.300	0.595	5.476	0.933	0.244
0.500	0.370	0.130	0.095	0.400	0.505	5.263	0.925	0.257
0.415	0.473	0.112	0.086	0.500	0.414	4.826	0.946	0.271
0.335	0.571	0.094	0.073	0.600	0.327	4.589	0.952	0.288
0.265	0.660	0.075	0.058	0.700	0.242	4.569	0.943	0.310
0.200	0.744	0.056	0.043	0.800	0.157	4.651	0.930	0.357
0.119	0.848	0.033	0.023	0.900	0.077	5.174	0.942	0.429
0.824	-	0.176	0.122	-	0.878	6.754	-	0.201
0.012	0.988	-	0.001	0.999	-	12.000	0.989	-
			100°F and 800 psia					
0.800	0.077	0.123	0.243	0.100	0.657	3.292	0.770	0.187
0.735	0.145	0.120	0.225	0.200	0.575	3.267	0.725	0.209
0.662	0.230	0.108	0.206	0.300	0.494	3.214	0.767	0.219
0.608	0.297	0.095	0.187	0.400	0.413	3.251	0.743	0.230
0.563	0.355	0.082	0.165	0.500	0.335	3.412	0.710	0.245
0.512	0.428	0.060	0.142	0.600	0.258	3.606	0.713	0.233
0.470	0.488	0.042	0.117	0.700	0.183	4.017	0.697	0.230
0.438	0.539	0.023	0.090	0.800	0.110	4.867	0.674	0.209
0.422	0.568	0.010	0.064	0.900	0.036	6.594	0.631	0.278
0.877	-	0.123	0.254	-	0.746	3.453	-	0.165
0.405	0.595	-	0.051	0.949	-	7.941	0.627	-
			100°F and 1200 psia					
0.797	0.083	0.120	0.374	0.100	0.526	2.131	0.830	0.228
0.737	0.146	0.117	0.358	0.200	0.442	2.059	0.730	0.265
0.680	0.210	0.110	0.336	0.300	0.364	2.024	0.700	0.302
0.630	0.271	0.099	0.307	0.400	0.293	2.052	0.678	0.338
0.565	0.367	0.068	0.274	0.500	0.226	2.062	0.734	0.301
0.538	0.417	0.043	0.237	0.600	0.163	2.270	0.695	0.276
0.525	0.445	0.030	0.195	0.700	0.105	2.692	0.636	0.286
0.514	0.472	0.014	0.152	0.800	0.048	3.382	0.590	0.292
0.880	-	0.120	0.381	-	0.619	2.310	-	0.194
0.508	0.492	-	0.110	0.890	-	4.618	0.553	-

Table 2 (continued)

Vapor Phase			Liquid Phase			Equilibrium Ratios		
CH_4	H_2S	$n\text{-}C_4H_{10}$	CH_4	H_2S	$n\text{-}C_4H_{10}$	CH_4	H_2S	$n\text{-}C_4H_{10}$
			40°F and 400 psia					
0.828	0.074	0.098	0.187	0.100	0.713	4.428	0.740	0.137
0.735	0.154	0.111	0.175	0.200	0.625	4.200	0.770	0.178
0.686	0.204	0.110	0.162	0.300	0.538	4.235	0.680	0.205
0.630	0.270	0.100	0.148	0.400	0.452	4.257	0.675	0.221
0.587	0.329	0.084	0.134	0.500	0.366	4.381	0.658	0.230
0.570	0.360	0.070	0.117	0.600	0.283	4.872	0.600	0.247
0.548	0.400	0.052	0.098	0.700	0.202	5.592	0.571	0.257
0.533	0.435	0.032	0.077	0.800	0.123	6.922	0.544	0.260
0.522	0.468	0.010	0.053	0.900	0.047	9.849	0.520	0.213
0.928	-	0.072	0.198	-	0.802	4.687	-	0.090
0.513	0.487	-	0.035	0.965	-	14.657	0.505	-
			40°F and 800 psia					
0.915	0.039	0.046	0.390	0.100	0.510	2.346	0.390	0.090
0.877	0.075	0.048	0.364	0.200	0.436	2.409	0.375	0.110
0.822	0.128	0.050	0.335	0.300	0.365	2.454	0.427	0.137
0.755	0.197	0.048	0.300	0.400	0.300	2.517	0.493	0.160
0.725	0.232	0.043	0.263	0.500	0.237	2.757	0.464	0.181
0.711	0.256	0.033	0.223	0.600	0.177	3.188	0.427	0.186
0.701	0.276	0.023	0.182	0.700	0.118	3.852	0.394	0.195
0.695	0.293	0.012	0.138	0.800	0.062	5.036	0.366	0.194
0.956	-	0.044	0.407	-	0.593	2.349	-	0.074
0.690	0.310	-	0.090	0.910	-	7.667	0.341	-
			40°F and 1200 psia					
0.905	0.045	0.050	0.545	0.100	0.355	1.661	0.450	0.141
0.835	0.108	0.057	0.508	0.200	0.292	1.644	0.540	0.195
0.777	0.160	0.063	0.464	0.300	0.236	1.675	0.533	0.267
0.747	0.195	0.058	0.416	0.400	0.184	1.796	0.488	0.315
0.734	0.216	0.050	0.363	0.500	0.137	2.022	0.432	0.365
0.726	0.237	0.037	0.303	0.600	0.097	2.396	0.395	0.381
0.724	0.252	0.024	0.241	0.700	0.059	3.004	0.360	0.407
0.725	0.260	0.015	0.174	0.800	0.026	4.167	0.325	0.577
0.950	-	0.050	0.567	-	0.433	1.676	-	0.116
0.727	0.273	-	0.162	0.838	-	4.488	0.326	-

Table 2 (continued)

Vapor Phase			Liquid Phase			Equilibrium Ratios		
CH_4	H_2S	$n\text{-}C_4H_{10}$	CH_4	H_2S	$n\text{-}C_4H_{10}$	CH_4	H_2S	$n\text{-}C_4H_{10}$
			$-20^{\circ}F$ and 400 psia					
0.925	0.039	0.036	0.275	0.100	0.625	3.364	0.390	0.058
0.900	0.067	0.033	0.254	0.200	0.546	3.543	0.335	0.060
0.885	0.085	0.030	0.232	0.300	0.468	3.815	0.283	0.064
0.860	0.116	0.024	0.206	0.400	0.394	4.175	0.290	0.061
0.852	0.126	0.022	0.182	0.500	0.318	4.681	0.252	0.069
0.840	0.143	0.017	0.154	0.600	0.246	5.455	0.238	0.069
0.827	0.160	0.013	0.125	0.700	0.175	6.616	0.229	0.074
0.812	0.182	0.006	0.096	0.800	0.104	8.458	0.228	0.058
0.805	0.192	0.003	0.067	0.900	0.033	12.015	0.213	0.091
0.957	-	0.043	0.294	-	0.706	3.255	-	0.061
0.797	0.203	-	0.054	0.946	-	14.759	0.215	-
			$-20^{\circ}F$ and 800 psia					
0.946	0.030	0.024	0.483	0.100	0.417	1.959	0.300	0.058
0.915	0.060	0.025	0.462	0.200	0.338	1.981	0.300	0.074
0.902	0.078	0.020	0.431	0.300	0.269	2.093	0.260	0.074
0.895	0.088	0.017	0.393	0.400	0.207	2.277	0.220	0.082
0.887	0.103	0.010	0.347	0.500	0.153	2.556	0.206	0.065
0.886	0.107	0.007	0.295	0.600	0.105	3.003	0.178	0.067
0.885	0.110	0.005	0.238	0.700	0.062	3.719	0.157	0.081
0.884	0.112	0.004	0.176	0.800	0.024	5.023	0.140	0.167
0.978	-	0.022	0.499	-	0.501	1.960	-	0.044
0.879	0.121	-	0.137	0.863	-	6.416	0.140	-
			$-20^{\circ}F$ and 1200 psia					
0.933	0.040	0.027	0.673	0.100	0.227	1.386	0.400	0.119
0.910	0.066	0.024	0.627	0.200	0.173	1.451	0.330	0.139
0.893	0.087	0.020	0.574	0.300	0.126	1.556	0.290	0.159
0.880	0.106	0.014	0.510	0.400	0.090	1.726	0.265	0.156
0.874	0.117	0.009	0.443	0.500	0.057	1.973	0.234	0.158
0.866	0.129	0.005	0.366	0.600	0.034	2.366	0.215	0.147
0.864	0.133	0.003	0.286	0.700	0.014	3.021	0.190	0.214
0.972	-	0.028	0.708	-	0.292	1.373	-	0.096
0.858	0.142	-	0.211	0.789	-	4.066	0.180	-

Table 3

Experimental Data in the CH_4-CO_2-nC_4H_{10} System

Run No.	Vapor Phase			Liquid Phase		
	CH_4	CO_2	$n\text{-}C_4H_{10}$	CH_4	CO_2	$n\text{-}C_4H_{10}$
		100°F			400 psia	
A-1	0.472	0.349	0.179	0.070	0.132	0.798
A-2	0.541	0.281	0.178	0.084	0.099	0.807
A-3	0.231	0.587	0.182	0.030	0.225	0.745
A-4	0.824	-	0.176	0.122	-	0.878
A-5	-	0.820	0.180	-	0.300	0.700
		100°F			800 psia	
A-6	0.466	0.412	0.122	0.169	0.275	0.556
A-7	0.713	0.158	0.129	0.224	0.094	0.682
A-8	0.199	0.694	0.107	0.073	0.549	0.378
A-9	0.877	-	0.123	0.254	-	0.746
A-10	-	0.920	0.080	-	0.735	0.265
		100°F			1200 psia	
A-11	0.464	0.429	0.107	-	-	-
A-12	0.399	0.487	0.114	0.212	0.445	0.343
A-13	0.520	0.369	0.111	0.260	0.313	0.427
A-14	0.237	0.656	0.107	0.152	0.595	0.253
A-15	0.743	0.140	0.117	0.336	0.122	0.542
A-16	-	-	-	0.203	0.458	0.339
A-17	0.880	-	0.120	0.381	-	0.619
		40°F			400 psia	
B-1	0.732	0.183	0.085	0.155	0.090	0.755
B-2	0.571	0.334	0.095	0.117	0.178	0.705
B-3	0.414	0.487	0.099	0.094	0.297	0.608
B-4	0.175	0.735	0.090	0.029	0.479	0.492
B-5	0.928	-	0.072	0.198	-	0.802
B-6	-	0.930	0.070	-	0.568	0.432

Table 3 (continued)

Run No.	Vapor Phase CH_4	Vapor Phase CO_2	Vapor Phase $n\text{-}C_4H_{10}$	Liquid Phase CH_4	Liquid Phase CO_2	Liquid Phase $n\text{-}C_4H_{10}$
		40°F			800 psia	
B-7	0.663	0.284	0.053	0.271	0.250	0.479
B-8	0.777	0.169	0.054	0.331	0.141	0.528
B-9	0.287	0.699	0.014	0.093	0.827	0.080
B-10	0.504	0.447	0.049	0.210	0.417	0.373
B-11	0.956	-	0.044	0.407	-	0.593
B-12	0.214	0.786	-	0.062	0.938	-
		40°F			1200 psia	
B-13	0.789	0.157	0.054	0.476	0.166	0.358
B-14	0.331	0.660	0.009	0.209	0.765	0.026
B-15	0.553	0.403	0.044	0.328	0.467	0.205
B-16	0.950	-	0.050	0.567	-	0.433
B-17	0.308	0.692	-	0.194	0.806	-
		-20°F			400 psia	
C-1	-	-	-	0.136	0.590	0.274
C-2	-	-	-	0.043	0.947	0.010
C-3	0.518	0.473	0.009	0.122	0.638	0.240
C-4	0.578	0.396	0.026	0.159	0.491	0.350
C-5	0.861	0.114	0.025	0.266	0.094	0.640
C-6	0.699	0.277	0.024	0.212	0.278	0.510
C-7	0.419	0.581	-	0.0395	0.9605	-
C-8	0.957	-	0.043	0.294	-	0.706
		-20°F			800 psia	
C-9	0.682	0.310	0.008	0.335	0.529	0.136
C-10	0.746	0.240	0.014	0.386	0.402	0.232
C-11	0.780	0.207	0.013	0.410	0.328	0.262
C-12	0.895	0.091	0.014	0.467	0.112	0.421
C-13	0.775	0.208	0.017	0.410	0.327	0.263
C-14	0.625	0.375	-	0.188	0.812	-
C-15	0.978	-	0.022	0.499	-	0.501
		-20°F			1200 psia	
C-16	0.927	0.047	0.026	0.678	0.059	0.263
C-17	0.879	0.095	0.026	0.647	0.136	0.217
C-18	0.837	0.146	0.017	0.624	0.211	0.165
C-19	0.972	-	0.028	0.708	-	0.292

Table 4

Smoothed Data in the CH_4-CO_2-nC_4H_{10} System

(all compositions are in mole fractions)

Vapor Phase			Liquid Phase			Equilibrium Ratios		
CH_4	CO_2	$n\text{-}C_4H_{10}$	CH_4	CO_2	$n\text{-}C_4H_{10}$	CH_4	CO_2	$n\text{-}C_4H_{10}$
			100°F and 400 psia					
0.696	0.128	0.176	0.102	0.050	0.848	6.824	2.560	0.208
0.561	0.260	0.179	0.082	0.100	0.818	6.842	2.600	0.219
0.420	0.400	0.180	0.062	0.150	0.788	6.774	2.667	0.228
0.282	0.538	0.180	0.041	0.200	0.759	6.878	2.690	0.237
0.150	0.670	0.180	0.020	0.250	0.730	7.500	2.680	0.247
0.824	-	0.176	0.122	-	0.878	6.754	-	0.201
-	0.820	0.180	-	0.300	0.700	-	2.733	0.257
			100°F and 800 psia					
0.700	0.174	0.126	0.223	0.100	0.677	3.139	1.740	0.186
0.563	0.310	0.127	0.193	0.200	0.607	2.917	1.550	0.209
0.438	0.438	0.124	0.160	0.300	0.540	2.738	1.460	0.230
0.345	0.535	0.120	0.126	0.400	0.474	2.738	1.338	0.253
0.246	0.641	0.113	0.093	0.500	0.407	2.645	1.282	0.278
0.158	0.738	0.104	0.055	0.600	0.345	2.873	1.230	0.301
0.044	0.870	0.086	0.014	0.700	0.286	3.143	1.243	0.301
0.877	-	0.123	0.254	-	0.746	3.453	-	0.165
-	0.920	0.080	-	0.735	0.265	-	1.252	0.302
			100°F and 1200 psia					
0.773	0.110	0.117	0.343	0.100	0.557	2.254	1.100	0.210
0.667	0.220	0.113	0.303	0.200	0.497	2.201	1.100	0.227
0.543	0.347	0.110	0.264	0.300	0.436	2.057	1.157	0.252
0.450	0.440	0.110	0.226	0.400	0.374	1.991	1.100	0.294
0.338	0.552	0.110	0.189	0.500	0.311	1.788	1.104	0.354
0.225	0.661	0.114	0.150	0.600	0.250	1.500	1.102	0.456
0.880	-	0.120	0.381	-	0.619	2.310	-	0.194

Table 4 (continued)

Vapor Phase			Liquid Phase			Equilibrium Ratios		
CH_4	CO_2	$n\text{-}C_4H_{10}$	CH_4	CO_2	$n\text{-}C_4H_{10}$	CH_4	CO_2	$n\text{-}C_4H_{10}$
			40^oF and 400 psia					
0.709	0.203	0.088	0.151	0.100	0.749	4.695	2.030	0.118
0.538	0.366	0.096	0.108	0.200	0.692	4.982	1.830	0.139
0.393	0.507	0.100	0.075	0.300	0.625	5.240	1.690	0.160
0.243	0.662	0.095	0.046	0.400	0.554	5.283	1.655	0.172
0.134	0.779	0.087	0.019	0.500	0.481	7.053	1.558	0.181
0.928	-	0.072	0.198	-	0.802	4.687	-	0.090
-	0.930	0.070	-	0.568	0.432	-	1.637	0.162
			40^oF and 800 psia					
0.832	0.118	0.050	0.350	0.100	0.550	2.377	1.180	0.091
0.714	0.231	0.055	0.298	0.200	0.502	2.396	1.155	0.110
0.614	0.332	0.054	0.254	0.300	0.446	2.417	1.107	0.121
0.517	0.433	0.050	0.215	0.400	0.385	2.405	1.083	0.130
0.457	0.498	0.045	0.182	0.500	0.318	2.511	0.996	0.142
0.351	0.620	0.029	0.124	0.700	0.176	2.831	0.886	0.165
0.301	0.679	0.020	0.098	0.800	0.102	3.071	0.849	0.196
0.242	0.753	0.005	0.073	0.900	0.027	3.315	0.837	0.185
0.956	-	0.044	0.407	-	0.593	2.349	-	0.074
0.214	0.786	-	0.062	0.938	-	3.452	0.838	-
			40^oF and 1200 psia					
0.854	0.096	0.050	0.513	0.100	0.387	1.665	0.960	0.129
0.763	0.187	0.050	0.457	0.200	0.343	1.670	0.935	0.146
0.683	0.270	0.047	0.406	0.300	0.294	1.682	0.900	0.160
0.603	0.352	0.045	0.358	0.400	0.242	1.684	0.880	0.186
0.528	0.432	0.040	0.314	0.500	0.186	1.682	0.864	0.215
0.452	0.518	0.030	0.272	0.600	0.128	1.662	0.863	0.234
0.375	0.609	0.016	0.233	0.700	0.067	1.609	0.870	0.239
0.950	-	0.050	0.567	-	0.433	1.676	-	0.116
0.308	0.692	-	0.194	0.806	-	1.588	0.859	-

Table 4 (continued)

Vapor Phase			Liquid Phase			Equilibrium Ratios		
CH_4	CO_2	$n\text{-}C_4H_{10}$	CH_4	CO_2	$n\text{-}C_4H_{10}$	CH_4	CO_2	$n\text{-}C_4H_{10}$
			-20°F and 400 psia					
0.838	0.122	0.040	0.262	0.100	0.638	3.199	1.220	0.063
0.742	0.223	0.035	0.232	0.200	0.568	3.198	1.115	0.062
0.674	0.296	0.030	0.204	0.300	0.496	3.304	0.987	0.061
0.625	0.350	0.025	0.179	0.400	0.421	3.492	0.875	0.059
0.577	0.403	0.020	0.155	0.500	0.345	3.723	0.806	0.058
0.532	0.453	0.015	0.132	0.600	0.268	4.030	0.755	0.056
0.500	0.490	0.010	0.108	0.700	0.192	4.630	0.700	0.052
0.468	0.526	0.006	0.085	0.800	0.115	5.506	0.658	0.052
0.451	0.546	0.003	0.057	0.900	0.043	7.912	0.607	0.070
0.419	0.581	-	0.0395	0.9605	-	10.608	0.605	-
0.957	-	0.043	0.294	-	0.706	3.255	-	0.061
			-20°F and 800 psia					
0.898	0.082	0.020	0.472	0.100	0.428	1.903	0.820	0.047
0.842	0.138	0.020	0.445	0.200	0.355	1.892	0.690	0.056
0.801	0.179	0.020	0.415	0.300	0.285	1.930	0.597	0.070
0.747	0.237	0.016	0.383	0.400	0.217	1.950	0.593	0.074
0.696	0.294	0.010	0.346	0.500	0.154	2.012	0.588	0.065
0.665	0.330	0.005	0.303	0.600	0.097	2.195	0.550	0.052
0.646	0.350	0.004	0.253	0.700	0.047	2.553	0.500	0.085
0.625	0.375	-	0.188	0.812	-	3.325	0.462	-
0.978	-	0.022	0.499	-	0.501	1.960	-	0.044
			-20°F and 1200 psia					
0.935	0.040	0.025	0.683	0.050	0.267	1.369	0.800	0.094
0.902	0.074	0.024	0.659	0.100	0.241	1.369	0.740	0.100
0.872	0.105	0.023	0.642	0.150	0.208	1.358	0.700	0.111
0.842	0.135	0.023	0.627	0.200	0.173	1.343	0.675	0.133
0.795	0.180	0.025	0.623	0.250	0.127	1.276	0.720	0.197
0.972	-	0.028	0.708	-	0.292	1.373	-	0.096

Table 5

Comparisons with the Chao-Seader Correlation

Percent Liquid (L), Experimental = 50%

a) The Methane (1)-Propane (2)-n-Pentane (3) System[8]

The Chao-Seader Constants[9]

Experimental			Predicted			
K_1	K_2	K_3	K_1	K_2	K_3	L
P = 500 psia and T = 100°F						
5.88	-	0.071	5.49	-	0.066	51.13
5.70	0.500	0.072	5.37	0.479	0.070	51.10
5.51	0.504	0.076	5.24	0.487	0.075	51.20
5.24	0.505	0.087	5.10	0.496	0.080	51.12
4.87	0.522	0.126	4.93	0.508	0.088	51.98
4.37	0.549	-	4.73	0.523	-	51.78
P = 1000 psia and T = 100°F						
3.08	-	0.077	3.04	-	0.070	50.78
2.94	0.403	0.077	2.98	0.379	0.076	50.03
2.81	0.403	0.084	2.91	0.393	0.084	49.02
2.65	0.415	0.097	2.83	0.412	0.095	47.64
2.38	0.458	0.158	2.73	0.438	0.112	46.61
1.99	0.530	-	2.55	0.489	-	39.47
P = 1500 psia and T = 100°F						
2.14	1.000	0.105	2.24	0.385	0.099	48.51
2.01	0.445	0.115	2.19	0.408	0.113	46.08
1.86	0.458	0.148	2.13	0.438	0.132	42.88
1.70	0.500	0.216	2.04	0.488	0.168	38.40
1.40	0.624	0.439	1.80	0.631	0.296	16.78
P = 2000 psia and T = 100°F						
1.58	-	0.204	1.84	-	0.153	42.19
1.44	0.582	0.263	1.79	0.500	0.185	35.72
1.28	0.644	0.462	1.72	0.562	0.237	30.46

b) The Methane (1)-Hydrogen Sulphide (2)-n-Butane (3) System

The Revised Chao-Seader Constants[72]

Experimental			Predicted			
K_1	K_2	K_3	K_1	K_2	K_3	L
		P = 400 psia and T = 100°F				
6.75	-	0.200	6.32	-	0.201	50.72
6.14	0.960	0.214	6.39	1.35	0.204	48.35
5.98	0.855	0.231	6.47	1.32	0.208	45.63
5.48	0.933	0.244	6.58	1.29	0.213	43.21
		P = 800 psia and T = 100°F				
3.45	-	0.165	3.45	-	0.170	49.56
3.29	0.770	0.187	3.49	0.818	0.176	49.02
3.27	0.725	0.209	3.55	0.797	0.181	48.69
3.21	0.767	0.219	3.63	0.771	0.188	48.81
		P = 1200 psia and T = 100°F				
2.31	-	0.194	2.49	-	0.199	46.06
2.13	0.830	0.228	2.51	0.712	0.211	44.82
2.06	0.730	0.265	2.54	0.696	0.224	43.38
		P = 400 psia and T = 40°F				
4.69	-	0.090	5.19	-	0.082	49.08
4.43	0.740	0.137	5.28	0.738	0.084	50.95
4.20	0.770	0.178	5.41	0.713	0.086	52.78
4.24	0.680	0.204	5.56	0.691	0.087	52.65
		P = 800 psia and T = 40°F				
2.35	-	0.074	2.91	-	0.080	42.61
2.35	0.390	0.090	2.96	0.469	0.082	42.06
2.41	0.375	0.110	3.02	0.454	0.084	42.33
2.45	0.427	0.137	3.13	0.435	0.087	44.21
		P = 1200 psia and T = 40°F				
1.68	-	0.115	2.17	-	0.109	35.54
1.66	0.450	0.141	2.21	0.420	0.114	34.79
1.64	0.540	0.195	2.26	0.404	0.121	38.07
1.68	0.533	0.267	2.34	0.341	0.127	42.52

Experimental			Predicted			
K_1	K_2	K_3	K_1	K_2	K_3	L
		P = 400 psia and T = -20°F				
3.26	-	0.061	3.85	-	0.027	48.88
3.36	0.390	0.058	3.93	0.328	0.027	49.19
3.54	0.335	0.060	4.04	0.315	0.028	49.56
3.82	0.283	0.064	4.17	0.303	0.028	49.59
		P = 800 psia and T = -20°F				
1.96	-	0.044	2.24	-	0.034	44.62
1.96	0.300	0.058	2.29	0.232	0.035	45.08
1.98	0.300	0.074	2.36	0.221	0.035	46.05
2.09	0.26	0.074	2.45	0.211	0.036	46.66
		P = 1200 psia and T = -20°F				
1.37	-	0.096	1.75	-	0.067	31.25
1.39	0.400	0.119	1.79	0.259	0.072	32.91

c) The Methane (1)-Carbon Dioxide (2)-n-Butane (3) System

The Grayson-Streed Constants[32]

Experimental			Predicted			
K_1	K_2	K_3	K_1	K_2	K_3	L
		P = 400 psia and T = 100°F				
6.75	-	0.200	5.74	-	0.193	52.48
6.82	2.56	0.208	5.71	2.22	0.196	53.43
6.84	2.60	0.219	5.68	2.21	0.199	54.88
6.77	2.67	0.228	5.63	2.21	0.203	56.64
6.88	2.69	0.237	5.59	2.20	0.207	58.78
7.50	2.68	0.247	5.53	2.20	0.211	61.36
-	2.73	0.257	-	2.19	0.216	65.68
		P = 800 psia and T = 100°F				
3.45	-	0.165	3.22	-	0.156	52.61
3.14	1.74	0.186	3.18	1.33	0.164	54.32
2.92	1.55	0.209	3.14	1.33	0.172	54.92
2.74	1.46	0.230	3.09	1.33	0.181	55.27
		P = 1200 psia and T = 100°F				
2.31	-	0.194	2.39	-	0.171	50.47
2.25	1.10	0.210	2.36	1.07	0.183	50.64
2.20	1.10	0.227	2.33	1.08	0.197	50.86
2.06	1.16	0.252	2.27	1.08	0.216	51.74
		P = 400 psia and T = 40°F				
4.69	-	0.090	4.56	-	0.077	51.25
4.70	2.03	0.117	4.52	1.34	0.080	56.44
4.98	1.83	0.139	4.47	1.34	0.083	61.08
5.24	1.69	0.160	4.42	1.34	0.085	65.08
		P = 800 psia and T = 40°F				
2.35	-	0.074	2.61	-	0.071	46.40
2.38	1.18	0.091	2.59	0.841	0.074	50.93
2.40	1.16	0.110	2.56	0.845	0.078	55.95
2.42	1.11	0.121	2.53	0.848	0.083	60.12
		P = 1200 psia and T = 40°F				
1.68	-	0.115	2.00	-	0.089	40.92
1.67	0.960	0.129	1.98	0.716	0.097	44.11
1.67	0.935	0.146	1.95	0.725	0.105	48.31
1.68	0.900	0.160	1.92	0.734	0.115	52.04

Experimental			Predicted			
K_1	K_2	K_3	K_1	K_2	K_3	L
		P = 400 psia and T = -20°F				
3.26	-	0.061	3.38	-	0.026	51.55
3.20	1.22	0.063	3.34	0.638	0.027	55.49
3.20	1.16	0.062	3.30	0.637	0.027	59.09
3.30	0.987	0.060	3.27	0.636	0.028	61.73
		P = 800 psia and T = -20°F				
1.96	-	0.044	2.00	-	0.031	49.88
1.90	0.820	0.047	1.98	0.436	0.032	53.71
1.89	0.690	0.056	1.96	0.438	0.034	56.70
1.93	0.597	0.070	1.94	0.440	0.036	59.43
		P = 1200 psia and T = -20°F				
1.37	-	0.096	1.60	-	0.055	37.79
1.37	0.800	0.094	1.59	0.420	0.058	40.46
1.37	0.740	0.100	1.58	0.424	0.062	43.26
1.36	0.700	0.111	1.57	0.429	0.066	45.00
1.28	0.720	0.197	1.55	0.439	0.075	48.57

d) Summary of Deviations

Set of Constants Used	Temperature Range °F	Pressure Range psia	PERCENT DEVIATIONS Average K_1	Average K_2	Average K_3	Average L	Standard K_1	Standard K_2	Standard K_3	Standard L
		System: Methane-Propane-n-Pentane								
O.C.S.*	100	500 to 2000	10.30	- 8.80	-15.67	-10.71	15.98	16.63	21.10	20.47
G.S.**	100	500 to 2000	6.29	-11.55	-31.27	- 3.52	17.73	18.72	34.92	11.89
R.C.S.***	100	500 to 2000	10.30	- 8.80	-15.67	-10.71	15.98	16.63	21.10	20.47
		System: Hydrogen Sulphide-n-Butane								
O.C.S.	-20 to 100	400 to 1200	14.93	- 3.00	-28.24	- 6.36	27.19	27.88	37.00	22.86
G.S.	-20 to 100	400 to 1200	3.40	-26.64	-35.07	5.74	10.03	32.32	39.37	12.37
R.C.S.	-20 to 100	400 to 1200	19.31	0.02	-26.97	- 9.72	21.86	22.46	34.01	14.56
		Systems: Methane-Carbon Dioxide-n-Butane								
O.C.S.	-20 to 100	400 to 1200	13.32	-28.17	-19.85	- 2.45	18.40	29.87	26.60	16.88
G.S.	-20 to 100	400 to 1200	3.09	-26.62	-28.61	5.66	12.64	29.21	32.91	14.01
R.C.S.	-20 to 100	400 to 1200	9.70	-10.89	- 5.69	-11.53	20.30	16.85	49.44	27.67

* Old Chao-Seader constants
** Grayson Streed constants
***Revised Chao-Seader constants

Table 6

Wilson Constants and Binary Interaction Energies in the Methane-Hydrogen Sulphide[51] System

Component (1) : Methane
Component (2) : Hydrogen Sulphide

P psia	T °F	x_1	x_2	γ_1†	γ_2†	Λ_{12}	Λ_{21}	$\lambda_{12}-\lambda_{11}$ Btu/lb.mole	$\lambda_{21}-\lambda_{22}$ Btu/lb.mole
1000	160	0.032	0.968	0.55	1.04	-0.011	4.543	-	-1632.5
1330	160	0.085	0.915	0.460	1.06	-0.020	4.574	-	-1640.7
1600	160	0.159	0.841	0.281	1.25	-0.106	5.301	-	-1822.2
600	100	0.034	0.966	1.07	1.008	0.049	3.381	3138.4	-1145.8
1200	100	0.105	0.895	1.10	1.007	0.277	2.043	1217.7	- 585.9
1800	100	0.280	0.720	0.555	1.484	-0.195	3.930	-	-1313.1
300	-59.8	0.04	0.96	19.7	1.72	-0.039	-7.567	-	-
500	-59.8	0.08	0.92	11.0	2.54	-0.080	-5.263	-	-
700	-59.8	0.103	0.897	8.64	3.56	-0.107	-4.931	-	-
400	40	0.034	0.966	2.08	1.11	-0.024	1.834	-	- 415.9
1000	40	0.122	0.878	1.90	1.10	0.012	1.829	4210.6	- 413.2
1600	40	0.256	0.744	1.21	1.54	-0.134	1.591	-	- 274.6
300	-29.92	0.03	0.97	10.3	1.42	-0.028	-6.040	-	-
500	-29.92	0.07	0.93	6.48	1.86	-0.067	-3.664	-	-
700	-29.92	0.095	0.905	5.49	2.18	-0.092	-3.070	-	-

† ideal vapor solutions assumed.

Table 7

Calculated Values of Excess Functions

System (1)-(2)	x_1	T °F	P psia	ΔF^E Btu/lb.mole	ΔH^E Btu/lb.mole	$T\Delta S^E$ Btu/lb.mole
CCl_4-C_6H_6 (49)	0.5	158	11.7	18.3	26.7	8.3
C_1-H_2S (51)	0.015	-60	200	-1437.0	-8736.1	-7299.1
C_1-H_2S (51)	0.075	-13	600	-1312.5	-5733.7	-4421.2
C_1-H_2S (51)	0.20	100	1600	- 697.5	-3258.9	-2561.4
nC_5-nC_7 (49)	0.50	310.28	147	- 19.3	121.4	140.7
nC_5-nC_7 (49)	0.50	447.26	443.9	- 435.2	-2462.3	-2027.1
C_1-nC_4 (101)	0.15	161.5	600	-1804.3	-6616.6	-4812.3
C_1-CO_2 (19)	0.15	-34.8	600	- 790.6	-5595.4	-4804.8
C_2-nC_7 (49)	0.5	198	600	-2556.2	-7573.7	-5017.5
CO_2-C_3 (83)	0.5	83	600	- 709.1	-4452.6	-3743.4
CO_2-nC_4 (83)	0.5	105.3	600	-1311.7	-4905.2	-3593.5
CO_2-nC_5 (83)	0.5	145.7	600	-1582.0	-3755.7	-2173.7
C_2-nC_5 (49)	0.5	188.4	600	-1490.7	-5557.1	-4066.4
H_2S-nC_4 (48)	0.5	195.6	600	- 292.0	-3333.6	-3041.6

Table 8

Values of Excess Functions Taken from the Literature[42,86,87,33,34,61]

P < 760 mm Hg

x = 0.5

System (1) - (2)	T °K	ΔF^E Btu/lb.mole	ΔH^E Btu/lb.mole	$T\Delta S^E$ Btu/lb.mole
$n\text{-}C_7\text{-}nC_{16}$	293	-14.0	26.0	40.0
$n\text{-}C_6$-Cyclohexane	293	16.6	50.6	34.0
$n\text{-}C_8$-tetraethylmethane	323	11.8	-21.2	-33.0
2-2-4 trimethylpentane-nC_{16}	297.9	5.0	55.0	50.0
$CO\text{-}CH_4$	90	28.9	25.9	- 3.0
$A\text{-}CH_4$	91	-	20.0	-
CH_4-Kr	115.5	14.0	-	-
$CH_4\text{-}CF_4$	110.5	86.0	-	-
$Kr\text{-}CF_4$	117.1	75.0	-	-
$CCl_4\text{-}C_6H_6$	343	17.9	30.2	12.3
$CS_2\text{-}C_6H_6$		69.0	128	59.0
C_6H_6-dibutyl Sebacate		≃88.0	negligible	88.0
Propyl bromide-Sebacate		≃64.0	negligible	64.0
benzene-butyl valerianate		≃42.0	negligible	42.0
Propyl bromide-butyl Sebacate		≃ 5.5	negligible	5.5
$CCl_4\text{-}C_6H_6$	298	19.55	26.1	6.55
CCl_4-Cyclohexane	298	16.4	35.5	19.1
CCl_4-Cyclohexane	313	16.5	34.0	17.5
Benzene-Cyclohexane	293	77.0	200.0	123.0
Benzene-Cyclohexane	343	62.5	162.0	99.5

Table 8 (continued)

System (1) - (2)	T °K	ΔF^E Btu/lb.mole	ΔH^E Btu/lb.mole	$T\Delta S^E$ Btu/lb.mole
Benzene-1,2-$C_2H_4Cl_2$	298	6.1	15	8.9
Benzene-1,2-$C_2H_4Cl_2$	343	3.7	14	10.3
Benzene-toluene	353	-2.1	11	13.1
CS_2-acetone	308	250.5	349	98.5
n-C_5F_{12}-nC_5H_{12}	277	295.2	370	74.8
Cy-C_6F_{12}-1,3,5$(CH_3)_3$Cy-C_6H_9	338	339.8	475	135.2
C_6H_6-toluene	297.6	-	68	-
toluene-p-xylene	297.6	-	16	-
benzene-p-xylene	297.6	-	172	-
benzene-cyclohexane	298	74.4	175.8	101.4
Cyclohexane-CCl_4	298	16.7	34.2	17.5
benzene-ethyldichloride	298	6.0	14.5	8.5
benzene-ethyldichloride	343	3.0	14.0	11.0
acetone-chloroform	308.17	-140.0	-458.0	-318.0
A-N_2	85	7.44	-	-
Kr-C_1	115.5	14.4	-	-
A-O_2	95	7.44	12.5	5.06
C_2-$C_2^=$	140-170	≤9.6	-	-
neo-pentane-cyclo Hexane	273	44.1	-	-
n-Hexane-Cyclo Hexane	293	16.8	51.6	34.8
n-Hexane-n-Heptane	293	-	3.84	-
Cyclo-Hexane-nC_7	293	-	64.8	-

Table 9

Comparison with the NGPSA Engineering Data Book

1. The methane-hydrogen sulphide-n-butane system

P_{cv} = 1500 psia

T = 40°F

P psia	Observed K_{C_1}	Observed K_{H_2S}	Observed K_{C_4}	Predicted K_{C_1}	Predicted K_{H_2S}	Predicted K_{C_4}	Percent Deviation* K_{C_1}	Percent Deviation* K_{H_2S}	Percent Deviation* K_{C_4}
400	4.10	0.600	0.277	4.90	0.820	0.115	19.51	36.67	-48.34
800	2.20	0.355	0.250	2.25	0.650	0.130	2.27	83.10	-48.00
1200	1.50	0.600	0.460	1.52	0.710	0.285	1.33	18.33	-38.04

Standard Deviations* K_{C_1} = 9.83%

K_{H_2S} = 46.33%

K_{C_4} = 39.33%

2. The methane-carbon dioxide-n-butane system

P_{cv} = 1700 psia

T = 40°F

P psia	Observed K_{C_1}	Observed K_{CO_2}	Observed K_{C_4}	Predicted K_{C_1}	Predicted K_{CO_2}	Predicted K_{C_4}	Percent Deviation* K_{C_1}	Percent Deviation* K_{CO_2}	Percent Deviation* K_{C_4}
400	5.20	1.40	0.256	5.10	1.25	0.106	- 1.92	-10.71	-58.59
800	2.70	0.94	0.156	2.35	0.68	0.110	-12.96	-27.66	-28.85
1200	1.70	0.86	0.207	1.55	0.62	0.173	- 8.82	-27.91	-16.43

Standard Deviations* K_{C_1} = 7.90%

K_{CO_2} = 20.36%

K_{C_4} = 33.67%

* For explanation, see page 77

APPENDIX B

SUMMARY OF EQUATIONS USED IN THE CHAO-SEADER CORRELATION

APPENDIX B

SUMMARY OF EQUATIONS USED IN THE CHAO-SEADER CORRELATION

$$K_i = \frac{\gamma_i^l \nu_i^l}{\phi_i' v} \tag{1}$$

$$\ln \gamma_i^l = \frac{V_i (\delta_i - \bar{\delta})^2}{RT} \tag{2}$$

$$\bar{\delta} = \frac{\sum_i x_j V_j \delta_j}{\sum_j x_j V_j} \tag{3}$$

$$T_{ri} = \frac{T}{T_{ci}} \tag{4}$$

$$P_{ri} = \frac{P}{P_{ci}} \tag{5}$$

where, T_{ri} and P_{ri} are reduced temperature and pressure and T_{ci} and P_{ci}, critical temperature and pressure of the i^{th} component

$$\log_{10} \nu_i = \log_{10} \nu_i^{(0)} + \omega_i \log_{10} \nu_i^{(1)} \tag{6}$$

where, ω_i = Acentric factor for the i^{th} component

$$\log_{10} \nu_i^{(0)} = a_o + \frac{a_1}{T_{ri}} + a_2 T_{ri} + a_3 T_{ri}^2 + a_4 T_{ri}^3 + P_{ri}(a_5 + a_6 T_{ri} + a_7 T_{ri}^2) + P_{ri}^2(a_8 + a_9 T_{ri}) - \log_{10} P_{ri} \quad (7)$$

$$\log_{10} \nu_i^{(1)} = a_{10} + a_{11} T_{ri} + \frac{a_{12}}{T_{ri}} - a_{13} T_{ri}^3 + a_{14}(P_{ri} - 0.6) \quad (8)$$

$$\ln \phi_i' = (Z'-1)\frac{B_i'}{B'} - \ln |Z - B'P| - \frac{A'^2}{B'}\left[\frac{2A_i'}{A'} - \frac{B_i'}{B'}\right] \ln\left[\left|1 + \frac{B'P}{Z'}\right|\right] \quad (9)$$

$$Z = \frac{1}{1-h} - \frac{A'^2}{B'}\left(\frac{h}{1+h}\right) \quad (10)$$

$$h = \frac{B'P}{Z'} \quad (11)$$

$$A' = \sum_j y_j A'_j \quad (12)$$

$$B' = \sum_j y_j B'_j \quad (13)$$

$$A'_i = \left(\frac{0.4278}{P_{ci} T_{ri}^{2.5}}\right)^{1/2} \quad (14)$$

$$B'_i = \frac{0.0867}{P_{ci} T_{ri}} \quad (15)$$

APPENDIX C

SAMPLE CALCULATIONS OF EXCESS FUNCTIONS

APPENDIX C

SAMPLE CALCULATION OF EXCESS FUNCTIONS

An example of the procedure employed for calculation of excess functions of Table 7 is presented below. The system is methane-hydrogen sulphide at a pressure of 1600 psia. The vapor-liquid equilibrium data are as follows:

System: Methane-Hydrogen Sulphide[51]

P = 1600 psia

$T^{\circ}F$	x_{CH_4}	x_{H_2S}	Y_{CH_4}	Y_{H_2S}	γ_{CH_4}	γ_{H_2S}
160	0.155	0.845	0.250	0.750	0.223	0.918
120	0.184	0.816	0.441	0.559	0.257	0.736
100	0.200	0.800	0.520	0.480	0.242	0.660
80	0.213	0.787	0.586	0.414	0.219	0.596
40	0.238	0.762	0.705	0.295	0.166	0.468

The variation of activity coefficients and temperature with composition is presented in Fig. 31. From this figure: at

$x_{CH_4} = 0.20$; $x_{H_2S} = 0.80$

$\gamma_{CH_4} = 0.24$

$\gamma_{H_2S} = 0.6525$, and

$T = 100^{\circ}F = 560^{\circ}R$

In Figure (32), activity coefficients are plotted against equilibrium temperature. From the slopes of activity coefficient curves at $100^{\circ}F$, values of the following partial derivatives can be calculated.

$$\frac{\partial \ln \gamma_{CH_4}}{\partial T} = \frac{1}{\gamma_{CH_4}} \frac{\partial \gamma_{CH_4}}{\partial T} = 0.005013$$

$$\frac{\partial \ln \gamma_{H_2S}}{\partial T} = \frac{1}{\gamma_{H_2S}} \frac{\partial \gamma_{H_2S}}{\partial T} = 0.005284$$

Knowing activity coefficients and partial derivatives of natural logarithm of activity coefficients with respect to temperature, all excess functions can be calculated at the desired composition.

$$\Delta F^E = RT(x_{CH_4} \cdot \ln \gamma_{CH_4} + x_{H_2S} \cdot \ln \gamma_{H_2S})$$

$$= 1.987(560)(0.2 \cdot \ln 0.24 + 0.8 \cdot \ln 0.6525)$$

$$= -1112.7(0.2854 + 0.3414)$$

$$= -697.5 \text{ Btu/lb.mole}$$

$$\Delta H^E = -RT^2\left(x_{CH_4} \frac{\partial \ln \gamma_{CH_4}}{\partial T} + x_{H_2S} \frac{\partial \ln \gamma_{H_2S}}{\partial T}\right)$$

$$= -1.987(560)^2(0.2 \cdot 0.005013 + 0.8 \cdot 0.005284)$$

$$= -1.987(31.36)\ 52.30$$

$$= -3258.9 \text{ Btu/lb.mole}$$

Therefore,

$$T\Delta S^E = \Delta H^E - \Delta F^E$$

$$= -3258.9 + 697.5$$

$$= -2561.4 \text{ Btu/lb.mole}$$

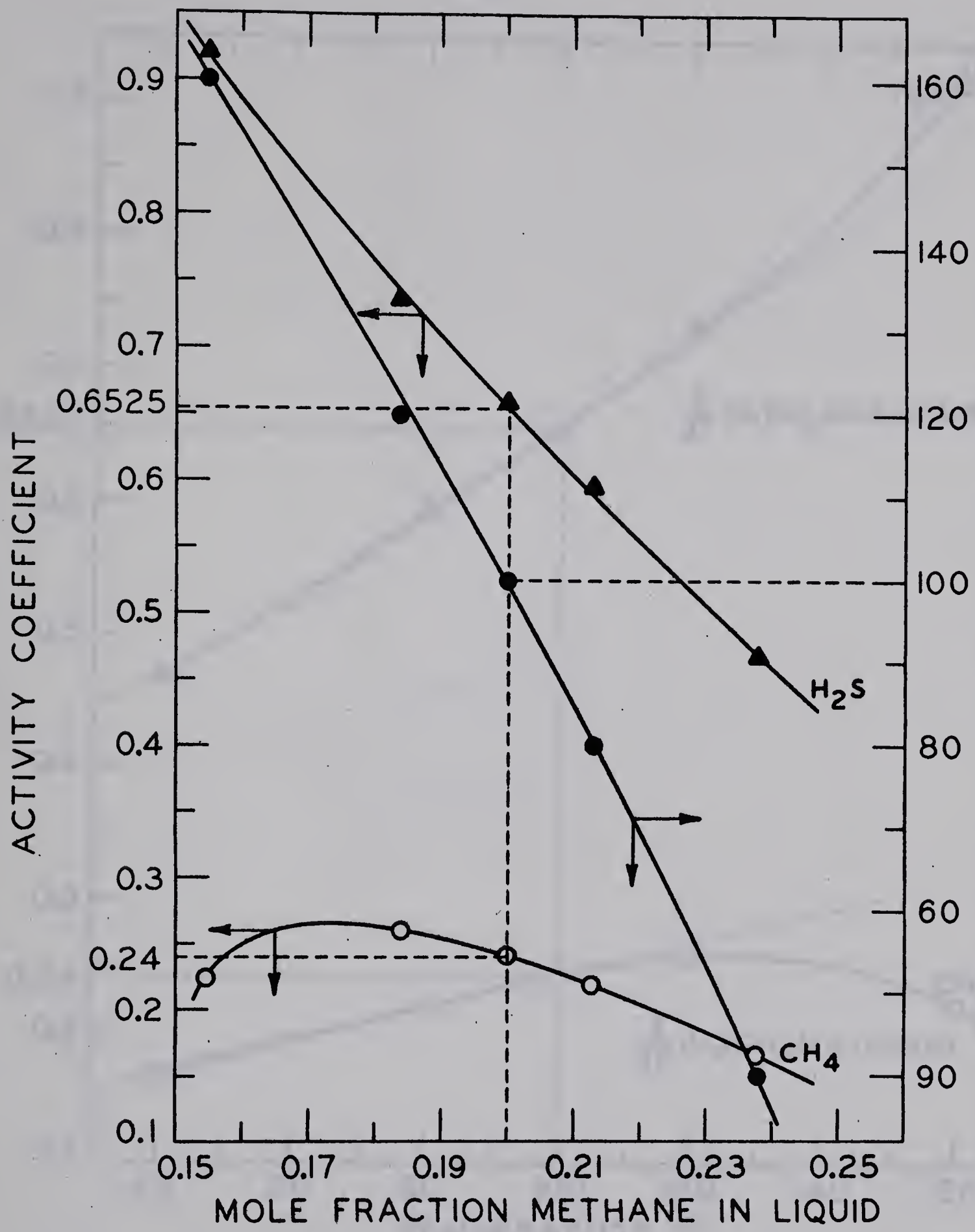

FIG. 31 Variation of Activity Coefficient and Equilibrium Temperature with Composition in the Methane Hydrogen Sulfide System at 1600 psia

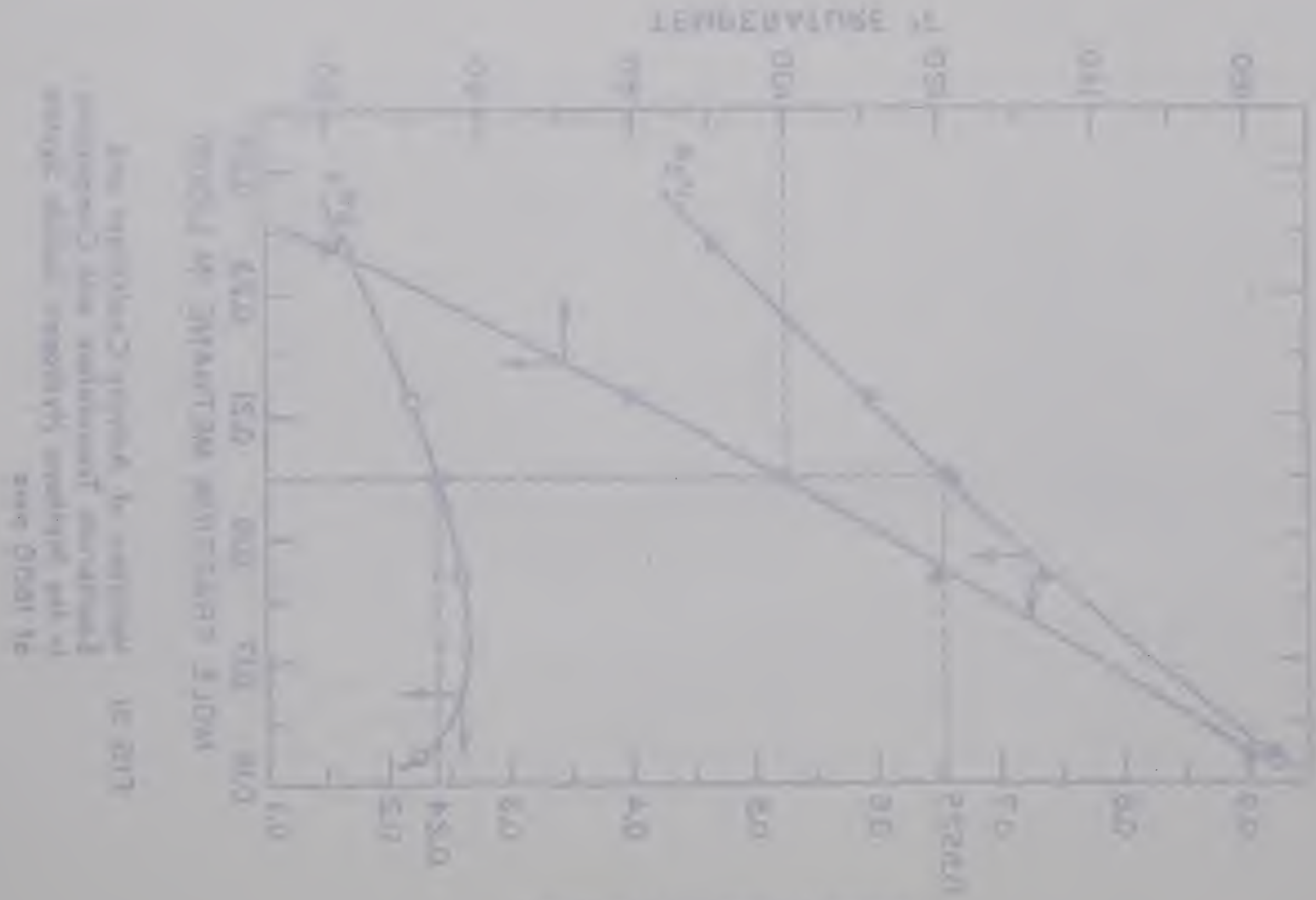

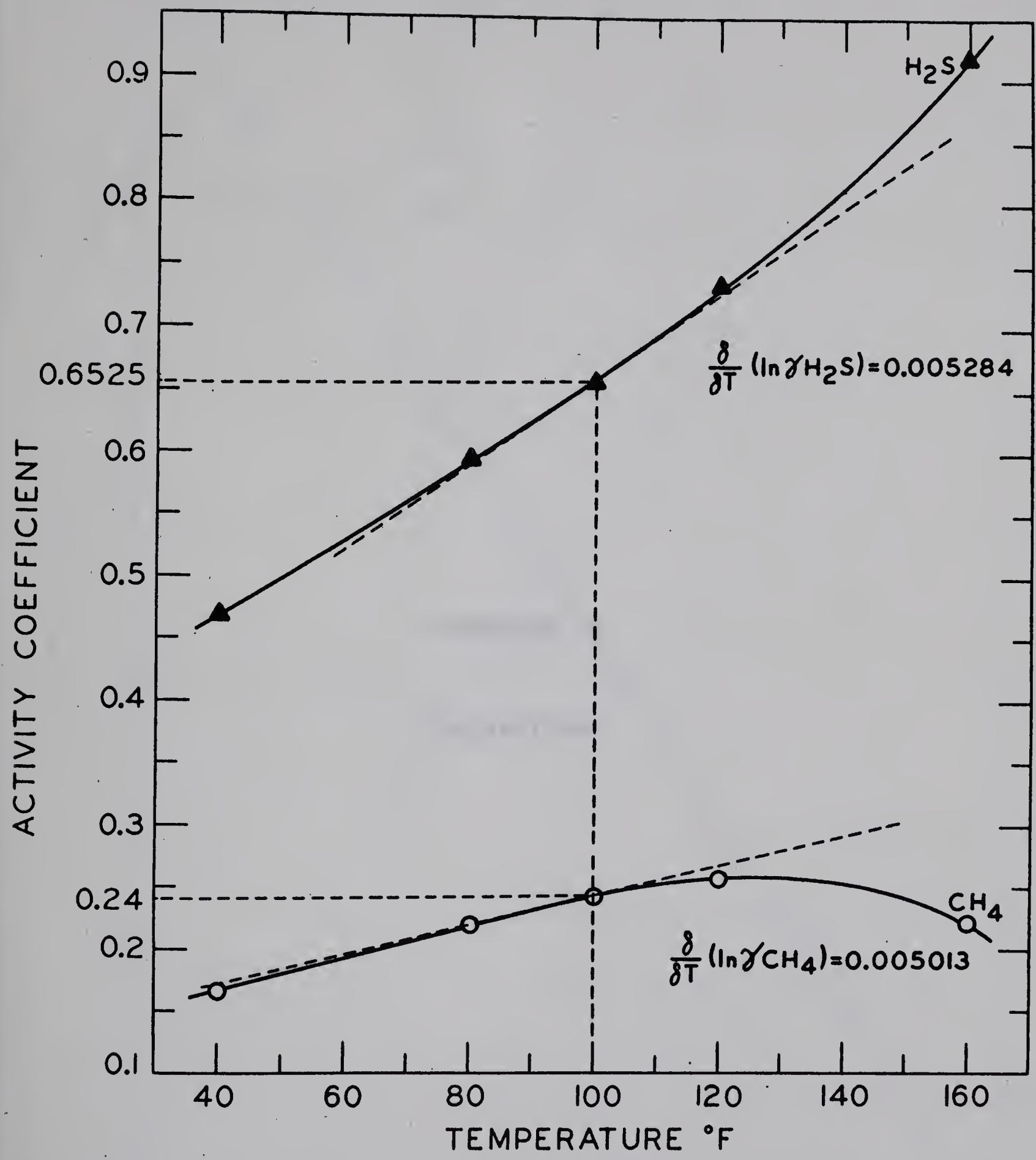

FIG. 32 Variation of Activity Coefficients with Temperature in the Methane–Hydrogen Sulfide System at 1600 psia

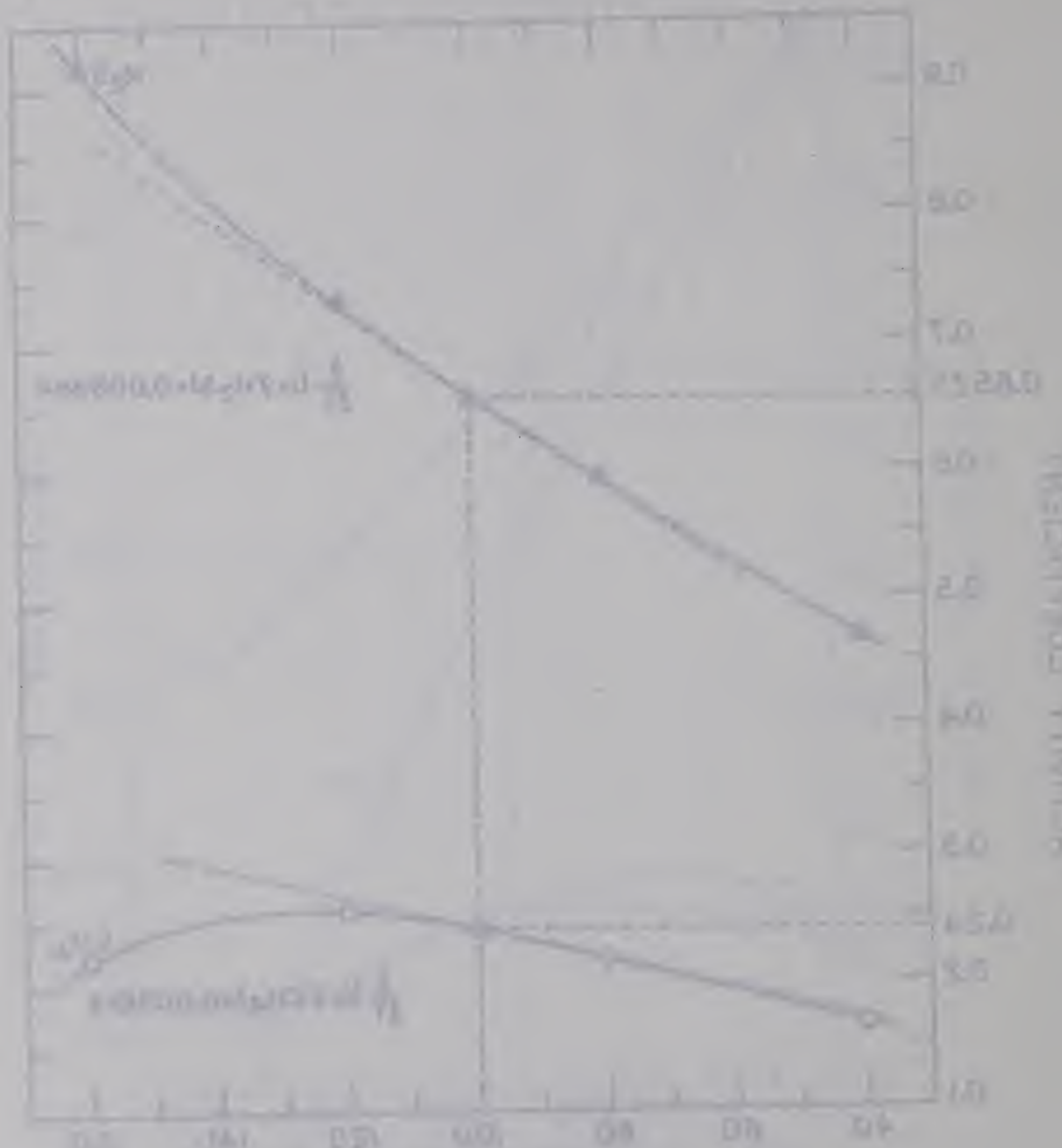

APPENDIX D

CALIBRATIONS

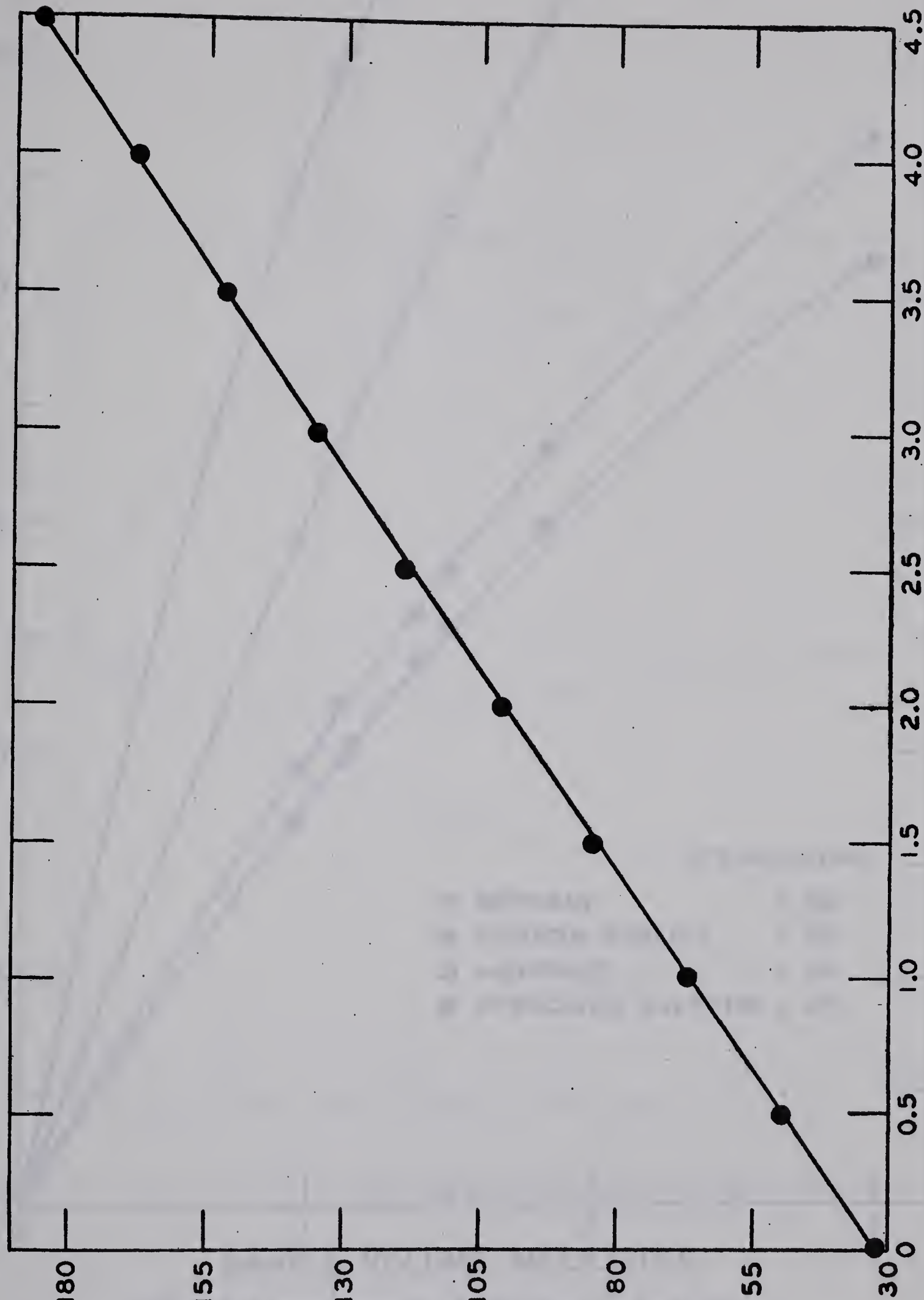

FIGURE IRON CONSTANTAN THERMOCOUPLD CALIBRATION

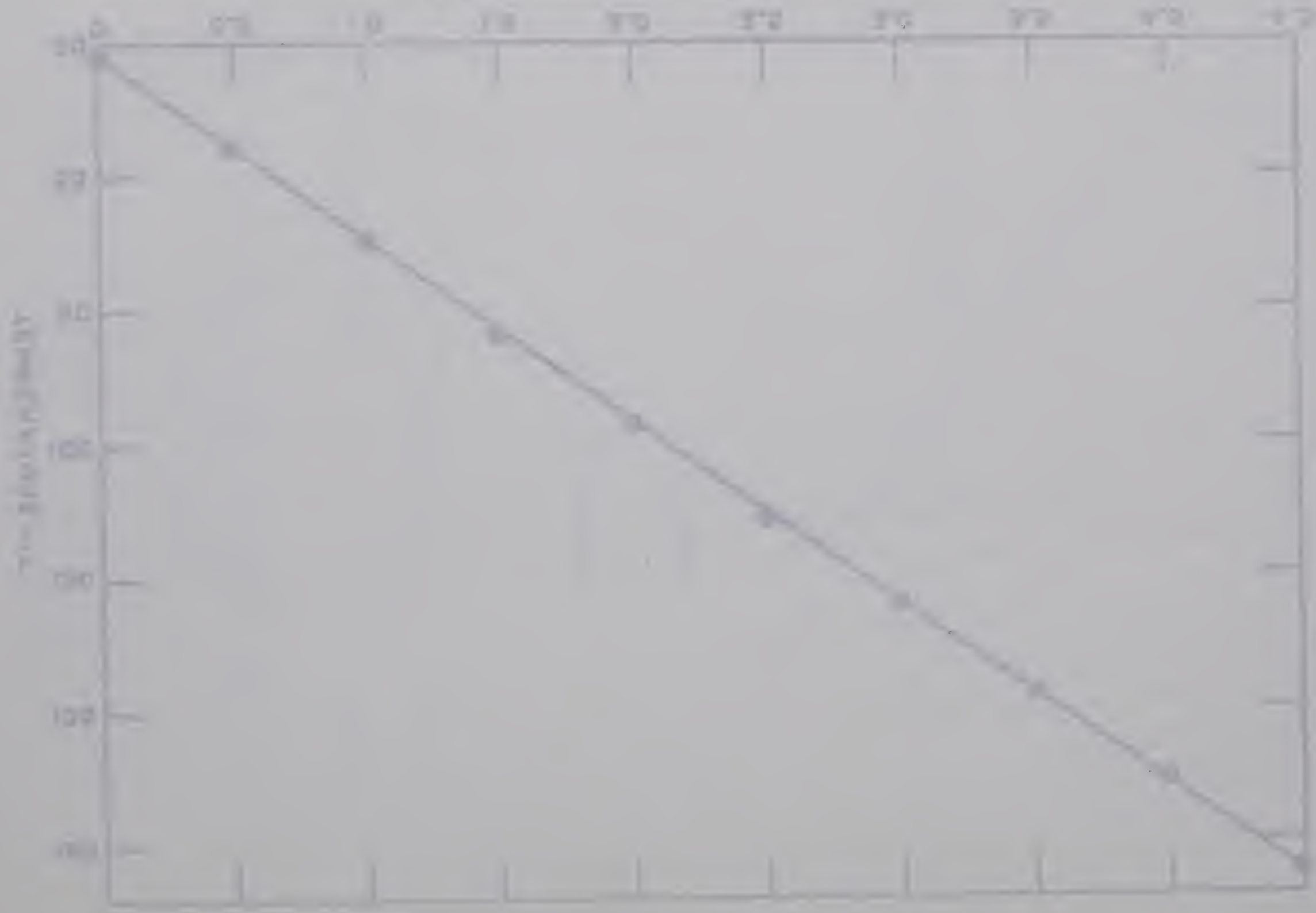

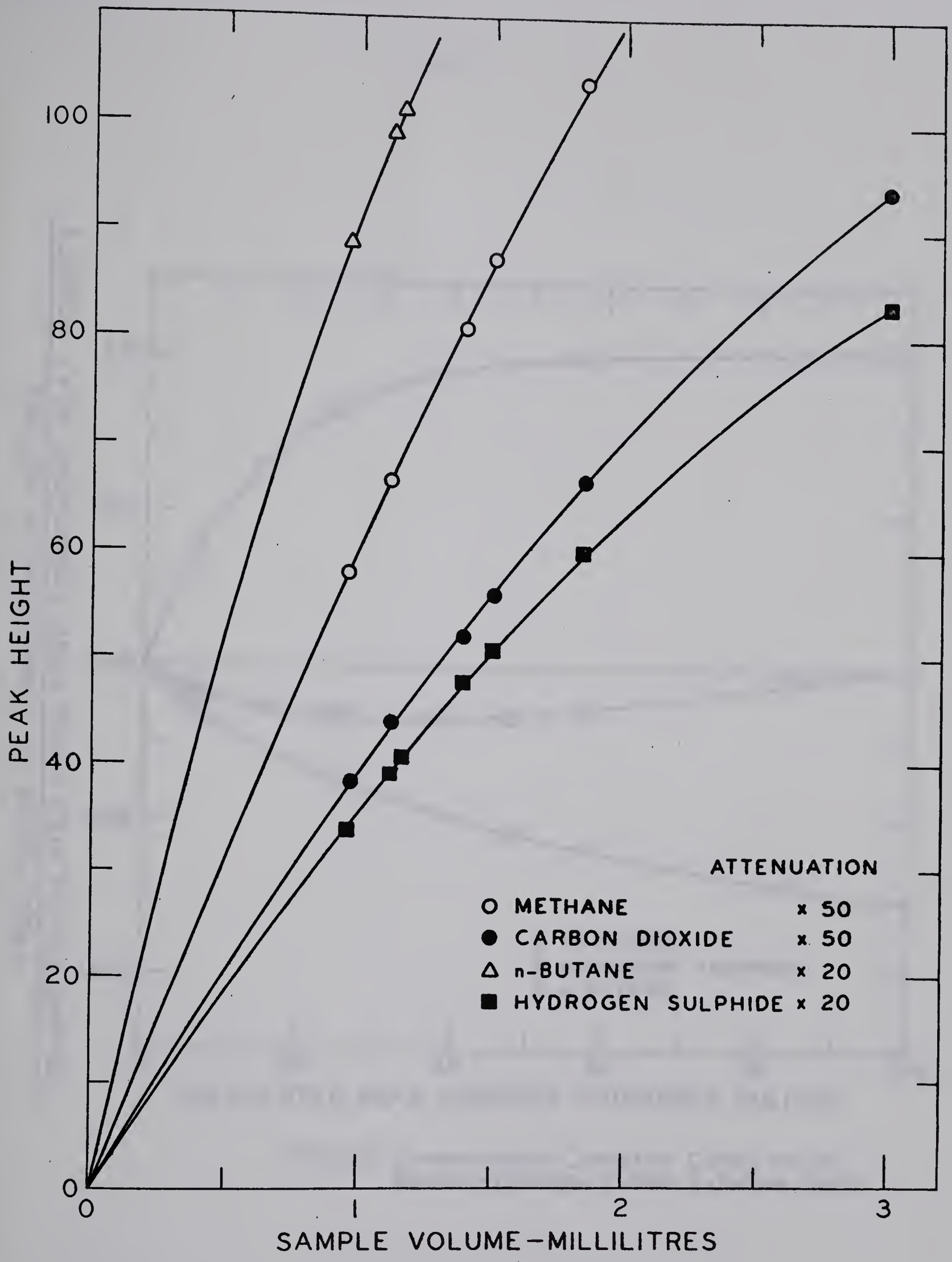

FIG. 34 Chromatograph Calibration Curves for CH_4, CO_2, H_2S, and $n\text{-}C_4H_{10}$

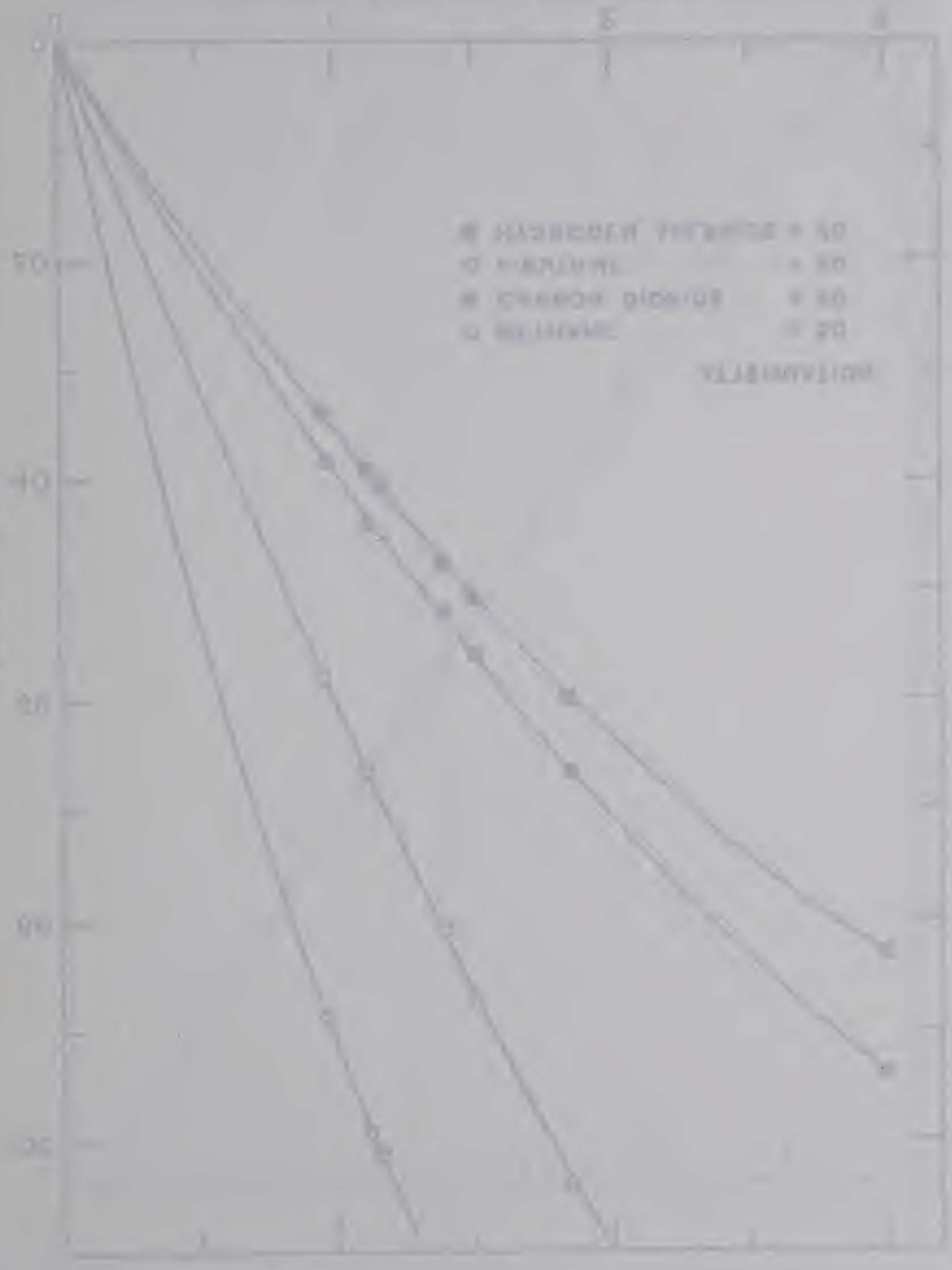

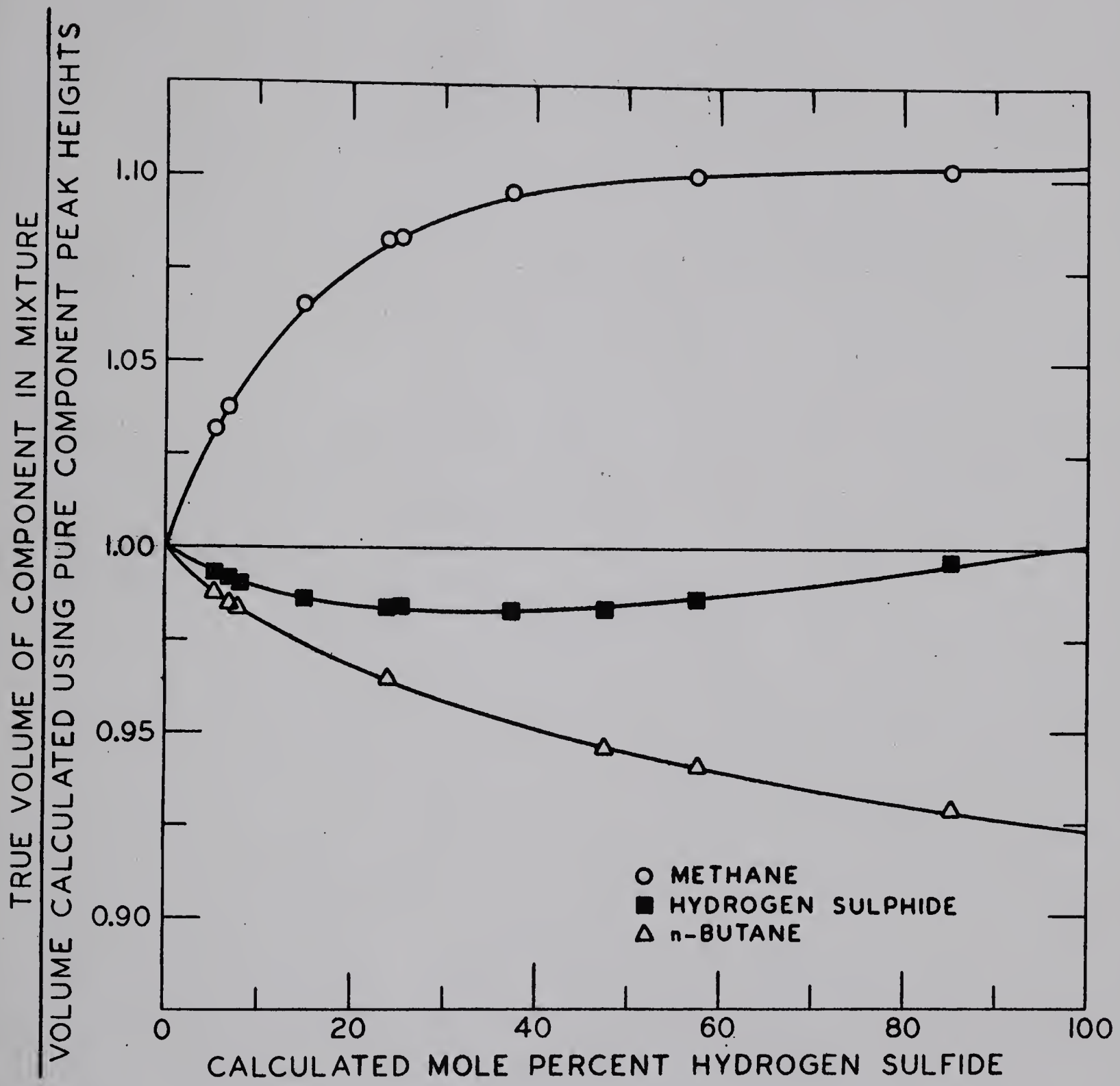

FIG.35 Chromatograph Correction Curves for the Methane-Hydrogen Sulfide-n-Butane System

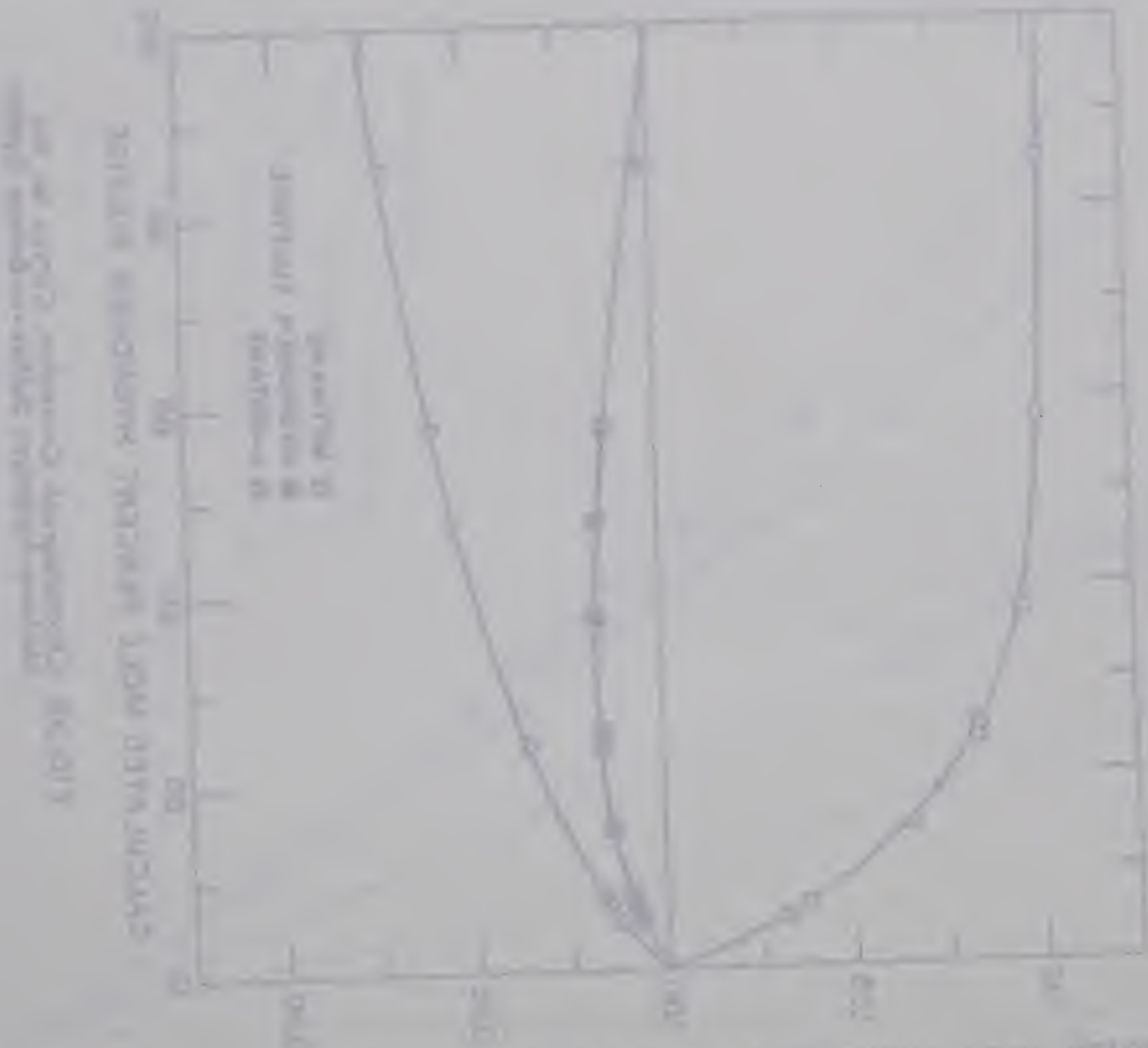

B29868